



**TRIBHUVAN UNIVERSITY
INSTITUTE OF ENGINEERING
PULCHOWK CAMPUS**

THESIS NO.: M-46-MSMDE-2019-2022

Design of Rotor Balancing System for Industrial Purpose

by

Sabin Adhikari

A THESIS
SUBMITTED TO THE DEPARTMENT OF MECHANICAL AND AEROSPACE
ENGINEERING IN PARTIAL FULFILLMENT OF THE REQUIREMENT FOR
THE DEGREE OF MASTER OF SCIENCE IN
MECHANICAL SYSTEMS DESIGN AND ENGINEERING

DEPARTMENT OF MECHANICAL AND AEROSPACE ENGINEERING
LALITPUR, NEPAL

MARCH, 2022

COPYRIGHT

The author has agreed that the library, Department of Mechanical and Aerospace Engineering, Pulchowk Campus, Institute of Engineering may make this thesis freely available for inspection. Moreover, the author has agreed that the permission for extensive copying of this thesis for the scholarly purpose may be granted by the Professor, who supervised the work recorded herein or, in their absence, by the Head of Department or concerning M.Sc. Program Coordinator or Dean of the Institute in which the thesis work was done. It is understood that recognition will be given to the author of this thesis and the Department of Mechanical and Aerospace Engineering, Pulchowk Campus, Institute of Engineering in any use of the material of the thesis. Copying or publication or the other use of this for financial gain without the approval of the Department of Mechanical and Aerospace Engineering, Pulchowk Campus, Institute of Engineering, and the author's written permission is prohibited. Request for permission to copy or to make any other use of the material in this in whole or in part should be addressed to:

Head of Department
Department of Mechanical and Aerospace Engineering
Pulchowk Campus, Institute of Engineering
Lalitpur, Nepal

TRIBHUVAN UNIVERSITY
INSTITUTE OF ENGINEERING
PULCHOWK CAMPUS

DEPARTMENT OF MECHANICAL AND AEROSPACE ENGINEERING

The undersigned certify that they have read, and recommended to the Institute of Engineering for acceptance, a thesis entitled “**Design of Rotor Balancing System for Industrial Purpose**” submitted by **Sabin Adhikari** in partial fulfillment of the requirements for the degree of Master of Science in Mechanical Systems Design and Engineering.

Supervisor, Laxman Poudel, PHD

Professor

Department of Mechanical and Aerospace
Engineering, Pulchowk Campus

External Examiner, Krishna Prasad Shrestha, PHD

Assistant Professor

Kathmandu University

Committee Chairperson, Surya Prasad Adhikari, PHD

Head, Department of Mechanical and Aerospace
Engineering, Pulchowk Campus

Date: 20th March, 2022

ABSTRACT

Most of the modern machines have the rotating parts containing bearings and gears. The mass distribution on either side of the rotary mass should be even. The unequal mass distribution leads to unbalanced forces causing vibrations and the noise. Hence, there is escalating demand of the reliable, safe, precise and versatile rotor balancing system. This research study focused on the design of the rotor balancing system with the balance quality grade G2.5 to G40. The structural and modal analysis of system component is being carried out according to Finite Element Method (FEM) in Ansys and Solidworks software after CAD model design in Solidworks.

The different positions of rotor in the shaft were studied, and the rotor at the center was found to deform less and with less chances of undergoing resonance. The machine components were analyzed and found to sustain the equivalent stress and deformation. The unbalance system was studied by considering two cases one with lumped mass and other with mass removed. The permissible unbalanced is also calculated for the different rpm and rotor weight. The target balancing of this study is for the disc type rotor of 3000 rpm as per ISO-1940-1 standard.

ACKNOWLEDGEMENT

I would like to express my special thanks of gratitude to my supervisors Professor Dr. Laxman Poudel sir and Assistant Professor Hari Bahadur Dura sir for providing professional guidance, continuous supervision, patience and valuable time during the project.

I would also like to express my due respect to Department of Mechanical and Aerospace Engineering for their constant coordination and support. My special thanks to Associate Professor Dr. Surya Prasad Adhikari, Head of Department of Mechanical and Aerospace Engineering, Pulchowk Campus for his constant encouragement. I would also like to thank the Department Professors, Lecturers for their extensive support and assistance throughout the project.

I would also like to give special thanks to my office, Directorate General of Army Aviation(DGAA), Nepal Army, Chief Engineer Sir, Rotor Wing In-charge, my respected senior sirs and colleagues for constantly supporting, encouraging and helping me to complete my research study.

Lastly, I would like to express my deep gratitude to my friends and family for their invaluable support, cooperation and motivation to accomplish the study within the time frame.

Table of Contents

COPYRIGHT.....	ii
ABSTRACT.....	iv
ACKNOWLEDGEMENT	v
List of figures.....	ix
List of tables.....	xi
CHAPTER ONE: INTRODUCTION.....	1
1.1 Background	1
1.1.1 Theoretical aspect of Rotor Balancing System	1
1.1.2 Types of Unbalance.....	3
1.1.3 Design and Construction of Rotor Balancing System.....	4
1.2 Objectives.....	7
1.2.1 Main Objective	7
1.2.2 Specific Objectives.....	7
1.3 Problem Statement	7
1.4 Limitations.....	8
CHAPTER TWO: LITERATURE REVIEW	9
2.1 Rigid and Flexible Rotors.....	9
2.2 Balancing Methods.....	10
2.2.1 Influence Coefficient Balancing Method (ICM)	11
2.2.2 Modal Balancing Method (MBM)	12
2.2.3 Modern Balancing Methods	13
2.3 Rotor Balancing Standard	17
2.4 Commercial Rotor Balancing System	21
CHAPTER THREE: METHODOLOGY	23
3.1 Design of Components	24
3.1.1 Selection of Components.....	24

3.1.2 CAD Model	25
3.1.3 Analytical Calculation	26
3.2 FEM Analysis.....	26
3.2.1 Geometry Design.....	27
3.2.2 Meshing	27
3.2.3 Setup/ FEA Solver	28
3.2.4 Solution/Post-processing	28
3.3 Dynamic Vibration	28
3.3.1 Free Vibration.....	30
3.3.2 Forced Vibration.....	33
3.4 Balancing Algorithm	36
3.5 Documentations.....	39
CHAPTER FOUR: DESIGN CALCULATIONS	40
4.1 Conceptual Design	40
4.1.1 Static Components.....	41
4.1.2 Dynamic Components	41
4.2 Equation of Motion	45
4.3 Machine Components Design	49
4.3.1 Machine Bench.....	49
4.3.2 Suspension System	50
4.3.3 Transmission System.....	51
4.3.4 Shaft and Rotor System.....	52
4.4 Safety and Aesthetic	52
CHAPTER FIVE: RESULTS AND DISCUSSIONS.....	54
5.1 Machine Specifications	54
5.2 Dynamic Analysis	54

5.2.1 Analysis of Shaft	55
5.2.2 Shaft with Rotor	58
5.2.3 Suspension System	66
5.2.4 Machine Frame	69
5.3 Unbalance System	71
5.4 Unbalance Characteristics	76
CHAPTER SIX: CONCLUSIONS AND RECOMMENDATIONS	79
6.1 Conclusions	79
6.2 Recommendations	80
References	81
APPENDIX A	85
APPENDIX B	87
APPENDIX C	88
APPENDIX D	89
APPENDIX E	91
APPENDIX F	92
APPENDIX G	93
APPENDIX H	94
APPENDIX I	95
APPENDIX J	96

List of figures

Figure 1.1 Spring-Mass System for Unbalanced Mass.....	2
Figure 1.2 Static Unbalance and Corrections (McMillan, 2020).....	3
Figure 1.3 Couple, Quasi-Static and Dynamic Unbalance	4
Figure 1.4 Basic Design of Balancing Machine	6
Figure 2.1 Deflection of flexible shaft at Critical Speed	10
Figure 2.2 System for Online Dynamic Balancing (Hongwei et al., 2011).....	16
Figure 2.3 Permissible Residual Unbalance	20
Figure 3.1 Methodology.....	23
Figure 3.2 Shaft and Suspension System system.....	27
Figure 3.3 Meshing	27
Figure 3.4 A simple 2 DOF spring-mass-damper system.....	30
Figure 3.5 Clampbell Diagram	32
Figure 3.6 SDOF System with Rotating Unbalance	34
Figure 3.7 Amplitude of response due to Unbalance.....	35
Figure 3.8 Shaft Whirl Geometry	35
Figure 3.9 Rotor Balancing Flowchart.....	36
Figure 3.10 Initial Run	38
Figure 3.11 Run with Trial Mass	38
Figure 3.12 Determination of Vector of Unbalance	38
Figure 3.13 Determination of Compensating Mass Position.....	38
Figure 4.1 Conceptual Design for Rotor Balancing System.....	40
Figure 4.2 Shaft Rotor (Disc) System.....	45
Figure 4.3 Machine Bench.....	50
Figure 4.4 Suspension System	51
Figure 4.5 Induction Motor.....	52
Figure 4.6 Flat Belt	52
Figure 5.1 Rotor Balance System Free Body Diagram.....	55
Figure 5.2 Clampbell Diagram for Shaft-Pulley Analysis.....	57
Figure 5.3 Maximum Equivalent Stress.....	58
Figure 5.4 Comparative Model Study and Deformation for Three Cases.	60

Figure 5.5 Clampbell Diagram for Shaft with Rotor Case 1	61
Figure 5.6 Clampbell Diagram for Shaft with Rotor Case 2	63
Figure 5.7 Clampbell Diagram for Shaft with Rotor Case 3	64
Figure 5.8 Mesh Independent Graph for Deformation	65
Figure 5.9 Mesh Independent Test Graph For Critical Speed	65
Figure 5.10 Free Body Diagram of Reaction Forces for Shaft and bearing	66
Figure 5.11 Forces acting on Suspension System.....	66
Figure 5.12 Deformation of Suspension System for First five modes.....	67
Figure 5.13 Structural Analysis of Suspension System	68
Figure 5.14 Modal Analysis of Machine Bench	69
Figure 5.15 Structural Analysis of Machine Bench.....	71
Figure 5.16 Unbalance System with Lumped mass and Removed mass.....	72
Figure 5.17 Clampbell Diagram for Rotor with Lumped Mass.....	73
Figure 5.18 Clampbell Diagram for Rotor with Mass Removed.....	74
Figure 5.19 Comparative Deformation Diagram	75
Figure 5.20 Comparative Equivalent Stress (Von Mises) Diagram.....	76
Figure 5.21 Permissible unbalance Weight	78
Figure A.1 Free Body diagram of Reaction forces for Shaft and Bearings.....	85

List of tables

Table 2.1 Guidance for Balance Quality Grades	19
Table 3.1 Selection of Single and Dual Plane.....	37
Table 4.1 Design Characteristics of Machine Bench.....	50
Table 4.2 Design Characteristics of Suspension System	51
Table 4.3 Transmission System Design Characteristics	52
Table 4.4 Design Characteristics of Shaft and Rotor.....	52
Table 5.1 Design Characteristics of Rotor Balancing System.....	54
Table 5.2 Different Forces Acting on Shaft.....	56
Table 5.3 Results of Modal Analysis of Shaft	57
Table 5.4 Equivalent Stress.....	58
Table 5.5 Results Showing Modes, Critical Speeds and Engine Orders for Case1	61
Table 5.6 Results Showing Modes, Critical Speeds and Engine Orders For Case 2... 62	
Table 5.7 Results Showing Modes, Critical Speeds and Engine Orders For Case 3... 63	
Table 5.8 Permissible Unbalance Mass	77
Table B.1 Results for Rotor with Lumped Mass	87
Table B.2 Results for Rotor with Mass Removed	87
Table C.1 Comparative Deformation Data	88
Table C.2 Comparative Equivalent Stress (Von Mises Stress).....	88
Table D.1 Comparative Deformation Diagrams	89
Table E.1 Comparative Equivalent Stress Diagram	91

CHAPTER ONE: INTRODUCTION

1.1 Background

The rotating components and the parts of the machine should be properly align and balanced. Any misalignment and unbalance in the system leads to the vibration. In turbo-machinery, the unbalance in the system is considered as the main source of vibration (Taylor, 2005), (Thomson, 2018). If the misalignments and the unbalances aren't identified and diagnose timely then they will lead to damage of machine components instead. Bearings, supports and housing are more susceptible to damages. The machine with vibration and unbalance within the permissible limits will have longer operational life before the failure occurs (Hongwei et al., 2011). This can be achieved primarily by balancing and aligning the machine and its components along with correction in the resonance problems. When the actual rotational axis of the rotor doesn't align with the geometric axis, vibration and unbalance is induced (Knowles et al., 2017). This is mainly caused by the material anisotropy, damaged of the components, defect manufacturing, installation eccentricity and other factors. For the rotor that operate in high speed machines like cutting tools, aircrafts rotors, propellers, manufacturing parts, actuators motors, etc and the system where precision and accuracy are important factors, the unbalance will leads to the deterioration in the quality and efficiency of whole system. The prolong use of these rotary machines will cause failure of the components and safety standard will not be met. Therefore, for rotor system application, the suppression of unbalance or induced vibration is of major concern while designing, maintaining and efficient operation.

Different approach has been made in the past to identify and solve the rotor induced unbalance. Various researches have been carried out and balancing techniques have been proposed. According to the applications, varieties of rotor balancing systems are designed and manufactured, different balancing software and the algorithm is being put forward. Details study of rotor balancing system and different related aspects are covered in this research study.

1.1.1 Theoretical aspect of Rotor Balancing System

The rotary system consists of shaft which is supported on the bearings. The unbalance mass or induce vibration imparts unequal load to the bearing resulting in the

misalignment. The unbalance is defined as the condition that persists in the rotating body when the vibratory motion is transferred to the bearings as the result of the centrifugal forces.

This can be written in equation form:

$$\vec{F} = m\omega^2 e \quad (1.1)$$

Where, \vec{F} is the centrifugal force, m is the unbalance mass, ω is the rotor angular velocity and e is the distance between the center of shaft rotation with the unbalance mass.

From the Equation (1.1), for the imbalance system, the centrifugal force which is directly proportional to the square of the rotational speed or angular frequency, mass of imbalance and the eccentricity.

Figure 1 shows a simple mass-spring system for the unbalance system. The vertical movement “x” is restricted. Mass (m) is the unbalance having the eccentricity (e) such that unbalance centrifugal force is generated in the radial direction.

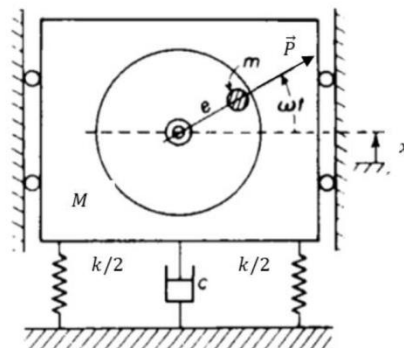


Figure 1.1 Spring-Mass System for Unbalanced Mass

As shown in Figure 1.1 any vibration in the rotary shaft, first of all it is checked for any residual weight and thus finding out the imbalance force imparted on the bearings for that corresponding frequency of rotation. The residual weight may be single or multiple in the numbers. Moreover, imbalance occurs when there is damaged in the rotor too. In case of imbalance or vibration due to residual mass, the balancing is carried out by placing or adding the mass in the position such that to counter balance the weight to the centrifugal forces. The maximum allowable unbalance for each rotating component is given in ISO 1940-1 for details.

The rotor balancing techniques are carried out in two ways. First being in-situ balancing where the balancing is carried out in the machine itself, second one being in-workshop where the component is taken out from the system and is balanced with the help of test-bench. These methods have their own procedures to balance the mass by reducing or nullifying the unbalance or vibration induced in the system.

1.1.2 Types of Unbalance

Basically there are four types of unbalances namely static unbalance, couple unbalance, quasi-static and dynamic unbalance.

1.1.2.1 Static Unbalance

In static unbalance as in Figure 1.2, the center of rotation of the rotor is displaced parallel to the geometric center of the rotating elements. For this system, amplitude and phase of vibration of the body will be same at the both ends. The system is corrected by adding or removing the proper amount of weight in the calculated plane. Single weight having the same mass as unbalance is placed at the same place of unbalance but exactly 180 degrees opposite as shown on Figure 1.2 (b). As in (c), two correction weights are placed at equal distance and 180 degrees from the unbalance for the balancing purpose.

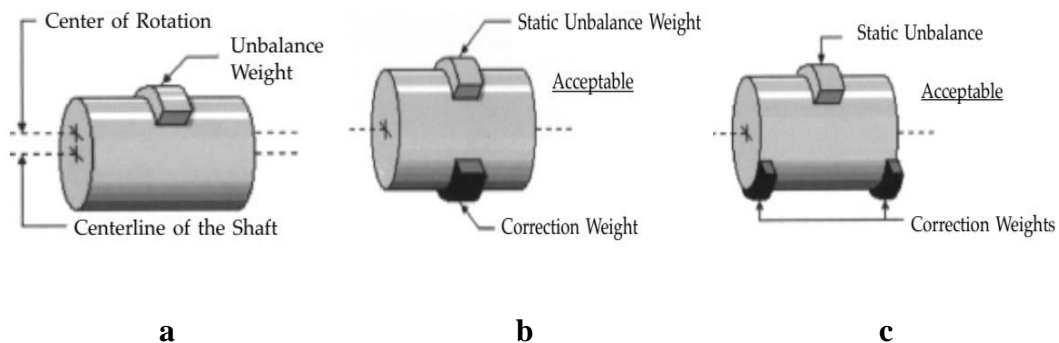


Figure 1.2 Static Unbalance and Corrections (McMillan, 2020).

1.1.2.2 Couple Unbalance

Even though the shaft is balanced statistically, the element tends to wobble around its center when shaft is under rotation such that both ends of shaft will undergo vibration with same amplitude but 180 degrees out of phase. Couple unbalance as shown in Figure 1.3 (a) cannot be corrected in single plane rather required two or multiple planes.

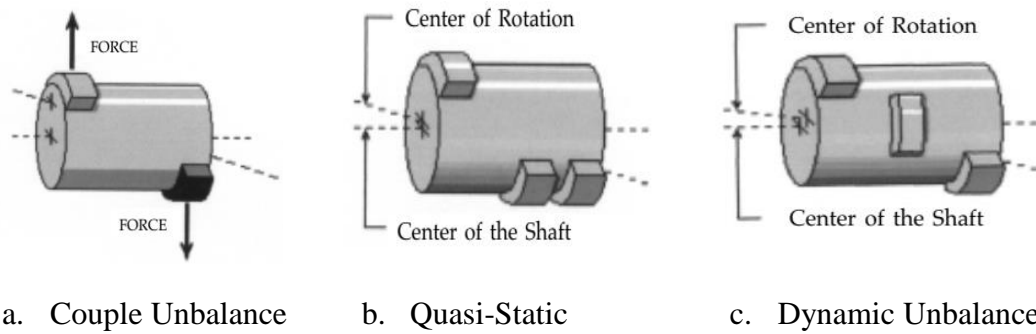


Figure 1.3 Couple, Quasi-Static and Dynamic Unbalance

1.1.2.3 Quasi-Static Unbalance

The Quasi-Static Unbalance as shown in Figure 1.3 (b) is detected by the vibration amplitude being very different at ends of shaft and being at phase difference of approximately 180 degrees. This is caused when the rotation center intersects the geometric center of element but not at the center of gravity. This is corrected in dual or multiple planes.

1.1.2.4 Dynamic Unbalance

The Dynamic Unbalance as shown in Figure 1.3 (c) takes place when the rotational axis of element doesn't coincide the geometric centerline. This kind of unbalance is most frequent in rotating machinery. The dynamic unbalance has the different vibration amplitude at ends of element and the phase angles are neither in phase nor directly opposite to each other. This type of unbalance is corrected in dual or multiple planes.

1.1.3 Design and Construction of Rotor Balancing System

Rotor balancing machines are classified into universal balancing machine, semi-automatic balancing machine and fully automatic balancing machine based on their design (McMillan, 2020). All of these machines can work efficiently for both rotating and non-rotating masses with the residual weight correction in single and multiple planes.

Universal balancing machines have the capacity for balancing a variety of sizes and types of rotors. The unbalance present in the system is easily observable with the suitable instruments present in the system. This type of machine is used for many small to medium scale production and balancing.

The performance of the semi-automatic balancing machine ranges between universal balancing machines to the fully automatic balancing system. This type of system can carry out the functions like retaining the amount and angular location of unbalance in the system for further use, couple the balancing machine to rotor, indicate and apply the correction weight, indication of any unbalance after correction, etc. The sophisticated semi-automatic balancing system performs most of the functions by itself but depend upon the operator for the loading, unloading and initiation of the operation.

Fully automatic balancing machine has the facility of automatic transfer of the rotor and the balancing is carried out either in the single stations or the multiple stations. The rotor is automatically transferred to the balancing system by the conveyor belt and taken away automatically after the completion. The processes like unbalance measurement, indication, location and the corrections are carried out sequentially in single station in automatic balancing machine where as in multiple station balancing machine the processes will be carried out in the different stations.

The basic design of balancing machine is shown in the Figure 1.4. The balancing system consists of the base or bench, the drive for transmission of rotation, pedestals, sensors in the bearing or supports and the measurement units which display the results transmitted by the sensors.

Major components of balancing system:

Base or bench: The base or the bench forms the main framework of the balancing machine. It is usually made up of tough and the hard materials like cast iron. It rest on the ground or floor and form the foundation supports for the other components of system. These other components are attached or connected to the base directly or indirectly.

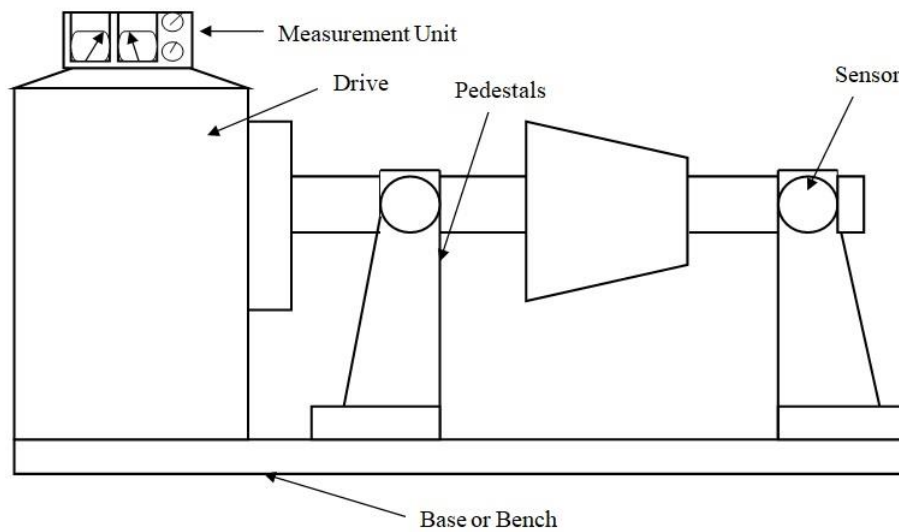


Figure 1.4 Basic Design of Balancing Machine

Measurement Units Display: Measurement unit is the main indication for deciding whether the system is balanced or not. Any alignment or misalignment or displacement due to unbalance in the rotors are transferred to the bearings which consists of sensors. The sensors shows the corresponding results in the measurement or display unit provided.

Pedestals: Pedestals are the supports for the rotor shaft. Usually two pedestals are provided to hold the shaft consisting of rotor. Each pedestals provided with the bearings and the sensors to measure the balancing.

Drive: The drive will be provided from the induction motor with different horse power depending upon the rotational velocity of the shaft. With respect to the balance quality grades for rotor and the permissible residual specific unbalance weight, the drive speed may vary.

Sensors: The balancing machine use different types of sensing elements at the rotor-bearing support to convert mechanical vibrations into an electrical signal(International Standard Organization, 2003). The sensing elements can be velocity sensors, magneto-restrictive piezoelectric sensors, capacitance or inductive sensor, accelerator or other types of indication sensors. This sensor information will be transferred to the measuring or display unit and hence the unbalance or vibration result will be displayed.

The rotor system to be analyzed for the balancing is kept in the drive supported between the pedestal having bearings placed for the rotary motion. The bearing consists of the sensors that give the information about the possible displacement corresponding to unbalance. This displacement will be shown in the measurement display unit. Accordingly correction is applied to the unbalance system.

1.2 Objectives

1.2.1 Main Objective

The main objective of this research is to design and analyze Rotor Balancing System for disc shape rotor having balance quality grade from G2.5 to G40.

1.2.2 Specific Objectives

The proposed research has following objectives

- To design Rotor Balancing System
- To carry out Modal and Structural analysis of the components and system.
- To study the unbalance rotor system and find out permissible limits.

1.3 Problem Statement

For any machine with the rotary system, the balancing of the rotatable component is essential. For the industrial machineries, the unbalance rotor system leads to deviation from the actual product and faulty or defective product may be manufactured. In case of cutting tools and machining process where high precision and accuracy is required, the unbalance of the system is intolerable. The unbalance mass will create the vibration and eventually damaged the supports and bearings. This may lead to the huge loss of economy and the resources.

It is very difficult to identify whether the system is balanced or not. For the system where high precision and accuracy is required, the balancing techniques are carried out frequently. The performance of the rotary machine should be within the tolerable limit, otherwise this will lead to the damage of the bearings, supports, bushings and even the machine components.

The industrial rotating machineries, aircraft rotors, machine cutting tools, manufacturing plants, etc where high precision and accuracy is required, the unbalance of the system directly impact the operational efficiency and safety. So,

there is the need for the rotor balancing system that can identify and balance the rotating components. Moreover the rotor balancing system should also be efficient enough to balance the self-induced unbalance in the system.

For the rotary system to work for longer duration, the system must be kept within the balance limit. To examine the condition, rotor balancing system must be designed and balancing need to be carried out. Before manufacturing the prototype, the designed prototype should be analyzed for effective performance at different conditions for the functional and the operational checks. In this research, the rotor balancing system for industrial purpose is designed and analyzed for proper functioning and balancing behavior.

1.4 Limitations

Mechanical system used in most of the modern industries like automobile, aerospace, hydropower, nuclear power plants, etc have the rotating components. Each of these system has the rotary components that have different characteristics. Similarly, the rotational speed, precision and the accuracy required for the system is diverse. For example, some rotary components can perform well within with certain unbalance in the system whereas other system cannot tolerate the unbalance for the high accuracy performance, so balancing system and the parameters cannot be generalized. In this research study, the system is designed for the rotation upto 5000rpm. The research work is limited to structural and modal analysis of CAD design made in SolidWorks software and simulation carried out in Ansys. If the prototype was manufactured and experiments were carried out, then the actual performance of the rotor balancing system could have been known.

CHAPTER TWO: LITERATURE REVIEW

The rotating machine undergoes the physical movement or the motion which is referred as vibration. The precise measurement of the vibration is quite difficult to be identified by the visualization or touch. So, to measure and analyze them, the vibration signal needs to be converted into electronic signal by the transducer. With the help of transducers, the frequency and the amplitude of moving machine is measured. These frequency and amplitude parameter provides whether the motion is harmonic or the random. The random motion leads to the vibration and unbalance in the system.

In wide range of machinery applications, the vibration of the rotating shaft is one of the major concerns. From the aircraft gas turbines, pumps, generators, fans, electrical generating power plants, chemical processing plants, etc. the vibration of shaft during the operation is unavoidable trouble to encounter. (Parkinson, 1991) in his article highlighted about the vibration experienced by various rotating machinery in different applications due to imbalance in the system. The balancing procedures for the both rigid and flexible shaft were discussed with special priority to high speed rotating shaft.

2.1 Rigid and Flexible Rotors

Most of the rotors are flexible in nature, however the rotors having comparatively lower speed of rotation are said to be rigid rotors (International Standard Organization, 2003). The rigid rotor at low speed rotate about its center axis, so there won't be significant bending and deformation. The shaft having high diameter to length (D/L) ratio, the operating speed of shaft being 70-75 percent less than the critical speed for which flexure may occurs possess this characteristics. Although the shaft is rigid but pedestals may deflect. (Neto et al., 2006) mentioned the historical definition for the rigid rotors as the rotor that operates below the first critical speed and operation above first critical speed is flexible one. Further defined the rotor based on the deformation due to unbalance and balancing of the rotor. If the unbalance force on the rotor cannot bend the rotor then, it is rigid one for which rigid balancing techniques are applied and flexible rotor balancing procedure is applied if the rotor deforms due to its own unbalance similar to the occurrence near the critical speed, then rotor is flexible. The new type of rotor is proposed as quasi-flexible rotor with its

operation ranges above half its first critical speed and below first critical speed where rigid balancing techniques are not effective enough. More definition and details of rotor type is available in (ISO 5406, 2014). The flexible rotors are used in alternators for generation of electrical power. The rigid rotors are mostly used in aircraft propulsion and other components where the cost of production is high as well as have high failure rates (Parkinson, 1991).

The amplitude of vibration of flexible rotor varies directly with the angular speed of rotation ω as shown in Figure 2.1. At the critical speed for angular velocity $\omega_1, \omega_2, \omega_3 \dots$, the amplitude becomes very high and undergoes the resonant vibration. At the critical speed, the straight shaft deflects into various shapes as shown in Figure 2.1. Therefore for the flexible shaft, allowance or tolerance limitation is provided.

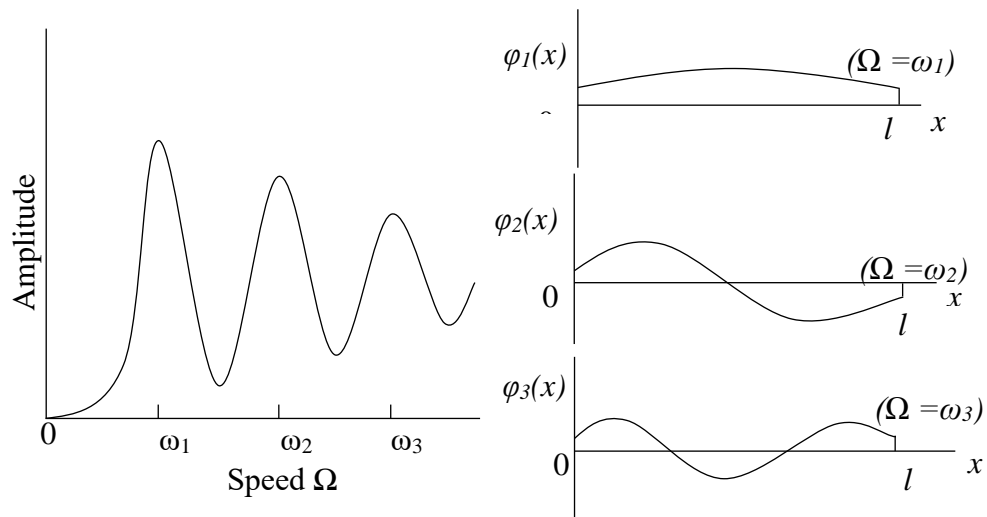


Figure 2.1 Deflection of flexible shaft at Critical Speed

From these observations, it is essential to consider design parameters like natural frequencies at different principal modes of rotor. So, different balancing procedures are applied to keep the vibration level within the tolerance limit.

2.2 Balancing Methods

Rotor imbalance is one of the main causes of vibration in rotating machines (Xu & Marangoni, 1994). Rotor imbalances can be caused by material defects, manufacturing defects along with assembly, asymmetric structure, rotor wear, temperature changes during operation, etc. If the inertia principal axis aligns with the rotational axis of rotor using the redistribution process, the unbalance can be removed. When the amplitude of rotor vibration is reduced and rotor operates steadily, then it is

said to be balanced. Three distinct methods were proposed for the rotor balancing which were included in (ISO 5406, 2014). Those three methods are:

1. Influence Coefficient Balancing Method(ICM)
2. Modal Balancing Method(MBM)
3. Modal balancing, proceed by rotor balancing

2.2.1 Influence Coefficient Balancing Method (ICM)

Although the research for rotor balancing system commenced in 1930, but the demand of precision balancing especially for heavy load and machine rotating at high speed is increasing at high rate and there is still lot to improve in existing methods like ICM, MBM and other methods (Zhou & Shi, 2001).

There was alarming requirements of the rotor balance after 1950 as rotor imbalance was becoming major problem. There was no assurance of rotor balance even after selecting the balancing speed. It was found that multiple balance speed and the planes to be chosen for the smooth passage for all bending critical speed. (Goodman, 1964) wrote a well-known study on how to use the least squares method to solve problems. Balance corrections were computed and verified through experimentation. The paper went into greater detail about the ICM theoretical foundation and the principle of the least squares approach was used to solve the problem. The minimization of residual vibrations at the measuring locations was crucial in this application. The number of measure points is not limited, and it might be significantly greater than the number of balancing planes. This approach meets the requirement for balancing flexible rotors and shaft systems in numerous planes and speeds. Post this method, the rotor balancing system was programmed which gave practical analogy to ICM.

(Tessarzik et al., 1972) calculated the balance correction using the improved ICM. The experiment was carried out and reduction in the vibration of large rotors was found to be effective with this balancing technique. The precision of balancing techniques can be enhanced greatly if the dynamic response of the unbalanced rotor system is known (Juergen M. Tessarzik, 1975).

Studied on four different aspect of balancing a. rotor balancing for multiple critical speeds b. rotor supported by rigid and flexible bearings c. balancing of rotor with different vibration information and different correction planes d. rotor balanced

through initial unbalanced configurations. The main purpose of ICM techniques is to select the correct mass to nullify the shaft vibration (or maintain within specified limits) at different section along the shaft for different shaft speed.

Balancing procedures for ICM method (Li et al., 2021):

1. Selection of balance planes and speed: During design of rotor, balance planes and the experimental speeds are selected for different working environment.
2. Vibration Measurement: Initial vibrations are measured for different speed at different points.
3. After the addition of trial weight vibrations are measured again
4. Influence coefficient and balance corrections are calculated.
5. The balancing of the rotor is carried out until the desired precision is achieved

2.2.2 Modal Balancing Method (MBM)

This method was originally developed in UK from the proposal of (Bishop & Gladwell, 1959). Modal balancing, proceed by rotor balancing is developed in Germany. The modal balancing techniques operate in the principle by separating the principal modes of vibration on the body and balancing is achieved when each individual mode is balanced. When the shaft containing rotor operated near the critical speed, the deformation produced can be called as vibration mode and is caused by modal imbalance. The deflection can be eliminated by the use of different balance corrections.(G. Urbikain et al., 2015), (Gorka Urbikain et al., 2017) put forward the vibration phenomena in turning process whereas (Grobel, 1953) researched on turbine rotor balancing method. Similarly (Kellenberger W, 1971) made study on MBM, experimented and proposed N ad N+2 plane balancing phenomena. (Meacham et al., 1988) suggested the method for linear flexible rotor without requiring the trial weight where the balancing is carried out by complex modal method having residual bow. (Palazzolo & Gunter, 1982) conducted an experiment verification of the unbalance distribution of flexible rotor without the requirement of trial weight. The modal balancing distribution was found out with the help of rotor modal mass and rotor mode shape. The differences in the theoretical models used for analysis of rotating and non-rotating structure were explained by (Bucher & Ewins, 2001) and experimental verification was carried out. Since the beginning of 21st century MBM procedures have been modernized in both theory and experiment. Although the

comparison modal balancing proceed by rigid rotor balancing seems even, the shaft still possess modal components of unbalance , which is corrected near to critical speed and the contradiction arise in these two methods are explain by (Parkinson, 1991).

Balancing procedures for MBM method(Li et al., 2021):

1. Measurement of Initial Vibration
2. After the addition of the trail weight vibration is measured again
3. Balance correction is calculated and 1st mode shape is balanced
4. Above mentioned procedures are repeated for balance of vibrations in different modes within the range of speed.

2.2.3 Modern Balancing Methods

The improvement in the balancing procedures after ICM and MBM is done and different methods have been developed. Along with the theoretical model, the experiment has also been carried out to propose new methods by different scholars will be explained in the following chapters.

Balancing Method for Non-linear Rotor

If the unbalance system undergoes the excitation which has nonlinear relationship with system response, then the nonlinear process needs to be employed. The non-linear response was studied by (Guskov et al., 2008) of modified Jeffcott rotor system which was multiple unbalances. Similarly, with the ICM and Lagrange's Approach, (Turpin & Sharan, 1994) researched on the non-linearity of the bearings and developed corresponding equivalent linear modal system.

Balancing Method for Transient Rotor

It is seen that conventional rotor balancing system operates normally at the steady speed. However, for the flexible rotor there is high chances and possibility of resonances leading to the vibrations near the critical speeds. So, different methods for the transient rotor balancing have been developed over the years.

Balancing Methods using Fusion Technology

Any rotating machinery possess multisource of information like temperature, pressure, vibration, flow, etc at the same time and the references. Compared to the single vibration signal received from sensors regarding the vibration only, these multi

source factors also impact the signal generated. To precisely receive the signal with high accuracy, multi-source real vibration signal should be received which gave rise to homologous information fusion technologies. Full spectrum technology (Capello & Kotlarek, 2016) of Bently Nevada Corporation, holospectrum technology of Academician (Qu et al., 1989) and full vector spectrum technology are the three fusion technologies. Based on the aforementioned fusion technologies several researchers have carried out the studies.

Balancing for Special Rotors

As the accuracy for rotating machinery has been increasing so does the selection of materials type, processing method and assembling techniques is also varying. The balancing methods for asymmetric and overhung rotors, dual-rotor system and bending rotors have been studied separately. The unbalance response developed in the anisotropic rotors was studied by (Han, 2007) found the process of multiple harmonics and proposed the idea of dominant balancing mode. The improved version of rotor balancing system is further highlighted by (Kang et al., 1997). The idea of separating the rotor vibration signal in dual-rotor system having small variation in speed is put forward by (Yang et al., 2004). The centrifuges having dual-rotor system can well be balanced by this method. The bending generally leads to the unbalance of the system (Deepthikumar et al., 2013). (Nicholas et al., 1975) proposed different methods with residual shaft bending by adjusting the amplitude, deflections at the balance speed. Including (Parkinson et al., 1984) different study has been carried out taking the considerations of thermal bending, temporary or the permanent bending.

Based on the plane of balancing following methods are there (Burgos Alconz & Zurita V., 2019):

Single Plane Balancing: Balancing is carried out in only one plane. Correction masses are added in single plane or equal weights are placed at two end of same plane. Most of the balancing is carried out by this single plane balancing phenomenon by the methods like graphical, influence coefficient method or by trial weight.

Dual Plane Balancing: The corrections are carried out by adding weight at two planes. The one of the planes being near to support bearing.

Multi-plane Balancing: In this technique corrections are carried out in more than two planes with multispeed of rotor.

Other Balancing Techniques

To enhance the accuracy of rotating machinery system different other balancing methods has been proposed and design. To mention some are transfer function method, balancing without trial weight, local balancing method, online balancing method, balancing by specific device, balancing of high speed rotor, etc. The calculations of unbalance using numerical simulations is carried out by (Tiwari & Chakravarthy, 2006). Similarly, balance for super critical structure can be carried out using slow speed data (Tresser et al., 2018).

(Hongwei et al., 2011) Proposed the program for the dynamic balancing of grinding wheel spindle. In this paper unbalanced factors for the grinding machine is identified. Those unbalances created the centrifugal forces which generated the vibration excitement of the system. For the rectification of this problem in CNC machine spindle system, online dynamic balancing system is proposed which consists of sensors, vibration signal and phase angle measurement component, signal amplifier, filters, dynamic balancing device and other essential components.

The rotor system consisting of wheel and spindle supported on bearings, the vibration sensors on the bearing senses the vibration amplitude, speed of spindle and vibration phase as in Figure 2.2. The signal processing generates the fundamental components of the frequency from original signal. DSP sampling, digital filter and signal analysis performs the unbalance calculation. Balancer drive, control and action actuate the auto balancer and carryout automatic balancing with the influence coefficient method.

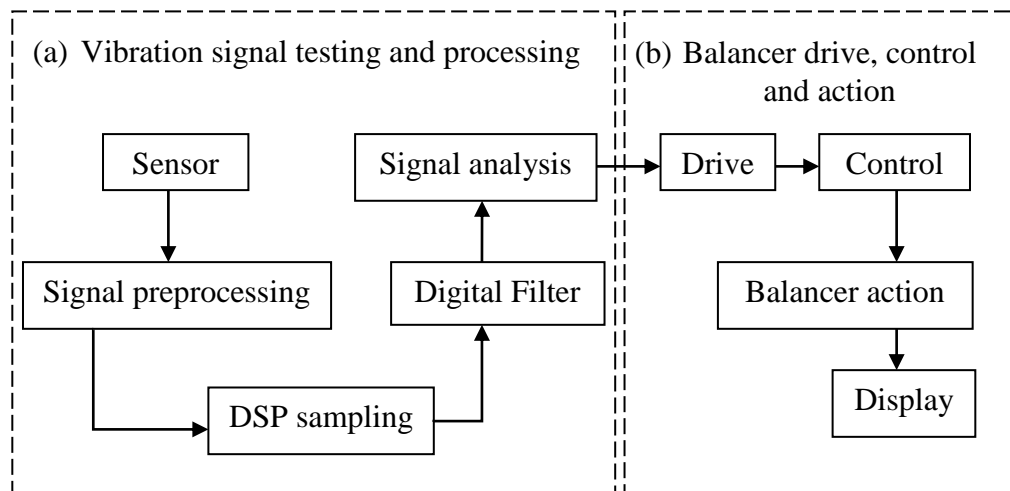


Figure 2.2 System for Online Dynamic Balancing (Hongwei et al., 2011)

A high-speed rotor unbalance-induced vibration has a direct impact on manufacturing accuracy. A modal-based balancing approach for a high-speed rotor without trial weights is provided to successfully suppress this unwanted vibration and eliminate the difficult process of employing trial weights during the balancing adjustment (Zhang et al., 2021). In the study, the imbalance equivalent plane is first acquired using the matrix sweep method (EP) and following that, the equivalent concentration approaches based on the vector feedback principle (VFP) and the modal equivalent principle (MEP) are investigated and contrasted, with the continuous imbalance vector being transferred to the EP in the same way. Then, using modal analysis and the MEP, a balancing approach for the high-speed rotor is proposed that does not require trial weights and only collects vibration data below critical speed.

The spindle bearings are used in most of the machine tools with the cutting rates of 5,000 m/min up to 10,000 m/min. for the cutting tools equipped with polycrystalline diamond (PCD) inserts or cubic boron nitride (CBN). High speeds, on the other hand, drastically limit the life of spindle bearings. Various writers explored the underlying major effects during the operating process, which were summarized in (Wock & Spachtholz, 2003), (Cao & Altintas, 2004). (Wock & Spachtholz, 2003) proposed spindle bearings with various inner geometry to decrease the harmful impact of centrifugal force on the ball added extra contact points to the raceways of traditional spindle bearings. This prevents axial and radial movement of the balls, allowing for stable contact angles and minimized axial displacement of the inner ring throughout a

wide speed range. The multipoint bearings are intended for the main spindle's fixed bearing unit. The movable bearing unit, on the other hand, may fail because to insufficient bearing bushes moving. (Brecher et al., 2007) developed high-rotational-speed cylindrical roller bearings. Compared to ordinary cylindrical roller bearings, the bearings have a higher compliance. These bearings achieved faster rotational speeds in practical tests than traditional ones. Finally, a-C: H:W coatings were added to improve the fail-safe qualities of spindle bearings in the event of inadequate lubrication. The coating reduced the possible wear and tear in case at higher rotational speed and enhances the life and reliability of the bearing in the absence of lubrication too.

(Knowles et al., 2018) proposed balancing mechanism for high-speed, flexible shafts. This method generates corrective balance moments, replicating the fixing moments of similar systems for the shafts placed in a double or single encastre. These phenomena can remove or nullify the 1st lateral critical speed and thus provide the reliable operation with the reduction in the lateral critical speed limiting margins. The research along with experimental verification provides the in depth study on balancing sleeve concept and facilitates imbalance analysis on any rotating shaft.

2.3 Rotor Balancing Standard

Mechanical Vibration ISO-1940-1(International Standard Organization, 2003) provides the different methods for the shaft selection, mass correction, and permissible residual and foremost balance quality grade of the rotor system. The part I of this paper covers the specification and verification of balance tolerances, the necessary number of correction planes and methods for varying residual unbalances. ISO 1925:2001, defined balancing as the procedure by which the mass distribution of a rotor is checked and, if necessary, adjusted to ensure that the residual unbalance or the vibration of the journals and/or forces on the bearings at a frequency corresponding to service speed are within specified limits. The same standard defines unbalance as condition which exists in a rotor when vibration force or motion is imparted to its bearings as a result of centrifugal forces.

According to ISO 1925:2001, the resultant unbalance is expressed by:

$$\vec{U}_r = \sum_{k=1}^K \vec{U}_k \quad (2.1)$$

Where,

\vec{U}_r is the resultant unbalance vector (g.mm);

\vec{U}_k are the individual unbalance vectors, numbered 1 to K.

The resultant moment is expressed by:

$$\vec{P}_r = \sum_{k=1}^K (\vec{z}_{U_r} - \vec{z}_k) \times \vec{U}_k \quad (2.2)$$

Where,

\vec{P}_r is the resultant moment unbalance (g.mm²);

\vec{U}_k are the individual unbalance vectors, numbered 1 to K;

\vec{z}_{U_r} is the axial position vector from a datum mark to the plane of the resultant unbalance \vec{U}_r ;

\vec{z}_k is the axial position vector from the same datum mark to the plane of \vec{U}_k .

The rotor which are out of balance tolerances need the correction. Depending upon the number of planes to be corrected they are classified to one correction plane, two correction plane and multiple correction plane (International Standard Organization, 2003). One correction plane applies usually to the disc type rotor having sufficiently large bearing distance and disc rotating with sufficiently large axial run out by properly choosing the correction plane for resultant unbalance. For the case of dynamic unbalance, i.e, the rotor having resultant unbalance and resultant moment unbalance need correction in two planes. In most of the cases the correction in two planes will be enough for the unbalance, however for the resultant unbalance, couple unbalance, and if the correction is spread along the rotor, more than two planes corrections will be required for the balancing.

The permissible residual unbalance U_{per} for the rotor is derived from the selected balance quality grade given by the expression:

$$U_{per} = 1000 \frac{(e_{per} \cdot \Omega) \cdot m}{\Omega} \quad (2.3)$$

Where,

U_{per} is the permissible residual unbalance, in g.mm; $(e_{per} \cdot \Omega)$ is balance quality grade, expressed in mm/s; m is the rotor mass, expressed in kg; Ω is the angular

velocity of the service speed, expressed in rad/s, with $\Omega \approx n/10$ and the speed n in revolutions per minute (r/min).

The rotors are balanced with respect to selected balance quality grades which also gives the indication regarding the permissible residual unbalance for the different rpm as in Table 2.1 and Figure 2.3.

Table 2.1 Guidance for Balance Quality Grades

Machinery types: General Examples	Balance quality grade, G	Magnitude per. Ω mm/s
Crankshaft drives for large slow marine diesel engines (piston speed below 9 m/s), inherently unbalanced	G 4000	4000
Crankshaft drives for large slow marine diesel engines (piston speed below 9 m/s), inherently balanced	G 1600	1600
Crankshaft drives, inherently unbalanced, elastically mounted	G 630	630
Crankshaft drives, inherently unbalanced, rigidly mounted	G 250	250
Complete reciprocating engines for cars, trucks and locomotives	G 100	100
Cars: wheels, wheel rims, wheel sets, drive shafts Crankshaft drives, inherently balanced, elastically mounted	G 40	40
Agricultural machinery, Crankshaft drives, inherently balanced, rigidly mounted, Crushing machines , Drive Shafts (Cardan shafts, propeller shafts)	G 16	16
Aircraft gas turbines , Centrifuges (separators, decanters) Electric motors and generators (of at least 80 mm shaft height), of maximum rated speeds upto 950 r/min, Electric motors of shaft heights smaller than 80 mm, Fans, Gears, Machinery, general, Machine-tools, Paper machines, Process plant machines, Pumps, Turbo-Chargers, Water turbines	G 6.3	6.3

Compressors, Computer drives, Electric motors and generators (of at least 80 mm shaft height), of maximum rated speeds, above 950 r/min, Gas turbines and steam turbines, Machine-tool drives, Textile machines	G 2.5	2.5
Audio and video drives, Grinding machine drives	G 1	1
Gyroscopes, Spindles and drives of high-precision systems	G 0.4	0.4

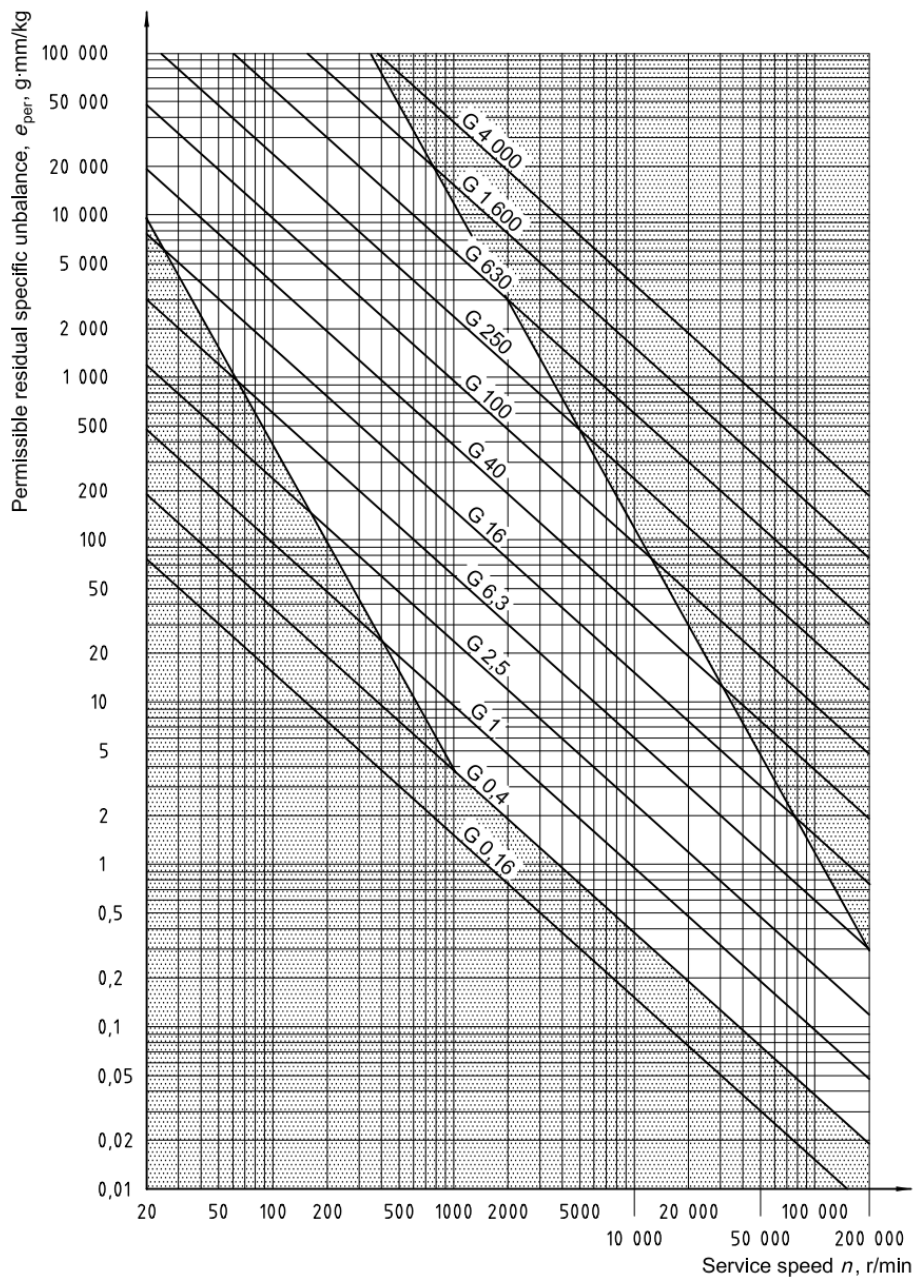


Figure 2.3 Permissible Residual Unbalance

2.4 Commercial Rotor Balancing System

Over the period of time, the balancing technique is regarded as the essential aspect in the industrial applications. From the turbo-machinery components in hydropower, generators, rotors of aircrafts, motors, etc the precision and accuracy of these components directly impact the outcomes (Parkinson, 1991). Different balancing machines have been developed to solve the unbalance problems.

Balancing System S.r.l is leading Italian company for manufacturing cutting edge products mainly balancing machines for rotating components and process control for machine tools. Horizontal balancing machine R5-G-B-VS-TO, R2KG-VS, R1KB-VS, R650B-VS and R300G-VS for dynamic and static balance of rotor upto 5000Kg, 2000kg, 1000Kg, 650Kg and 300Kg respectively are some of the commercial products of this company. The balancing operation is electromechanical with properties of high accuracy, two plane balancing, high speed and modular. The balancing techniques are fully computerized, with varieties of drive systems, gearbox and variable speed motor.

Similarly, Blue Star Engineering and Electronics, Mumbai, India manufacture the vertical balancing machine which is used for balancing disc shaped rotors like fan blades, magnetos, impellers, spinning spindles, clutch plates, etc. The machine is provided with microprocessor based instrument panel for balancing in single and dual planes.

Technology for Energy Corporation (TEC-USA), having the branch company named ACES system provides balancing solution for different critical industries like material testing, nuclear power, electric power and aviation. This industry has the main working area in the field of vibration analysis, balancing, inlet guide vane adjustment, engine performance analysis and other dynamic structures. Similarly, SpectraQuest, Inc, USA has been working for the online training package for field and shop balancing. The company has been providing interactive training program, software, data acquisition hardware and accessories, diagnosis and training in Machine Vibration Analysis, Shaft/Coupling Alignment and Rotor Balancing.

Universal Balancing, UK has been manufacturing different balancing machines according to applications and type. Some balancer are e-rotor balancer, driveshaft

balancer, brake rotor balance, axle balancer, crankshaft balancer, transmission component balancer, pump balancer, aircraft wheel balancer, flywheel balancer, etc and according to type vertical, horizontal, static and dynamic balancer are some name. SchenckRoTec, Germany company is also actively involved in designing and manufacturing variety of balancing system. In spite of these, there are lots of company which are working in the field of balancing around the globe.

CHAPTER THREE: METHODOLOGY

The methodology is the main framework of any research study. Different task carried out for accomplishment of the study is clearly mentioned in the methodology. In-fact, it is the work flow-chart that display the information regarding the sequence or the order in which wok has been done. This research is also carried out in the sequence order. Initially started with research topic and objectives from the literature review ended with documentations and publications. Between literature reviews and the publication different activities has been done which can be seen in Figure 3.1 below.

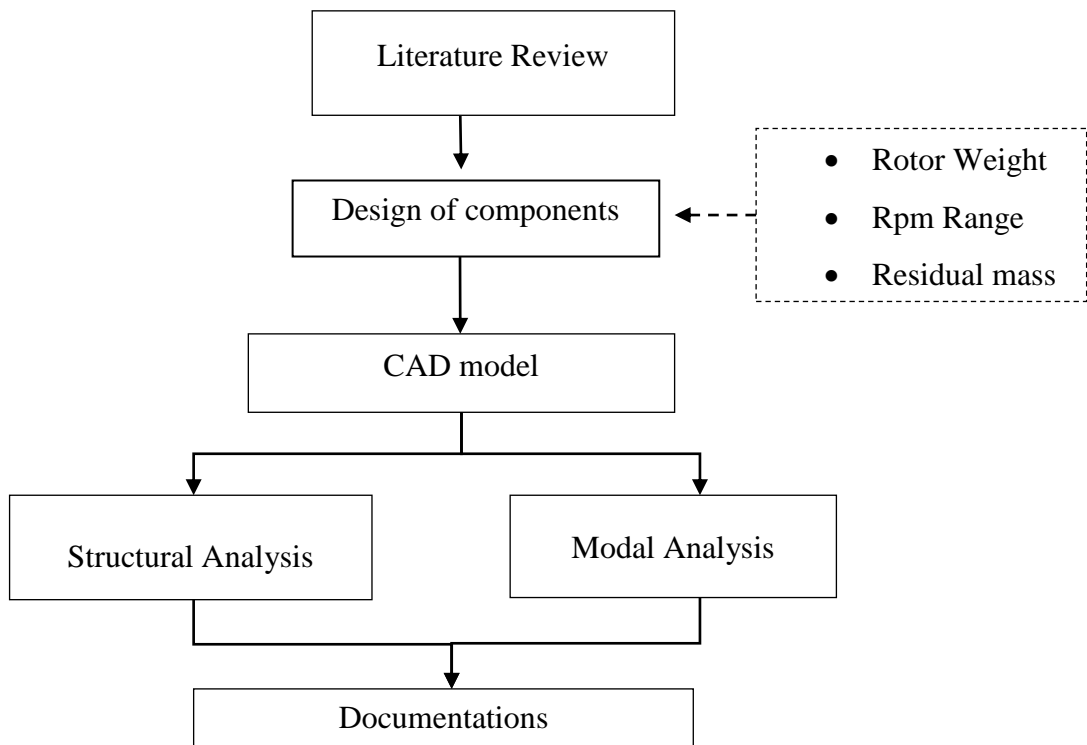


Figure 3.1 Methodology

For the confirmation of the topic of research study, literature review is the foremost step. The good literature review can help to select objectives of the study and guide to carry research efficiently and effectively. The procedure to be followed, task to be carried out, area to be focus on, previous research made, scopes on different, etc can easily be obtain from the references of the literature review.

For this study also different articles, journals, publications, books and other sources were consulted. Based on this the rotor balancing topic was finalized and the

objectives were set up. Different previous studies made on these topics were reviewed and the possible ways to give justice to the objectives for the successful completion of the study were identified. The procedures were laid down so that the sequence can be maintained. As, rotor balancing techniques is inseparable part of mechanical design, many articles related to it were available. The research documents which are closely related to our topic of interest and synchronizing with our objectives were shortlisted and reviewed for the guidance of this research to be carried out smoothly.

3.1 Design of Components

For any machinery system, the designing of system and components is the preliminary and the important task. Once the design is made ready, it is then analyzed using the simulations software to check the integrity and functioning of the system. After this process only, the system will go for manufacturing. The design of the components for rotor balancing system is explained in following sub topics.

3.1.1 Selection of Components

After the literature review the procedures to be followed for the research is laid down. The completion of the research study will not be enough unless the results are authentic and can be valid. For this purpose, it is essential to select different design and analysis parameter correctly and wisely. The random selection of the parameters leads to divergence in the final output that cannot be validated. Considering aforementioned things, various design parameters were selected and analysis data were identified from the literature review.

For this rotor balancing study, there were plenty of ways on the basis of which research can be proceed. Many research studies have been put forward previously with different design and the experimental models. In this research, the balancing procedure is carried out for the balance quality grade of rotor in constant (rigid) state from G2.5 to G40 as per ISO-1940-1 standard for the mechanical vibrations. Accordingly the design components like structural frame works, suspension system, motor, and rotor weight limitations, shaft diameter, length, component material along with design and analysis software were selected to accomplish the task with high accuracy.

3.1.2 CAD Model

After selecting the components, they are transformed into the CAD model using SolidWorks software. Suitable dimensions and the materials were assigned as per the literature review. Solidworks is a user friendly mechanical design automation software which is feature-based and provided with parametric solid modeling design tool(Portal, 1995).

- **Feature based:** Solidworks model is made up of number of individual constituent elements which are called features. The geometric features such as cuts, bosses, holes, ribs, fillets, chamfers and drafts applied to the work piece. The software provides the special window called feature manager design tree that shows the sequence in which features are used and the information related to it.
- **Parametric:** This features stores and captures different dimensions and relation used for the design. Along with the design intent, easy and quick modification of the model is possible.
- **Solid Modeling:** 3D CAD model or the solid model is the final outcome of the design in the Solidworks. It contains geometry features like wireframe and surface geometry necessary to fully describe the model.
- **Fully Associative:** The model is fully associated with the sketches, drawings or the assemblies from which it is design. Any changes in the reference part or drawing will automatically changes the model, i.e. it is reflected back.
- **Constraints:** Equations can be used to define the mathematical relationship between the parameters in the Solidworks along with the pre-defined constraint relationships like parallel, perpendicular, horizontal, vertical, coincident and concentric to mention some.
- **Design Intent:** It is the pre conceived idea of the designer about how the model will behave when it is changed. From the way the model is designed, it determines the relative change in the model. Some of the factors that contribute to design intent includes automatic relations, equations, added relations and dimensioning.

In this CAD model, the 2D sketch is made, then using the sketched features of Solidworks, the 3D model was generated as a part. Different parts are assembled

together with suitable mates and the constraints to get the model as our requirements. The Solidworks provides the information about the mass properties, material selection and appearance selection as per requirements. The software also entertains the simulation facilities for analysis.

3.1.3 Analytical Calculation

As the research is limited to the simulation aspect only, the CAD model is analysed using Finite Element Method(FEM) for structural and modal analysis in Ansys software. Finite Element Analysis(FEA) is one of the most popular analytical tool for structural dynamic analysis because of advancement in the numerical method and the rise in modern computing technology. FEA in fact is the simulation techniques to identify the possible workability of the structures or the component before actually manufacturing and testing is carried out. With the result from the FEA , optimizations for the improvement of the design is carried out. The numerical modelling is basically divided into three major categories viz. analysis, prediction and design to ease the process of analysis (Nazri & Sani, 2017).

3.2 FEM Analysis

In our study, finite element analysis is carried out in Solidworks and Ansys workbench consisting of structural and modal analysis. Ansys workbench is a user friendly platform among many other commercial simulation software with advanced engineering simulation technology (Chen & Liu, 2014). The workbench interference provides ease for product development and improving the productivity.

The general procedure for FEA includes following steps in general (Chen & Liu, 2014).

- Divide the CAD/geometric model into parts to create a “mesh” (mesh is the collection of elements and nodes)
- Describe the behavior of the physical quantities on each element
- Connect(assemble) the element at the nodes to form an approximate system of the equations for the entire model
- Apply loads and the boundary conditions
- Solve the system of the equations involving unknown quantities at the nodes
- Calculate the desired quantities at the elements or nodes

In the commercial simulation software, the aforementioned procedures are typically arranged into the following processes:

- Pre-processing: It includes building the FEM model, defining the element properties and applying the loads and the constraints as required
- FEA solver: It involves the assembling and solving the FEM system of equations and calculating the element results.
- Post-processing: In post processing the result are sorted as per the requirements and they are displayed.

Following different processes of analysis in Ansys workbench, the results for modal and structural analysis is obtained. For the modal analysis critical speed is main factor to be considered.

3.2.1 Geometry Design

The model for the rotor balancing system is designed in the Solidworks as per the convenience. The design file is saved with .stp file for compatible import to Ansys workbench.

After the generation of the model, the components which are not necessary for the analysis can be made suppress. The imported and generated model of suspension system and shaft is given in the Figure 3.2 and Figure 3.3 respectively.



Figure 3.2 Shaft and Suspension System



Figure 3.3 Meshing

3.2.2 Meshing

Meshing is one of the most important steps in performing an accurate simulation using FEA (Chen & Liu, 2014). A mesh is made up of elements which contain nodes (coordinate locations in space that can vary by element type) that represent the shape

of the geometry. Meshing is the process of turning irregular shapes into more recognizable volumes called elements.

There are two main types of meshing methods for 3D models. They are Tetrahedral element meshing or “tet” and Hexahedral element meshing or “hex”. Hex or “brick” elements generally result in more accurate results at lower element counts than tet elements. If it is a complex geometry, tet elements may be the best choice. These default or automatic meshing methods may be enough; however, there are additional methods that can give more mesh control. Hybrid meshing which is a hybrid of hex and tet elements that allows to mesh different parts of the geometry with different methods. This allows you to perform less geometry preparation and have more local control meshes. In this research, the default meshing is use which is programmed controlled. For the accuracy and the precision mesh sizing is used and as per the requirements the element size is defined for the analysis.

3.2.3 Setup/ FEA Solver

This is the main step in the analysis where the input and the governing equations are defined. Depending upon the type of analysis carried out, the FEA solver or setup will have different name, however the purpose will be the same. In the modal analysis, the set up provides the facilities of material selections, define the connection types, different boundary conditions as per the requirement and the governing principle for the analysis.

3.2.4 Solution/Post-processing

This is the final step in the analysis where the results are generated. Depending upon the requirement of the analysis, deformation, displacement, force reaction, strain, stress, etc. parameters are selected for the visualization and the display of the result. In this research study, structural and modal analysis of design components and system are carried out.

3.3 Dynamic Vibration

The oscillation of any system about its equilibrium is known as the vibration. The vibratory system comprises the means for storing potential energy (spring), kinetic energy (mass or inertia) and the means by which the energy is gradually dampens (damper). There is alternating transfer of energy between the potential and the kinetic

energy in between which some part of energy is dissipated to the surroundings(He & Fu, 2001).

Considering the vibration of the body, the natural frequency plays a significant role. Natural frequency is the frequency at which objects or system vibrate when it is subjected to an external load. Natural frequency is an important criterion in understanding and analyzing the rotor balancing system, so that any rotation or the imbalance in the system doesn't cause vibration in the regime of natural frequency.

$$\omega_n = \sqrt{\frac{K}{m}} \quad (3.1)$$

Equation (3.1) represents the general equation for natural frequency of a single degree of freedom where,

ω_n is the natural frequency of system

K is the Stiffness of the material

m is the mass of the system

For a system which is subjected to dynamic load, it undergoes vibration and the induced vibration if matches the natural frequency of the system. This will result in condition known as resonance where the vibration of the system is amplified. For a rotating body the speed of rotation at which resonance occurs is an important aspect in design consideration and the speed at which resonance occurs is known as the critical speed of the system. In case of rotor balancing system, which is made up of complex rotating mass system with multiple degree of freedom (MDOF) will have multiple critical speed for the resonance.

For any machine and system operating at high dynamic load region, it is necessary to avoid resonance. In rotor balancing system, effect of resonance can be reduced by operating the shaft-rotor at rotational speed below the critical speed or operating at speed which is higher than the critical speed. Campbell diagram can be used to plot these variables and predict the behavior in response to the operating loads. It can help in assessing the vibratory response of the balancing system and prediction of resonance. Natural frequencies are not avoidable and are inherent property of the system.

As seen in Equation (3.1), the ways to vary natural frequencies are:

1. Changing the mass of the system
2. Changing the stiffness of the system

A mass-spring- damper system can be used to understand the complexity of rotor balancing system where the shaft with rotor rotates at different frequency and the system has multiple degree of freedom. A two degree of freedom model can be used to understand the mode shapes occurring in the whole assembly.

For a 2 DOF system the equation of motion is:

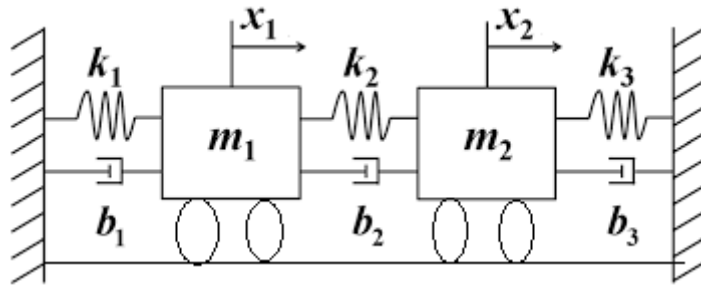


Figure 3.4 A simple 2 DOF spring-mass-damper system

In matrix form the equations can be represented as:

$$\begin{pmatrix} m_1 & 0 \\ 0 & m_2 \end{pmatrix} \begin{bmatrix} \ddot{x}_1 \\ \ddot{x}_2 \end{bmatrix} + \begin{bmatrix} b_1 + b_2 & b_2 \\ b_2 & b_2 + b_3 \end{bmatrix} \begin{bmatrix} \dot{x}_1 \\ \dot{x}_2 \end{bmatrix} + \begin{bmatrix} k_1 + k_2 & k_2 \\ k_2 & k_2 + k_3 \end{bmatrix} \begin{bmatrix} x_1 \\ x_2 \end{bmatrix} = \begin{bmatrix} f_1 \\ f_2 \end{bmatrix} \quad (3.2)$$

This equation can further be compacted to form

$$[M](\ddot{x}) + [B](\dot{x}) + K(x) = (f) \quad (3.3)$$

Where,

[M], [B] and [K] are mass, damping and stiffness matrices for the system. The matrices are square matrices of order $N \times N$ where N represents the number of degrees of freedom for the system.

3.3.1 Free Vibration

For a free vibration condition without damping the Equation (3.3) can further be simplified into

$$[M](\ddot{x}) + K(x) = 0 \quad (3.4)$$

The differential equation obtained can further be solved and solution obtained is

$$(x) = \{X\}e^{i\omega t} \quad (3.5)$$

Euler solution to the Equation (3.5) for real part gives us cosine function and the equation of motion can be formed as:

$$[-\omega^2[M] + [K]]\{X\}e^{i\omega t} = 0 \quad (3.6)$$

Since, $e^{i\omega t} \neq 0$

$$[-\omega^2[M] + [K]]\{X\} = 0 \quad (3.7)$$

This equation is forms the Eigen value problem which when solved by multiplying by $[M]^{-1}$ we get,

$$[[M]^{-1}[K] - \omega^2[M]^{-1}[M]]\{X\} = 0 \quad (3.8)$$

If we take $[M]^{-1}[K] = [A]$ and $\lambda = \omega^2$ the equation can be written as

$$[[A] - \lambda [I]]\{X\} = 0 \quad (3.9)$$

The solution of Equation (3.9) gives results in form of Eigen values that is $\omega_1^2, \omega_2^2, \omega_3^2, \dots \dots \omega_N^2$ where N is the corresponding value for number of degrees of freedom in the system. The Eigen values give the natural frequencies of the system and the values when substituted in the main equation give us Eigen vectors which represents mode shape of the system (Ritto et al., 2011). The mode shapes are numerically calculated in modern FEA software like Solidworks, ANSYS, LS-DYNA, and Abacus to name few.

3.3.1.1 Critical Speed

Critical speed is one of the important factors in studying vibration excitation in material. It is the angular speed of the rotating material which corresponds to natural frequency of the shaft or rotor and rotating shaft or rotor operating in the regime of critical speed undergo resonance effect leading to amplified vibration response. Determination of critical speed can help in understanding vibration response of rotor balancing system and can be done by plotting Campbell diagram.

Campbell diagram as shown Figure 3.5 consists of frequency of shaft vibration per cycles along the vertical axis and rotor speed in rpm along the horizontal axis. In addition to these radial lines are drawn in the graph which represents order of excitation. These lines represent the points along which the frequency of vibration of rotor is integral multiple of rotational speed. While there are inclined lines called

Engine Order lines (EO) which are to be considered for a vibration analysis and Campbell diagram is used to determine critical speeds.

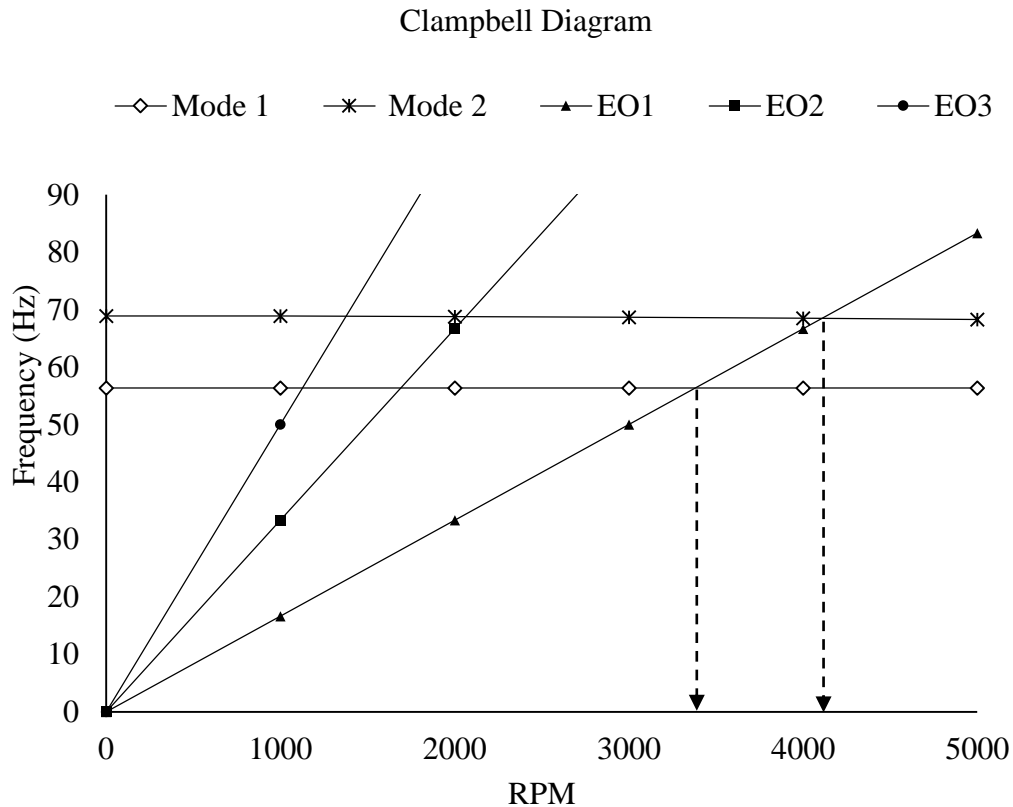


Figure 3.5 Campbell Diagram

First order excitation can be considered to be the source of all other order of vibrations, but it is important that the first order does not normally intersect the natural frequency line and contribute in resonance. Near horizontal lines labeled as mode represent the natural frequency lines and vary with rotational speed for different modes. This effect is represented by the given equation:

$$f^2 = f_0^2 + \beta N^2 \quad (3.10)$$

Here,

f = Natural frequency at rotational speed of N cycles per second

f_0 = Static natural frequency of shaft in cycles per second

β = Constant (depends on the physical shape and dimension)

N = Rotational speed of rotor in revolutions per second

The intersection between order lines and natural frequency lines gives us the critical speed and occurrence of resonance. The rotating shaft or rotor possess wide range of

critical speeds and possible resonance can be narrowed down by operating at high or low rotational speed.

3.3.1.2 Forward Whirl and Backward Whirl

Campbell diagram consists of modal values at each rpm plotted along the near horizontal lines known as mode. Each mode represents modal frequencies of the rotating shaft at various rotations and the mode number corresponds to the mode of frequency of vibration. These near horizontal looking lines can sometimes be seen to diverge or converge with change in rotational speed. The divergent and convergent lines represent forward and backward whirl in rotors and all practical rotors have these frequencies. BW (Backward Whirl) and FW (Forward Whirl) are conditions where the vibration of rotors is in opposite and same direction to that of the rotation of the shaft respectively. Corresponding frequencies of rotor swirl with engine order frequencies in both BW and FW indicate resonant frequency.

3.3.2 Forced Vibration

In the mechanical vibrating system, free response only gives the complementary solution to the homogeneous equation of motion. For the in-homogeneous equation in a forced linear lumped parameter SDOF system with constant coefficients and viscous damping, the equation of motion:

$$M\ddot{x}_d + C\dot{x}_d + Kx_d = f(t) \quad (3.11)$$

Figure 3.6 shows a basic rotating system with eccentric mass. This system can be rotating system (such as fan, disk drive, etc) with an imbalance in the distribution. The center of rotation of body does not coincide with the center of mass. M is the system total mass, m is the eccentric mass, ω is the operating frequency and e is the eccentricity. This system is supported by viscous dampers and linear springs. The equation of motion for this system is:

$$M\ddot{x} + C\dot{x} + Kx = me\omega^2 \sin(\omega t) \quad (3.12)$$

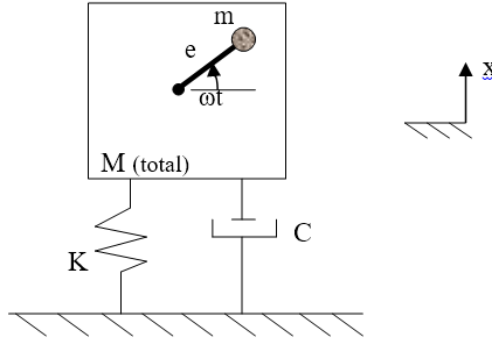


Figure 3.6 SDOF System with Rotating Unbalance

For the harmonic excitation (Bishop, 1958), frequency response function(FRF) is shown in Equation (3.13).

If $f(t) = me\omega^2 \sin(\omega t) = F_i \sin(\omega t)$, then $x_p(t) = X_p \sin(\omega t + \Phi_p)$ where,

$$H(j\omega) = \frac{X(j\omega)}{F(j\omega)} = \frac{1/K}{1 - \left(\frac{\omega}{\omega_n}\right)^2 + j2\zeta\left(\frac{\omega}{\omega_n}\right)} \text{ and} \quad (3.13)$$

$$\frac{MX_p}{me} = \frac{\left(\frac{\omega}{\omega_n}\right)^2}{\sqrt{\left[1 - \left(\frac{\omega}{\omega_n}\right)^2\right]^2 + \left[2\zeta\left(\frac{\omega}{\omega_n}\right)\right]^2}}$$

The Equation (3.13) is plotted in Figure 3.7.

Another important application for vibration analysis in rotating systems is whirling shafts as shown in Figure 3.8 . Both the shaft, which is assumed massless and bearings provide stiffness through restoring force to the disk when it rotates about the axis through point P. The axis through point O is a reference for the motion of points P and the disk center of mass, G. The distance OP is called the whirling amplitude and the rotational velocity of the line segment OP is the whirl velocity. Newton's method results the following:

$$M\ddot{x} + K_x x = Me\omega^2 \cos \omega t \quad (3.14)$$

$$M\ddot{y} + K_y y = Me\omega^2 \sin \omega t \quad (3.15)$$

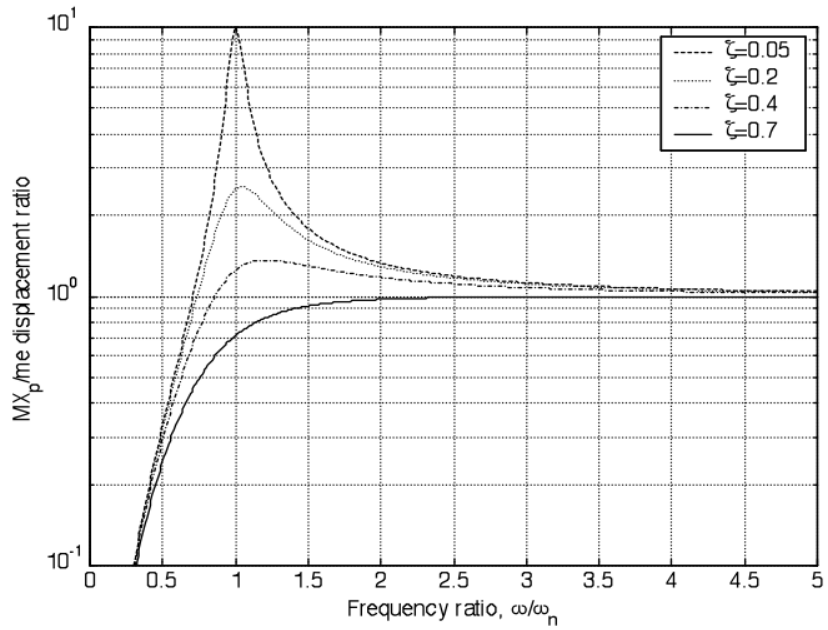


Figure 3.7 Amplitude of response due to Unbalance

The magnitudes and phases of the x and y responses in the steady-state can be shown to be governed by the following FRFs in Equation (3.16).

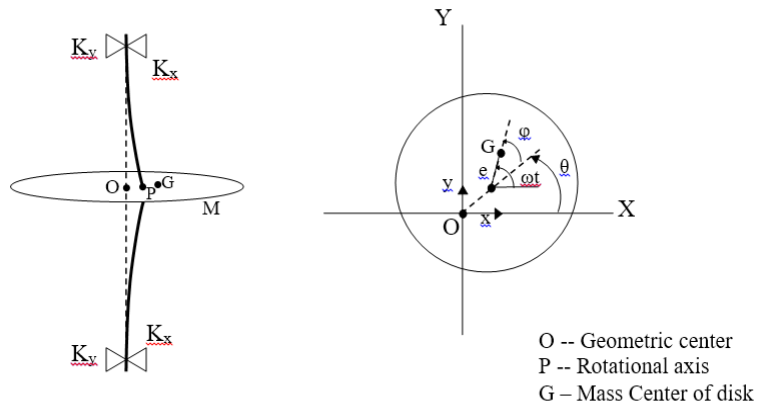


Figure 3.8 Shaft Whirl Geometry

$$\frac{X(j\omega)}{e} = \frac{\left(\frac{\omega}{\omega_{nx}}\right)^2}{1 - \left(\frac{\omega}{\omega_{nx}}\right)^2} \text{ and } \frac{Y(j\omega)}{e} = \frac{\left(\frac{\omega}{\omega_{ny}}\right)^2}{1 - \left(\frac{\omega}{\omega_{ny}}\right)^2} e^{-j\pi/2} \quad (3.16)$$

The whirl angle and speed are found as follows:

$$\theta = \tan^{-1} \frac{y}{x}, \quad \omega_{whirl} = \frac{d\theta}{dt} = \left(\sec^2 \frac{y}{x}\right) \left(\frac{\dot{y}x - \dot{x}y}{x^2}\right) \quad (3.17)$$

3.4 Balancing Algorithm

Balancing algorithm is the soul of rotor balancing system. Identifications of the unbalances to the balancing procedures are covered under this topic. Any disc or rotor is found to be vibrating or unbalance, it should undergo the balancing procedures as per balancing algorithm which is shown in Figure 3.9 and are described in following steps:

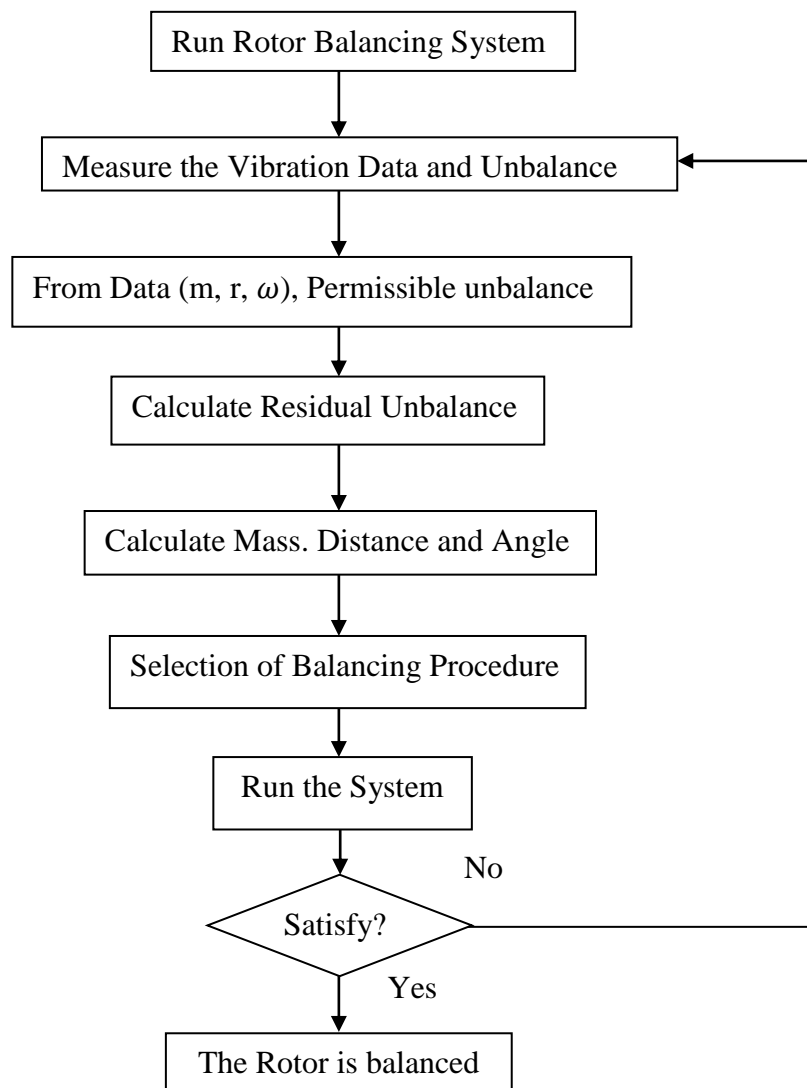


Figure 3.9 Rotor Balancing Flowchart

Unbalance Measurement: If any unbalances are found in the system, it is then checked in the rotor balancing system for finding the magnitude and geometry of

unbalances. The unbalances vary the centrifugal force of the system which is the converted in to the vibratory motion of the system.

Balancing: For the given components to balance with balance quality grade (International Standard Organization, 2003), from equation (2.3) the permissible unbalance U_{per} is calculated.

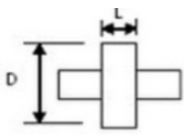
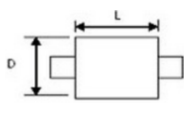
$$U_{per} = 1000 \frac{(e_{per} \cdot \Omega) \cdot m}{\Omega} \quad (3.18)$$

The centrifugal unbalance is given by:

$$F_{unbalance} = m r \omega^2 = U_{per} \times \omega^2 \quad (3.19)$$

From the vibration data residual unbalance is calculated which is then balance by using trial weight whether it is in single, double or multiple planes. The single planes and dual plane is decided by the L/D ratio and the speed of rotor which is shown in Table 3.1.

Table 3.1 Selection of Single and Dual Plane

Rotor	L/D ratio	Balance Correction	
		Single Plane	Dual Plane
	Less than 0.5	0-1000RPM	Above 1000RPM
	More than 0.5	0-500RPM	Above 500RPM

For the initial run, machine needs to be run-up to the operating speed. The velocity of vibration is detected. The velocity level and phase angle together give a vector that represents the rotor's original unbalance as shown in Figure 3.10. The vector's length equals the vibration amplitude, and the phase angle determines its direction.

A new vibration velocity level and a new phase angle are obtained as in Figure 3.11 whose values are represented by the resultant effect of the trial mass and the initial unbalance. Then, the procedure to determine the vector of unbalance is illustrated in Figure 3.12.

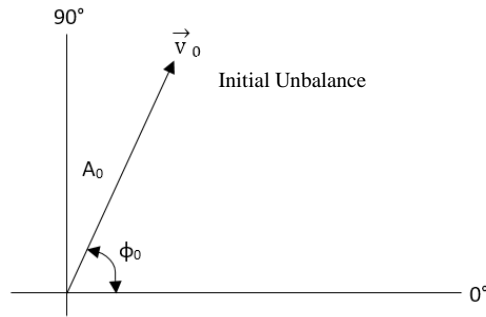


Figure 3.10 Initial Run

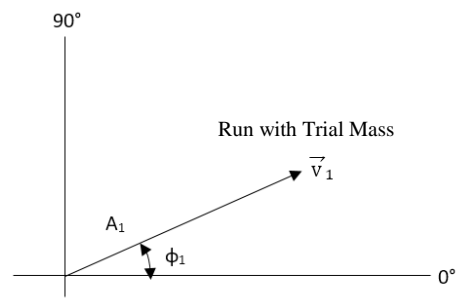


Figure 3.11 Run with Trial Mass

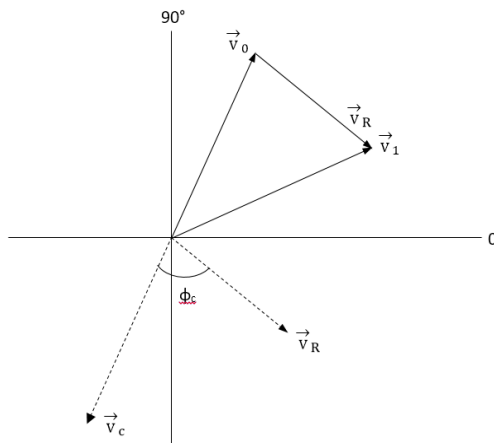


Figure 3.12 Determination of Vector of Unbalance

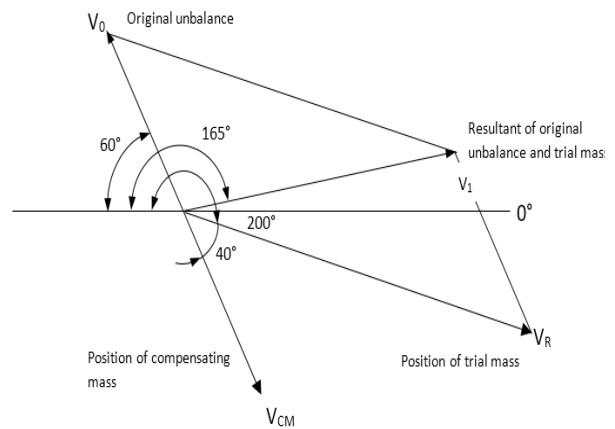


Figure 3.13 Determination of Compensating Mass Position

Where, \vec{V}_R denotes the effect of the trial mass alone and \vec{V}_C denotes the position and magnitude of the mass that is required to counteract the original unbalance. If the vibration's amplitude is assumed to be proportional to the unbalance mass, an expression that allow us to calculate the compensating mass value (M_{CM}) is obtained.

$$\frac{M_R}{\vec{V}_R} = \frac{M_{CM}}{\vec{V}_{CM}} = \frac{M_0}{\vec{V}_0} \quad (3.20)$$

$$M_{CM} = M_0 = \frac{\vec{V}_0}{\vec{V}_R} \times M_T \quad (3.21)$$

The vector diagram to determine the mass's position relative to the position of the trial mass is shown in Figure 3.13.

Balancing Iteration: After multiple trial runs, if the unbalance comes within the prescribed unbalance as per balance quality grade, then the system is said to be balanced. And if the vibration amplitude or unbalance still found above the permissible limit then the balancing process is repeated until the balancing is carried out.

3.5 Documentations

The rotor balancing machine is being studied in detail. The components and optimize designs of the system is considered for the analysis. The system which gives the output of better performance is concluded as comparatively best model for the prototype design and manufacture. After the analysis is carried out, the whole process is described in the report form. Further, the articles will be forwarded for the publication purposes to the science and engineering journals for the publications.

CHAPTER FOUR: DESIGN CALCULATIONS

4.1 Conceptual Design

The rotor balancing techniques is the process of finding out the mass distribution of the system. For the every rotor system there is specified limit of acceptable unbalance. The unbalance is basically caused by the fault in the design, manufacturing, assembly of parts and the material failure. The permissible limit of unbalance is defined in the ISO 1940-1. So, for the correction of the unbalance, it is essential to design, develop and test the rotor balancing measurement system. This study proposed the conceptual design for the balancing machine.

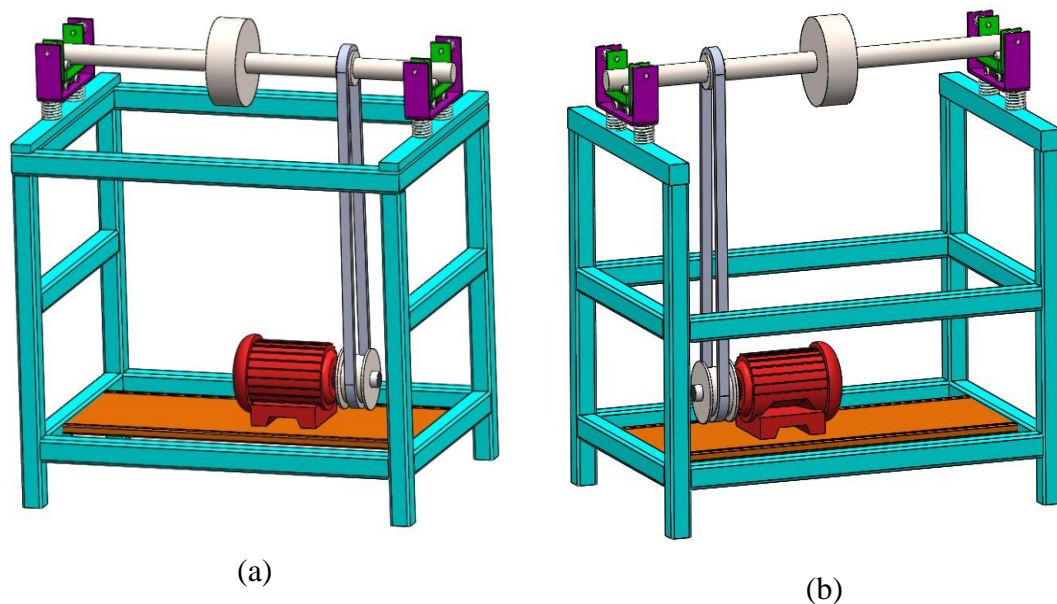


Figure 4.1 Conceptual Design for Rotor Balancing System

Two designs cases were considered for the research study as shown in (a) and (b) of Figure 4.1. The details of the components are given in APPENDIX G. Both the designs are almost similar in the designs and system components. Only the supporting machine bench configuration is different. The Figure (a) has the 4 square tubes in the top connected together to form strong top section. The load in the top section will be shared between the tubes and transferred to other vertical frames. The Figure (b) has the load directly transferred to the vertical frames and then to other frames. The Figure (b) type balancing system can be used for balancing the rotor with larger dimensions, however, the vertical frame in figure (b) may get displaced due to lack of

interconnecting frames at the top. So, from load sharing and aesthetic point of view, Figure (a) type design is considered for the further study.

4.1.1 Static Components

The machine bench and induction motor supports come under the static components. The machine bench structure holds the suspension system consisting the shaft and the rotor at the top where as it is firmly stand on the ground. At the bottom part of the machine bench consist of the platform to place the induction motor on it. The platform plate is also bonded with the main structure whereas the motor assembly is fixed on it. Primary function of the machine bench is to support the other structural member and provides the attachment point for each of other component in one way or other. The four legs of the machine bench are provided with the rubber harness at the bottom which dampens the vibrations and damage of the ends. Similarly, the induction motor base in also provided with the elastic support at the base, so any vibration induced from the induction motor will be transferred to the ground then to body and other components. The rectangular type machine bench is chosen so the structure will be more stable and prevent failure. (Salinger, 1964) laid down about different aspects of interaction between frames and the foundations. The loads and the vibrating behavior of the body will ultimately go to the ground. And the vibration and damping level depends upon the type of ground that is being used for the fixation of the machine bench. Regarding the motor supporting base, provided with the damper in the bottom to eliminate any induced vibration of the motor and the structural components. These structural components are made up of the material which can dampens the vibration level, grey cast iron is best option from structural and damping point of view.

4.1.2 Dynamic Components

Different dynamic components are present in the rotor balancing system that not only bear the loads but also transfer the motion. Induction motor, suspension system, belt transmission system, rotor-shaft and bearings are the main components under this topic.

Induction Motor: The induction motors operates in the principle of rotating magnetic field in which the stator creates the rotating magnetic field where the rotor rotates called as synchronous speed, N_s .

$$N_s = 120 \times \frac{F}{P} \text{ RPM} \quad (4.1)$$

Where, F is the frequency of supply

P is the number of poles

The rate of rotation of magnetic field generated by rotor depended upon the number of pole pairs per the phase of stator. The generated magnetic field rotates once per cycle of sine wave, i.e, 50 Hz power means that the field rotates at 50 rotation per second or 3000rpm. The power factor for high speed rotor is 90%, at $\frac{3}{4}$ of full load capacity, the largest high speed motors can have 92% power factor and for small low speed rotor its value can be as low as 50%. Similarly, large 3 phase induction motors are more efficient than smaller 3 phase one and other single phase motors. Large induction motor have common efficiency of 90% whereas at full load can be upto 95%. The 3 phase motors are self-starting such that the starters provide greater starting torque than required.

Suspension System

There are basically two types of supports for the shaft-rotor system one being hard other being soft support bearing (Salinger, 1964). The soft support bearing has the horizontal spring support of low stiffness having the free vibration period of one or two second and has higher vertical stiffness. The hard support bearing is comparatively stiff in horizontal direction and possess very high stiffness in vertical direction. The soft support compared to hard support bearing have larger signal to strength ratio for same level of unbalance measurement and the imbalance data can be taken with less sophisticated electronic equipment and such machines are simple in design and cheaper too. These kinds of machines are suited for balancing the rigid rotors like crankshafts, armatures, impellers, fan, drive shafts, etc. However, the hard support bearings are used in most of modern designs of supports like journal pedestals and the hard spring. The hard supports are provided with the advanced electronic equipment like displacement probes, capacitance sensors, inductance sensors, acceleration sensors, strain gauges, etc. that measure the unbalance signals precisely. The suspension system takes the loads and the displacement of shaft and rotor, the electronic sensors provided on it gives the indications of the unbalance. Moreover, the

suspension system materials and the stiffness of the spring also have vital importance for the vibration information.

Transmission System (Belt Type)

The power transmission system of belt either consists of belts with friction drive or the positive drive. The friction drive depends upon the frictional effect between the belt and the pulley and requires tension to maintain the sufficient friction where as positive drive relies on the teeth engagement on the belt and grooves of pulley. Flat belt is the main example of friction drive while V-belt relies upon the wedging action of the pulley. The modern flat belts eliminate the need for high tension in belt that lowers shaft and bearing loads. (Habasit, 2015) Efficiency of this belt is about 99% and 2.5-3% better than V belts. The flat belts have smaller cross section and work efficiently at higher rpm. Moreover the vibration of belt is an important factor for the selection and design point of view. The rpm of the belt is given by the following formula:

$$RPM\ of\ Belt = 3.14159 * \frac{Pulley\ Diameter}{Belt\ Length} \quad (4.2)$$

Velocity Ratio (VR) is given by:

$$VR = \frac{N1}{N2} = \frac{D1}{D2} \quad (4.3)$$

Where, N1 rpm of driving pulley

N2 rpm of driven pulley

D1 diameter of driving pulley

D2 diameter of driven pulley

The material selection of the belt system is important for the transmission of the power. (Ashby, 2011) gives the properties of the different materials. Kevlar, the composite thick fabric is used for heavy duty conveyor. Being bulky, temperature and impact resistant and comparatively higher modulus of elasticity value with durability makes Kevlar ideal material for the belt.

Shaft System

The rotating components of the machine that transmits power is called shaft. The shafts are made to transfer the torque and support the rotating parts like pulleys and

gears. As shaft takes the rotating load acted upon it, for high speed machinery, greater strength is essential. The shaft materials are made up of alloy steel such as Ni, Cr or Vanadium steels for high strength considerations. The shaft takes the rotation from the motor and the rotation is transferred to the rotor. During the rotation of shaft with rotor attached to it, shaft may undergo both torque and the bending moment. Maximum stress of this shaft is given in Equation(4.15) (R.K Bansal, 2014).

$$\tau_{max} = \frac{16}{\pi d^3} \sqrt{M_b^2 + M_t^2} \quad (4.4)$$

Where, M_t is torsional moment or torque

M_b is the bending moment

d is the diameter of shaft

τ is allowable shear strength

The critical speed of the shaft is also important parameter in the rotor dynamics, the speed is calculated by Equation (4.5)

$$\omega_c = \sqrt{\frac{k}{m}} = \sqrt{\frac{g}{\delta}} \quad (4.5)$$

Where,

K is the stiffness of shaft

m is the mass of shaft

δ is the static deflection of shaft

4.2 Equation of Motion

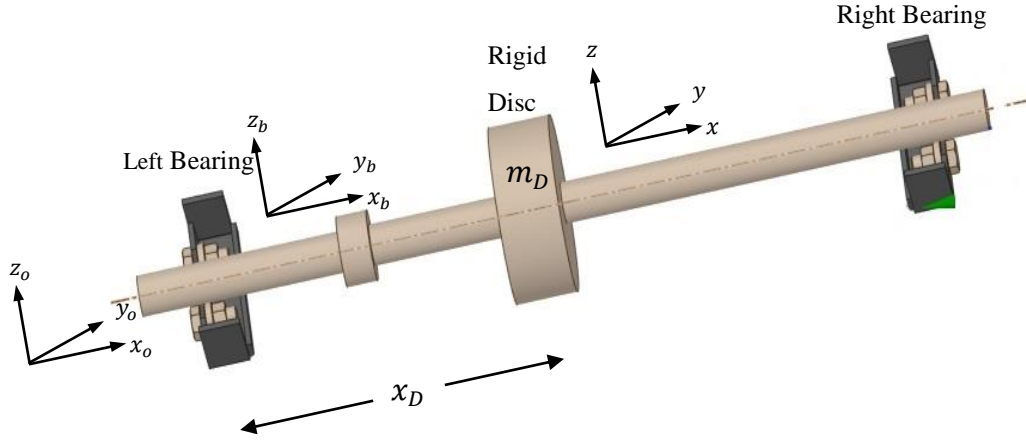


Figure 4.2 Shaft Rotor (Disc) System

The following coordinate systems are used to describe the motion of the rotor–shaft–bearing system in relation to the rigid, moving base (Das et al., 2010).

- (i) $X_0-Y_0-Z_0$: inertial reference frame.
- (ii) $X_b-Y_b-Z_b$: Located at left bearing and fixed to the moving base.
- (iii) $X-Y-Z$: Translating and rotating with the shaft and fixed at a generic location.

$(v(x), w(x))$ are the transverse deflection components of a generic point on the elastic line of the shaft owing to bending (w.r.t. frame $X_b-Y_b-Z_b$) and $v', -w'$ are the corresponding slopes, where the operator $(\cdot)'$ means the first partial derivative of the operand with respect to 'x'. $\bar{V}_a(x) \equiv [\dot{u}_a, \dot{v}_a, \dot{w}_a]^T$ is the absolute velocity of that point. $(\omega_x, \omega_y, \omega_z)$ are the absolute angular velocity components of the frame $X-Y-Z$. Ω , which is assumed to be constant, is the spin speed of the shaft about its own axis.

Equations of motion of the Rotor (disc)

The kinetic energy of a rigid disc is given by:

$$T_D = \frac{1}{2} m_D \left(\dot{v}_a^2(x_D) + \dot{w}_a^2(x_D) \right) + \frac{1}{2} (I_p \omega_x^2 + I_d \omega_y^2 + I_d \omega_z^2) \quad (4.6)$$

Where,

m_D, I_d, I_p are the mass, transverse mass-moment inertia and polar mass-moment inertia respectively of the Rotor(disc) present at a distance x_D from the left bearing.

$$\begin{aligned}
T_D = & \frac{1}{2}m_D(\dot{v}^2 + \dot{w}^2) + \frac{1}{2}I_D(\dot{v}'^2 + \dot{w}'^2) + \dot{\alpha}_b m_D(v\dot{w} - w\dot{v}) \\
& + \dot{\alpha}_b I_d(\dot{v}'w' - \dot{w}'v') - (\Omega + \dot{\alpha}_b)I_p \dot{v}'w' + \frac{1}{2}\dot{\alpha}_b^2 m_D(v^2 + w^2) \\
& + \frac{1}{2}\dot{\gamma}_b^2 m_D v^2 + \frac{1}{2}\dot{\beta}_b^2 m_D w^2 + \frac{1}{2}\dot{\alpha}_b^2 I_d(w'^2 + v'^2) \\
& + \frac{1}{2}\dot{\gamma}_b^2 I_p w'^2 + \frac{1}{2}\dot{\beta}_b^2 I_p v'^2 \\
& + m_D x_D(\dot{\gamma}_b \dot{v} - \dot{\beta}_b \dot{w} - \dot{\alpha}_b \dot{\beta}_b v - \dot{\alpha}_b \dot{\gamma}_b w + p_5) \\
& + m_D(p_1 \dot{v} + p_2 \dot{w} + p_3 v + p_4 w - \dot{\beta}_b \dot{\gamma}_b v w + p_6) \\
& + I_d(\dot{\gamma}_b \dot{v}' + \dot{\beta}_b \dot{w}' - \dot{\alpha}_b \dot{\beta}_b v' - \dot{\alpha}_b \dot{\gamma}_b w' + \dot{\beta}_b \dot{\gamma}_b v' w') \\
& + I_p((\dot{\alpha}_b + \Omega)(\dot{\beta}_b v' - \dot{\gamma}_b w') - \dot{\beta}_b \dot{\gamma}_b v' w') \\
& + \frac{1}{2}(m_D x_D^2 + I_d)(\dot{\beta}_b^2 + \dot{\gamma}_b^2) + \frac{1}{2}I_p(\Omega + \dot{\alpha}_b)^2
\end{aligned} \tag{4.7}$$

$$\begin{aligned}
p_1 = & \dot{y}_b + \dot{\gamma}_b x_b - \dot{\alpha}_b z_b; \\
p_2 = & \dot{z}_b + \dot{\alpha}_b y_b - \dot{\beta}_b x_b; \\
p_3 = & \dot{\alpha}_b p_2 - \dot{\gamma}_b(\dot{x}_b - \dot{\gamma}_b y_b + \dot{\beta}_b z_b); \\
p_4 = & \dot{\beta}_b(\dot{x}_b - \dot{\gamma}_b y_b + \dot{\beta}_b z_b) - \dot{\alpha}_b p_1; \\
p_5 = & \dot{\gamma}_b \dot{y}_b - \dot{\beta}_b \dot{z}_b + \dot{\beta}_b^2 x_b + \dot{\gamma}_b^2 x_b - \dot{\alpha}_b \dot{\beta}_b y_b - \dot{\alpha}_b \dot{\gamma}_b z_b; \\
p_6 = & \dot{x}_b^2 + \dot{y}_b^2 + \dot{z}_b^2 + \dot{\alpha}_b^2(y_b^2 + z_b^2) + \dot{\beta}_b^2(x_b^2 + z_b^2) + \dot{\gamma}_b^2(x_b^2 + y_b^2) \\
& + 2\dot{\alpha}_b(y_b \dot{z}_b - \dot{y}_b z_b) + 2\dot{\beta}_b(\dot{x}_b z_b - x_b \dot{z}_b) \\
& + 2\dot{\gamma}_b(x_b \dot{y}_b - \dot{x}_b y_b) - 2(\dot{\alpha}_b \dot{\beta}_b x_b y_b + \dot{\alpha}_b \dot{\gamma}_b x_b z_b \\
& + \dot{\beta}_b \dot{\gamma}_b y_b z_b)
\end{aligned} \tag{4.8}$$

From Lagrange's principle, the equations of motion for a disc are obtained as follows:

$$\begin{aligned}
& [M]_D \{\ddot{q}\}_D - (\Omega + \dot{\alpha}_b)[G]_D \{\dot{q}\}_D + 2\dot{\alpha}_b [C]_D \{\dot{q}\}_D + \ddot{\alpha}_b([C]_D - [H]_D)\{q\}_D \\
& - \left(\dot{\alpha}_b^2 [M]_D + \dot{\gamma}_b^2 [K_{p11}]_D + \dot{\beta}_b^2 [K_{p22}]_D - 2\dot{\beta}_b \dot{\gamma}_b [K_{p12}]_D \right) \{q\}_D \\
= & -(\dot{\gamma}_b + \dot{\alpha}_b \dot{\beta}_b) \{S_{2y}\}_D + (\ddot{\beta}_b - \dot{\alpha}_b \dot{\gamma}_b) \{S_{2p}\}_D \\
& - (\Omega + \dot{\alpha}_b) \left(\dot{\gamma}_b \{S_{1p}\}_D - \dot{\beta}_b \{S_{1y}\}_D \right) - (\dot{p}_1 - p_3) \{S_1\}_D \\
& - (\dot{p}_2 - p_4) \{S_2\}_D + \{Q\}_D
\end{aligned} \tag{4.9}$$

In the Equation (4.9), for the rotor (disc) node (subscript 'D'), the nodal displacement vector is defined by

$$\{q\}_D = [v, w, -w', v']_D^T. \quad (4.10)$$

Equations of motion of a shaft finite element

$$\{q\}_S^e = [v_1, w_1, -w'_1, v'_1, v_2, w_2, -w'_2, v'_2]^T. \quad (4.11)$$

Within the element, the interpolation of the relative transverse displacement components of a point on the shaft elastic line can be done as

$$\begin{Bmatrix} v(x) \\ w(x) \end{Bmatrix} = [\psi\{x\}]^2 \{q\}_S^e. \quad (4.12)$$

The kinetic energy of a differential section of a shaft element of length dx can be calculated as follows:

$$dT_S^e = \frac{1}{2} m (\dot{v}_a^2(x) + \dot{w}_a^2(x)) dx + \frac{1}{2} (i_p \omega_x^2 + i_d \omega_y^2 + i_p \omega_z^2) dx. \quad (4.13)$$

In the Equation (4.13), m , i_d , i_p are the mass, transverse mass moment of inertia, and polar mass moment of inertia per unit length of the shaft element, respectively. The expression of the kinetic energy for an element is determined by substituting different translational and rotational velocities components, neglecting the terms of the higher order and integrating Equation (4.13) over the length of an element (l).

$$\begin{aligned} T_S^e = & \frac{1}{2} \int_0^l [m(\dot{v}^2 + \dot{w}^2) + i_d(\dot{v}'^2 + \dot{w}'^2)] dx + \alpha_b \int_0^l [m(v\dot{w} - w\dot{v}) \\ & + i_d(v'\dot{w}' - w'\dot{v}')] dx - (\Omega + \dot{\alpha}_b) \int_0^l i_p \dot{v}' w' dx + \frac{1}{2} \\ & \times \int_0^l m [\dot{\alpha}_b^2 (v^2 + w^2) + \dot{\gamma}_b^2 v^2 + \dot{\beta}_b^2 w^2] dx \\ & + \frac{1}{2} \int_0^l [i_d \dot{\alpha}_b^2 (v'^2 + w'^2) + i_p (\dot{\gamma}_b^2 v'^2 + \dot{\beta}_b^2 w'^2)] dx \\ & + \int_0^l [mx(\dot{\gamma}_b \dot{v} - \dot{\beta}_b \dot{w} - \dot{\alpha}_b \dot{\beta}_b v - \dot{\alpha}_b \dot{\gamma}_b w) \\ & + m(p_1 \dot{v} + p_2 \dot{w} + p_3 v + p_4 w - \dot{\beta}_b \dot{\gamma}_b v w)] dx \\ & + \int [i_d (\dot{\gamma}_b \dot{v}' + \dot{\beta}_b \dot{w}' - \dot{\alpha}_b \dot{\beta}_b v' - \dot{\alpha}_b \dot{\gamma}_b w' + \dot{\beta}_b \dot{\gamma}_b v' w')] \\ & + i_p ((\dot{\alpha}_b + \Omega)(\dot{\beta}_b v' - \dot{\gamma}_b w') - \dot{\beta}_b \dot{\gamma}_b v' w')] dx + \frac{1}{2} \\ & \times \int_0^l [mxp_5 + mp_6 + (mx^2 + i_d)(\dot{\beta}_b^2 + \dot{\gamma}_b^2) \\ & + i_p (\Omega + \dot{\alpha}_b)^2] dx. \end{aligned} \quad (4.14)$$

For the shaft element, the strain energy (V_S^e) due to bending and the Rayleigh dissipation function (D_S^e) due to viscous form of internal material damping are written as

$$(V_S^e) = \frac{1}{2} \int_0^l (EI) \begin{Bmatrix} -w'' \\ v'' \end{Bmatrix}^T \begin{Bmatrix} -w'' \\ v'' \end{Bmatrix} dx, \quad (4.15)$$

$$(D_S^e) = \frac{1}{2} \eta_v \int_0^l (EI) \begin{Bmatrix} -\dot{w}'' + \Omega v'' \\ \dot{v}'' + \Omega w'' \end{Bmatrix}^T \begin{Bmatrix} -\dot{w}'' + \Omega v'' \\ \dot{v}'' + \Omega w'' \end{Bmatrix} dx. \quad (4.16)$$

In the expressions above, E is the shaft material's Young's modulus; I is the area-moment of inertia of the shaft cross-section about the neutral axis and η_v is the coefficient of the viscous form of internal damping. From Lagrange's principle, equations of motion for the shaft finite element are obtained by using finite element interpolation functions and expressions of kinetic energy, strain energy, and dissipation functions.

$$\begin{aligned} & [M]_S^e \{\ddot{q}\}_S - (\Omega + \dot{\alpha}_b) [G]_S^e \{\dot{q}\}_S + 2\dot{\alpha}_b [C]_S^e \{q\}_S + \eta_v [K_B]_S^e \{\dot{q}\}_S \\ & \quad + \dot{\alpha}_b ([C]_S^e - [H]_S^e) \{q\}_S + ([K_B]_S^e + \eta_v \Omega [K_C]_S^e) \{q\}_S \\ & \quad - \left(\dot{\alpha}_b^2 [M]_S^e + \dot{\gamma}_b^2 [K_{p11}]_S^e + \dot{\beta}_b^2 [K_{p22}]_S^e - 2\dot{\beta}_b \dot{\gamma}_b [K_{p12}]_S^e \right) \{q\}_S \\ & = -(\dot{\gamma}_b + \dot{\alpha}_b \dot{\beta}_b) \{S_{2y}\}_S^e + (\dot{\beta}_b - \dot{\alpha}_b \dot{\gamma}_b) \{S_{2p}\}_S^e \\ & \quad - (\Omega + \dot{\alpha}_b) \left(\dot{\gamma}_b \{S_{1p}\}_S^e - \dot{\beta}_b \{S_{1y}\}_S^e \right) - (\dot{p}_1 - p_3) \{S_1\}_S^e \\ & \quad - (\dot{p}_2 - p_4) \{S_2\}_S^e + \{Q\}_S^e. \end{aligned} \quad (4.17)$$

Equations of motion for concentrated mass unbalance associated with a disc

A disc's mass unbalance is represented as a concentrated mass m_u at a location with eccentricity 'e'. The unbalanced mass kinetic energy of is written as:

$$T_u = \frac{1}{2} m_u e \{ \bar{V}_a^u \cdot \bar{V}_a^u \}. \quad (4.18)$$

The components of the unbalance mass absolute velocity \bar{V}_a^u are given below:

$$\bar{V}_a^u = \begin{Bmatrix} \dot{x}_b + \dot{\beta}_b (z_b + w + e \sin(\Omega t)) - \dot{\gamma}_b (y_b + v + e \cos(\Omega t)) \\ \dot{y}_b + \dot{\gamma}_b (x + x_b) - \dot{\alpha}_b (z_b + w + e \sin(\Omega t) + \dot{v} - \Omega e \sin(\Omega t)) \\ \dot{z}_b - \dot{\beta}_b (x + x_b) + \dot{\alpha}_b (y_b + v + e \cos(\Omega t) + \dot{w} + \Omega e \cos(\Omega t)) \end{Bmatrix} \quad (4.19)$$

From Lagrange's principle, the equations of motion of the unbalance mass are obtained by substituting the expression of \bar{V}_a^u in Equation (4.18).

$$\begin{aligned}
& -m_u e^{\left[\{(\Omega + \dot{\alpha}_b)^2 + \dot{\gamma}_b^2\} \cos(\Omega t + \gamma) + (\ddot{\alpha}_b - \dot{\beta}_b \dot{\gamma}_b) \sin(\Omega t + \gamma) \right]} = 0, \\
& -m_u e^{\left[\{(\Omega + \dot{\alpha}_b)^2 + \dot{\beta}_b^2\} \sin(\Omega t + \gamma) - (\ddot{\alpha}_b + \dot{\beta}_b \dot{\gamma}_b) \cos(\Omega t + \gamma) \right]} = 0. \quad (4.20)
\end{aligned}$$

Where, γ is the initial phase angle of the unbalance.

4.3 Machine Components Design

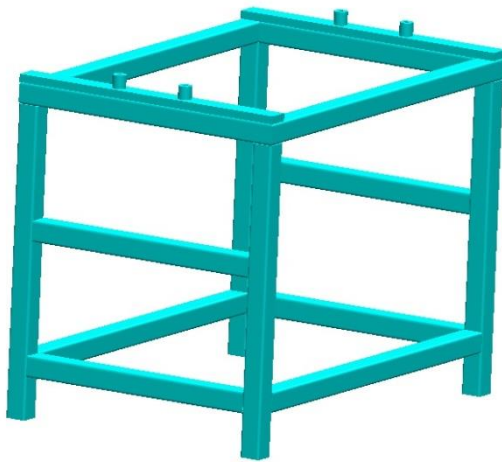
The designing of the balancing system consists of different essential components. These components form the inseparable part of the balancing system. If any of the rotor balancing system components undergo damage or malfunction, the whole system will be faulty and the machine need to be changed. Following components are incorporated in the system:

4.3.1 Machine Bench

The machine bench is made up of 14 square tube of the grey cast iron each tube having dimensions $80 \times 80 \times 5 \text{mm}^3$. These square tubes are bonded together to form the structure with high strength. The hollow tube makes the structure light in weight so that it is easier to move and transport. Any vibration induced in the shaft due to unbalance weight is transferred to the suspension system then to the machine bench to ground. After the complete connection of all the members of machine bench the height of structure becomes 1.27m where 1.58m*1.08m becomes length and breadth respectively. The details about the machine bench are shown in Table 4.1.

The structure is made up of grey cast iron. Gray iron is not as ductile as other forms of cast iron and its tensile strength is also lower. However, it has a damping capacity that is 20–25 times higher than steel and superior to all other cast irons, easier to machine and wear resistance property make grey cast iron best material for machine bench.

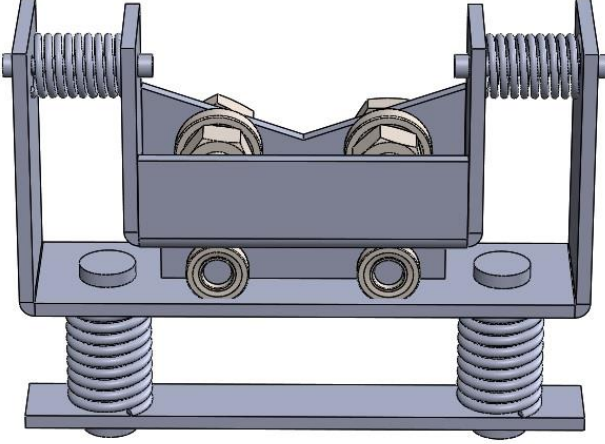
Table 4.1 Design Characteristics of Machine Bench

 <p>Figure 4.3 Machine Bench</p>	Charateristics	Value
	Materials	Grey Cast Iron
	Square Tube	14 Number
	Each Tube Dimension	80×80×5mm ³
	Length	1.58m
	Breadth	1.08m
	Height	1.27m

4.3.2 Suspension System

The suspension system is the main component where the balance and unbalance of the rotor system is identified. The system consists of the rotating shaft which rest upon the bearings. Roller bearings are used as these kinds of bearings are used in the all shaft applications to support pure axial load. These bearings are connected to small bracket which has the roller at the bottom and connected by spring with larger bracket. The larger bracket rest upon the machine bench with the spring. In the suspension system Figure 4.4, it can be seen, supporting shaft and rotor with three degrees of freedom: horizontal, vertical and pendulum in the axial direction. The characteristic of this system is that it can isolate or at least reduce the external vibrations phenomena.

Table 4.2 Design Characteristics of Suspension System

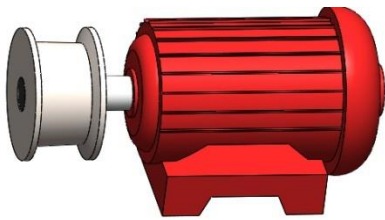
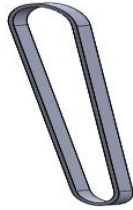
 <p>Figure 4.4 Suspension System</p>	Characteristics	Value
	Quantity	2
	Distance between	1.4m
	Dimensions	0.38mx0.07m
	Material	Grey Cast Iron
	Bearing Type	Hard Support Roller Bearing
	Spring Stiffness	1000N/mm

4.3.3 Transmission System

6hp 3phase AC induction motor is used for this study. These kinds of motor are capable of rotating at 1500-6000 rpm and are heavy duty motor. This induction motor is self-starting, reliable and economical, and doesn't have brushes and slip rings so the maintenance cost is less. Carbon brushes and slip rings are sources of error and noise due to spark and other friction effects. Due to lack of slip rings and the carbon brushes the noise will be less and the motor is environmental friendly.

The torque generated by the motor is transmitted to the shaft by the flat belt system. Belt transmission is more flexible, quieter, doesn't require any lubrication, don't require parallel shaft, the clutch action can be activated by release of the belt and also provide protection against overload and obstruction.

Table 4.3 Transmission System Design Characteristics

 <p>Figure 4.5 Induction Motor</p>		 <p>Figure 4.6 Flat Belt</p>	
Characteristics	Value	Characteristics	Value
Motor Type	AC induction 3 phase 6Hp	Dimensions	Length 2.34m, Thickness 2mm Width 4mm
RPM	1500-6000, 50-100Hz	Materials	Kevlar

4.3.4 Shaft and Rotor System

The shaft is chosen as per the ISO 1940-1 standard with pre assigned permissible unbalance. The shaft is made of Alloy Steel providing high index of strength, high level of machine ability and have wear resistant properties. The rotor/disc to be balanced is placed in the shaft. For the study cast iron is chosen as the study material. The design characteristics of shaft and rotor is shown in Table 4.4.

Table 4.4 Design Characteristics of Shaft and Rotor

Shaft Parameter		Rotor Parameter	
Characteristics	Value	Characteristics	Value
Length	1.68m	Length	12cm
Diameter	7cm	Inner/Outer Dia	7cm/30cm
Material	Alloy Steel	Materials	Cast Iron

4.4 Safety and Aesthetic

The rotor balancing system consists of high speed rotating component, electrical and electronic components and other structural assemblies. So care should be taken while handling and operating the system.

Following safety precautions can be taken:

- This machinery system is to balance, the unbalance system which are at some vibration level. If the vibration amplitudes are already high then those system may damage the balancing system instead. These kinds of unbalance rotor or disc shouldn't be brought for balancing.
- The response of the system isn't always linear and predictable, so addition of some trial weight instead may result in high vibration and displacement. The trial weight should be added after proper study only.
- Only limited and operator should be near the balancing system and the vibration sensor with the long cable should be used to avoid long exposure to the system.
- The device should be operated in no wind condition.
- Never take the vibration data of the pump, compressor, etc where the fluid is leaking
- Never operate the machine with the mechanical faults, in case of any fault stop the operation and find the escape.
- Electric wiring and cables should be properly insulated.
- Before operation of the machine, each and every components should be checked thoroughly and in case of possible fire, fire extinguisher should be made ready all the time.

Not only safety, the aesthetic aspect also plays determining role for the design of the system. The aesthetic component includes following considerations like shape of components, color, size, weight, purpose, surface finish and material, Tolerance, Noise, etc. The modular components are easier to work with and maintain for any problems, instead of single structure, the balancing system is designed with different components assembled together. Depending upon the application of machine, size and weight should be suitable with good surface finish. For different components different types of materials are selected such that it sustains the failures. The noise of the motor and the vibrating components can be reduce by addition of harness and damper between the mounting parts and operate the machines such that it won't resonant. Moreover, the dynamic components should be well lubricated and the color of the assembly should be appealing such that any structural damaged can easily be identified.

CHAPTER FIVE: RESULTS AND DISCUSSIONS

This chapter covers the actual task and the analysis done for the research. Each and every step followed for the research is explained in detail. First the model is designed in Solidworks CAD designing software. In the Ansys the geometry is imported. With the suitable element size, the meshing is carried out. If the number of elements and nodes are found satisfactory further processing of the analysis is done. Suitable boundary conditions are assigned to the model and governing effects are selected. Hence, the solution is generated, if the results are not within the satisfactory limits, then modifications in the geometry or boundary conditions or governing equations are carried out.

5.1 Machine Specifications

The major machine design characteristics of rotor balancing system are shown in Table 5.1.

Table 5.1 Design Characteristics of Rotor Balancing System

Design Characteristics	Value
Dimensions	1.68mx1.08mx1.61m
Materials	Structure: Grey Cast Iron, Shaft: Alloy Steel
Bearings	Hard support Roller type
Motor Type	6Hp 3Phase Ac induction, 1500-6000 RPM
Operating Shaft RPM	3000 RPM
Belt Type	Flat Belt, Kevlar material
Shaft Dimension	1.68m length and 7cm Diameter
Balance Quality Grade	G2.5 to G40

5.2 Dynamic Analysis

Rotor balancing system comprises of different components. Some of the components are static whereas some are dynamic. Motor, Pulley, Belt, Shaft and Rotor, Bearings and Suspension system undergo the some displacement over the period of time whereas machine bench takes the structural load of the system. The structural and modal analysis of these components will studied in detail in following sub topics.

5.2.1 Analysis of Shaft

The shaft and machine components in contact with the shaft form the basic balancing system. The torque of the induction motor is delivered for the rotation of the shaft through the pulley attached with the shaft. The shaft is simply supported at the two ends with the bearing. Any imbalance or the vibratory motion of the shaft is transferred to the bearings. The rotor to be balanced is also placed in the shaft which rotates along with the shaft. The simple free body force diagram of the balancing system is shown in Figure 5.1.

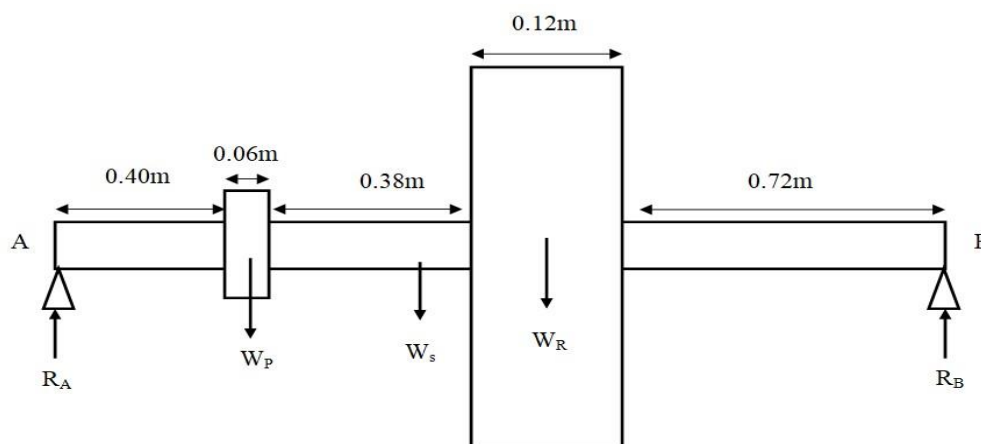


Figure 5.1 Rotor Balance System Free Body Diagram

From the Equation of weight balance given by Newton's Law,

$$R_A + R_B = W_R + W_S + W_P \quad (5.1)$$

Where,

R_A and R_B are the two reaction forces at the two end supports A and B respectively,

W_R is the weight of the Rotor

W_S is the weight of the Shaft

W_P is the weight of the Pulley

From the law of equilibrium,

$$R_A \times 1.68 = W_R \times 0.78 + W_P \times 1.25 + W_S \times 0.84$$

$$R_A \times 1.68 = 608 \times 0.78 + 32 \times 1.25 + 490 \times 0.84 \quad (5.2)$$

$$R_A = 539\text{N}$$

Similarly,

The Reaction at the support B i.e, R_B is calculated by:

$$R_A + R_B = W_R + W_S + W_P$$

$$539 + R_B = 608 + 490 + 32 \quad (5.3)$$

$$R_B = 591 \text{ N}$$

As per the design in the Solidworks software, the material selections and the design parameter, the Table 5.2 shown below shows the forces acting on the system.

Table 5.2 Different Forces Acting on Shaft

Data Characteristics	Notation	Weight(N)
Rotor	W_R	608
Shaft	W_S	490
Pulley	W_P	32
Reaction Force R_A	R_A	539
Reaction Force R_B	R_B	591
Suspension System	W_{Ss}	64
Unbalanced Force	W_u	60

The research is targeted for the balance quality grade of rotor in constant (rigid) state from G2.5 to G40. The rotational speed of most of the components in this grade ranges from 2000-4000rpm. Accordingly, for this research, the rotational speed of shaft-rotor is taken to be 3000rpm which correspond to 50Hz frequency. The permissible residual specific unbalance, e_{per} gm.mm/kg for quality grade G40 at speed 3000rpm is 150 from the Figure 2.3. 60N of arbitrary weight is taken as unbalance weight for the rotor. The shaft is analyzed for possible resonances and the stresses in the following subtopics.

Table 5.3 Results of Modal Analysis of Shaft

Modes	Mode 1	Mode 2	Mode 3	Mode 4	Mode 5	1st EO	2nd EO	3rd EO
Critical Speed	2503.9 rpm	3040. rpm						
RPM	Mode 1	Mode 2	Mode 3	Mode 4	Mode 5	1st EO	2nd EO	3rd EO
0	83.46	101.33	258.25	298.92	586.16	0.00	0.00	0.00
1000	83.46	101.33	258.25	298.92	586.16	16.67	33.33	50.00
2000	83.46	101.33	258.25	298.92	586.16	33.33	66.67	100.00
3000	83.46	101.33	258.25	298.92	586.16	50.00	100.00	150.00
4000	83.46	101.33	258.25	298.92	586.16	66.67	133.33	200.00
5000	83.46	101.33	258.25	298.92	586.16	83.33	166.67	250.00

For the shaft and pulley without rotor, the critical speed isn't present for the first Engine Order (EO) line. However, the critical speeds are for the first EO line will be present for higher rpm only which isn't applicable in our case. The possibility of resonance is at rpm greater than 5000 which is out of scope of this study as shown in Figure 5.2.

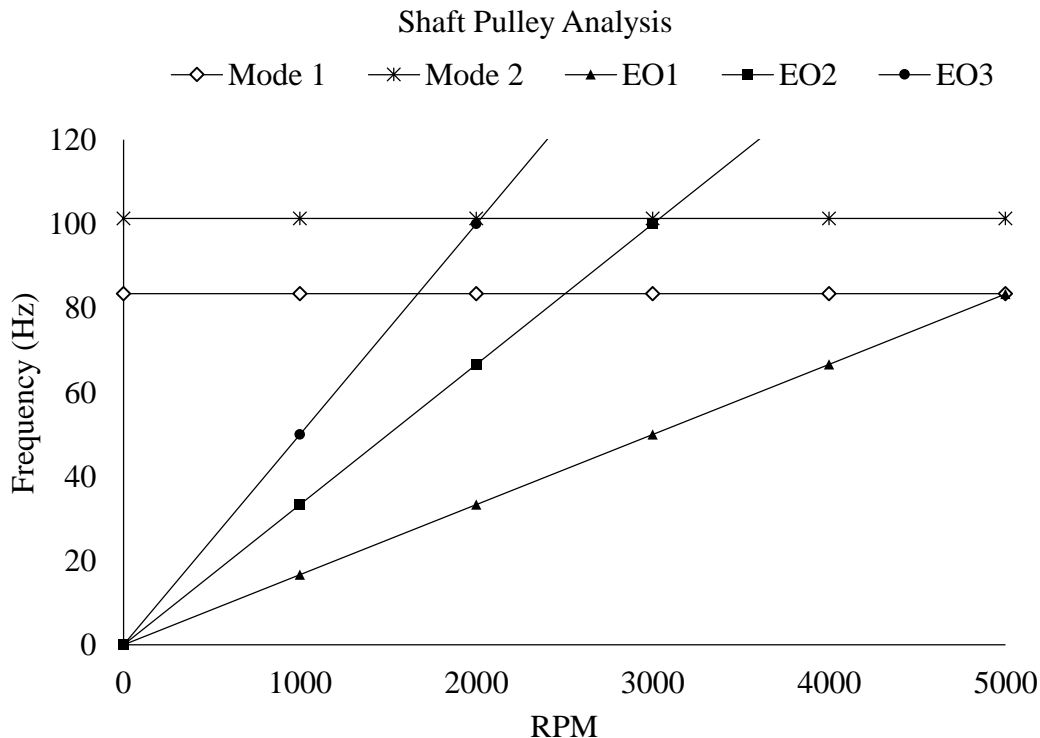


Figure 5.2 Clampbell Diagram for Shaft-Pulley Analysis

It can be noted that critical speeds at 2503.9 rpm and 3040 rpm which corresponds to 83.46Hz and 101.33Hz respectively for the 2nd Engine Order(EO). This is the condition of the shaft without any rotor, so the critical speed and corresponding frequency will vary for the loaded configurations.

Table 5.4 Equivalent Stress

Mode	Frequency	Equivalent Stress
1	48.427 Hz	1.03 x10 ¹⁰ Pa
2	58.531 Hz	1.34 x10 ¹⁰ Pa
3	135.6 Hz	3.56 x10 ⁹ Pa
4	224.77 Hz	2.03 x10 ¹⁰ Pa
5	259.85 Hz	3.92 x10 ¹⁰ Pa

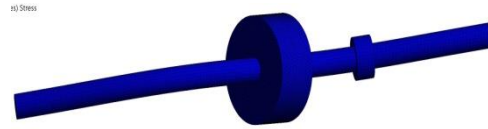


Figure 5.3 Maximum Equivalent Stress

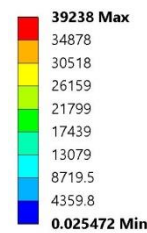


Table 5.4 Equivalent Stress

Table 5.4 shows the Equivalent (Von Mises) stress for different modes. The maximum stress of 39238Mpa was found to be in mode 5 for the frequency of 259.85Hz. The material of the shaft is alloy steel having the Young's Modulus value 2.129x10¹¹Pa and Yield stress 1511MPa. This value is much higher than the maximum stress induced in the shaft. For the shaft rotation of 3000 rpm frequency is 50Hz, however for the shaft in all the cases, the frequency is more than the rotational speed of shaft, so possible resonance due to this also avoided. As a result, this shaft can operate safely within this region.

5.2.2 Shaft with Rotor

The rotor balancing system consists of shaft along with the rotor to be balanced. The positioning of the rotor in the shaft plays an important role for determining the structural and the modal integrity of the system. In this research study 3 different cases of rotor position in shaft is being studied and analyzed. The disc shaped rotor is taken and positioned which is described in detail below:

5.2.2.1 Case 1: Shaft with Rotor on Right Side

In this case the disc shape rotor is kept at one fourth distance from the side B on the right side. Here the distance between the pulley of the shaft and the rotor is comparatively more. As most of the heavy part is being on the right side, the more forces will act upon the supporting bearings of right this can be visualized in the Figure 5.4.

5.2.2.2 Case 2: Shaft with Rotor at the Center of Shaft

The rotor is kept at the center of the shaft. The driving pulley and the rotors are in close proximity. The heavy or the concentrated weight remains almost at the geometric center of the shaft, so there will not be much difference in the reaction forces calculated at the supports.

5.2.2.3 Case 3: Shaft with Rotor at the Center between Pulley and Right End

In this case, the rotor to be balance is at the equidistance between the pulley of the shaft and the right end point B. This location of the rotor impacts much on the structural and harmonic performance of the system, so this case is taken into considerations.

5.2.2.4 Comparative Model Study and Deformation for Three Cases

Three different cases as described earlier are visualized and their behavioral characteristics are being compared in this topic. Design along with the different position of the rotor in the shaft is analyzed for the deformation in the different modes.

On the basis of position of the rotor in the shaft three different geometries were studied. Provided with the same boundary conditions for all three cases, first mode data were analyzed for the deformation which is shown in Figure 5.4. In the first mode, the case 1 having rotor near the right end undergo the maximum deformation of 136.17mm in the frequency of 56.37Hz. Similarly, case 2 has the maximum deformation of 3.59mm in the frequency of 48.43Hz. Case 3 for first mode frequency of 50.17Hz has maximum deformation of 118.08 mm. From this comparative study, it was found that when the rotor position is at the center or near the geometric center, then maximum deformation is small with comparatively low frequency for the first modes and the behavior of shaft is similar for the higher modes. So, it is wise to

position the rotor at the near the geometric center of the shaft to prevent deformation and the failure of the shaft.

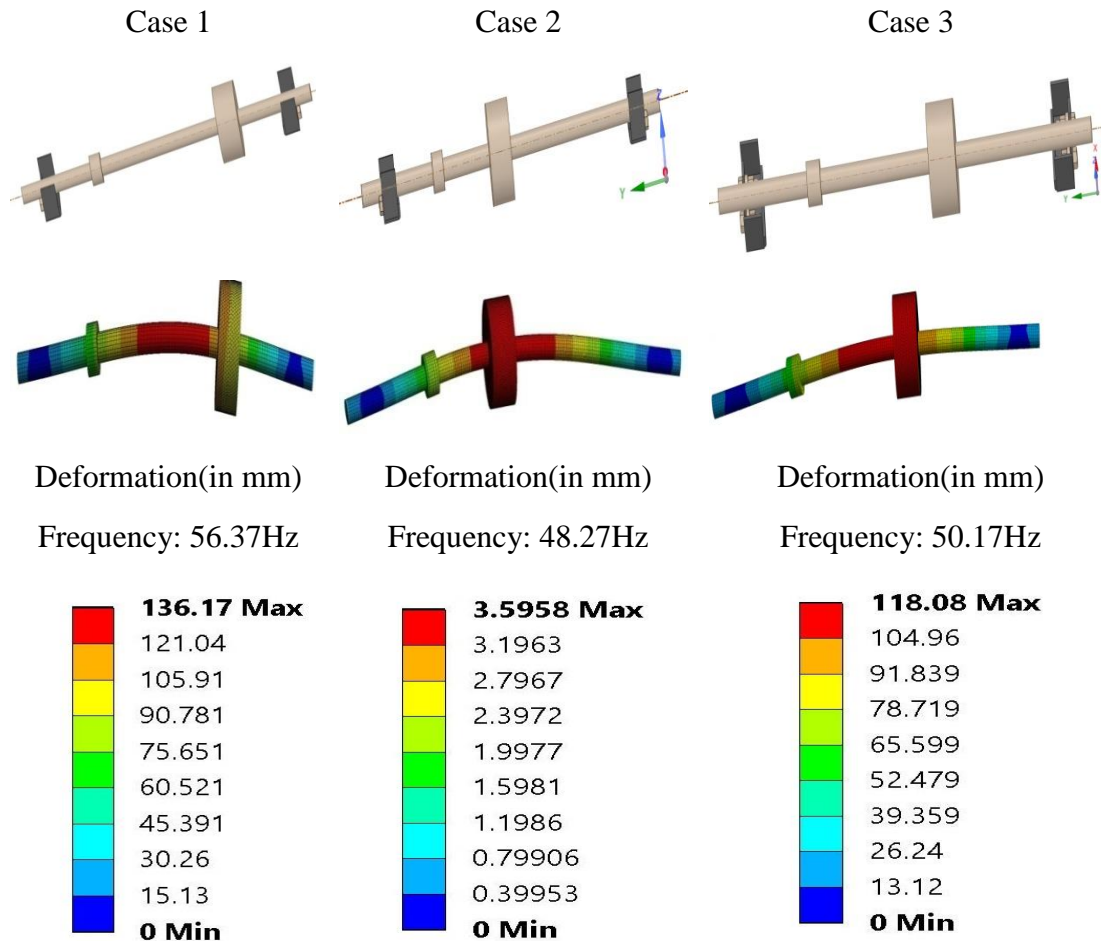


Figure 5.4 Comparative Model Study and Deformation for Three Cases.

5.2.2.5 Free Vibration Analysis of the Shaft

Shaft vibration is the main challenge while designing and the operating the rotor balancing system. The shaft containing rotor must not undergo the vibration by itself instead of sensing the unbalance in the system. So, it is essential to restrict the shaft from the possible vibration. The shaft will resonant with high amplitude when it operates in the regime of the critical speed. The critical speeds are known from the Clambell diagram for the different modes and the engine order (EO) lines. All three cases were analyzed for the vibration and the results are presented in the Tables and Clambell diagrams.

Table 5.5 Results Showing Modes, Critical Speeds and Engine Orders for Case1

	Mode 1(Hz)	Mode 2	Mode 3	Mode 4	Mode 5	1st EO	2nd EO	3rd EO
Critical Speed	3382. rpm	4110.1rpm						
RPM	Mode 1(Hz)	Mode 2	Mode 3	Mode 4	Mode 5	1st EO	2nd EO	3rd EO
0	56.37	68.91	133.70	191.48	222.24	0.00	0.00	0.00
1000	56.37	68.88	133.61	191.48	222.46	16.67	33.33	50.00
2000	56.37	68.81	133.34	191.49	223.14	33.33	66.67	100.00
3000	56.37	68.69	132.89	191.51	224.27	50.00	100.00	150.00
4000	56.37	68.52	132.29	191.53	225.82	66.67	133.33	200.00
5000	56.36	68.31	131.55	191.55	227.78	83.33	166.67	250.00

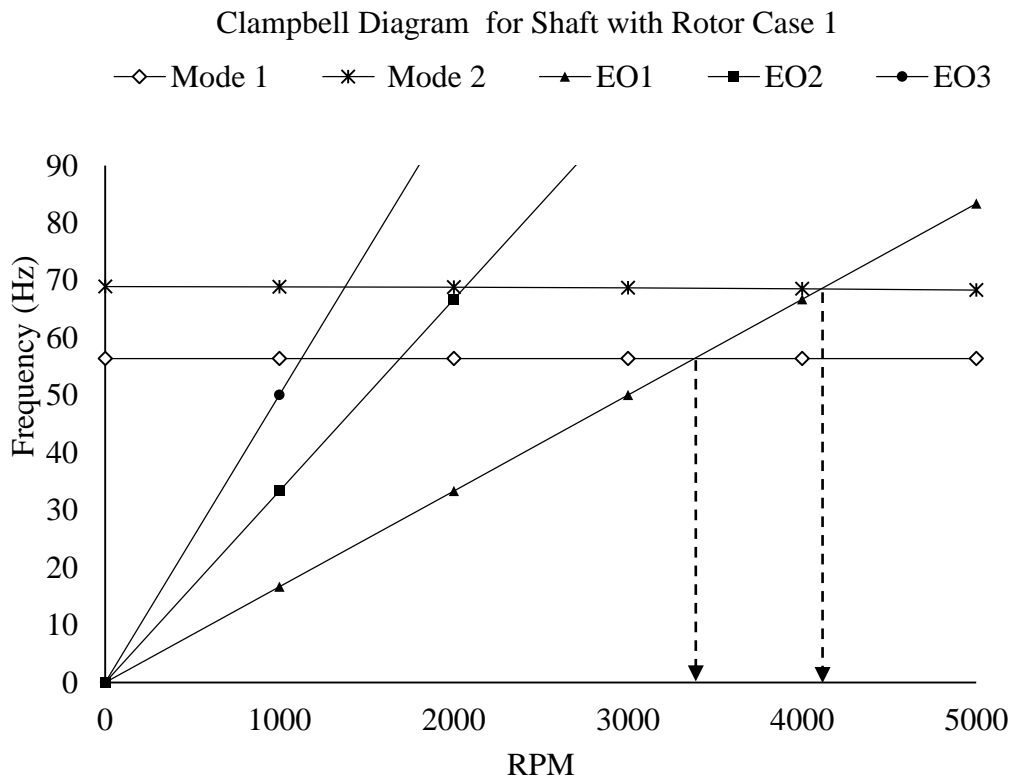


Figure 5.5 Clampbell Diagram for Shaft with Rotor Case 1

For the shaft containing rotor at the right end, i.e, Case 1, 56.37Hz and 68.91Hz frequencies are obtained for the mode 1 and mode 2 respectively. Higher modes frequencies are shown in the Table 5.5. From the Clampbell diagram shown in Figure 5.5 for the 1st Engine Orders (EO), critical speeds are found to be 3382RPM and

4110.1RPM. Similarly, for the higher engine orders critical speeds can be obtained from diagram. As our shaft RPM is 3000, it will avoid the critical speed and the possible resonance.

Table 5.6 Results Showing Modes, Critical Speeds and Engine Orders For Case 2

	Mode1 (Hz)	Mode 2	Mode 3	Mode 4	Mode 5	1st EO	2nd EO	3rd EO
Critical Speed	2905rpm	3500rpm						
RPM	Mode1 (Hz)	Mode 2	Mode 3	Mode 4	Mode 5	1st EO	2nd EO	3rd EO
0	48.43	58.53	135.60	224.77	259.85	0.00	0.00	0.00
1000	48.43	58.52	135.58	224.77	259.96	16.67	33.33	50.00
2000	48.43	58.47	135.53	224.77	260.26	33.33	66.67	100.00
3000	48.43	58.39	135.45	224.77	260.77	50.00	100.00	150.00
4000	48.43	58.28	135.33	224.77	261.48	66.67	133.33	200.00
5000	48.43	58.14	135.19	224.77	262.38	83.33	166.67	250.00

For Case 2, 48.43Hz and 58.53Hz frequencies are obtained for the mode 1 and mode 2 respectively for 0 RPM. Modes frequency accordance with RPM are shown in the Table 5.6. From the Campbell diagram shown in Figure 5.6 for the 1st Engine Orders (EO), critical speeds are found to be 2905RPM and 3500RPM. Similarly, for the higher engine orders critical speeds can be obtained from diagram. So, these critical speeds must be avoided for the efficiency and effectiveness of the balancing system. As our design RPM is 3000 and 50Hz frequency, it is close to the lower critical speed. However, close observation should be taken for the shaft not to operate in the regime of critical speed.

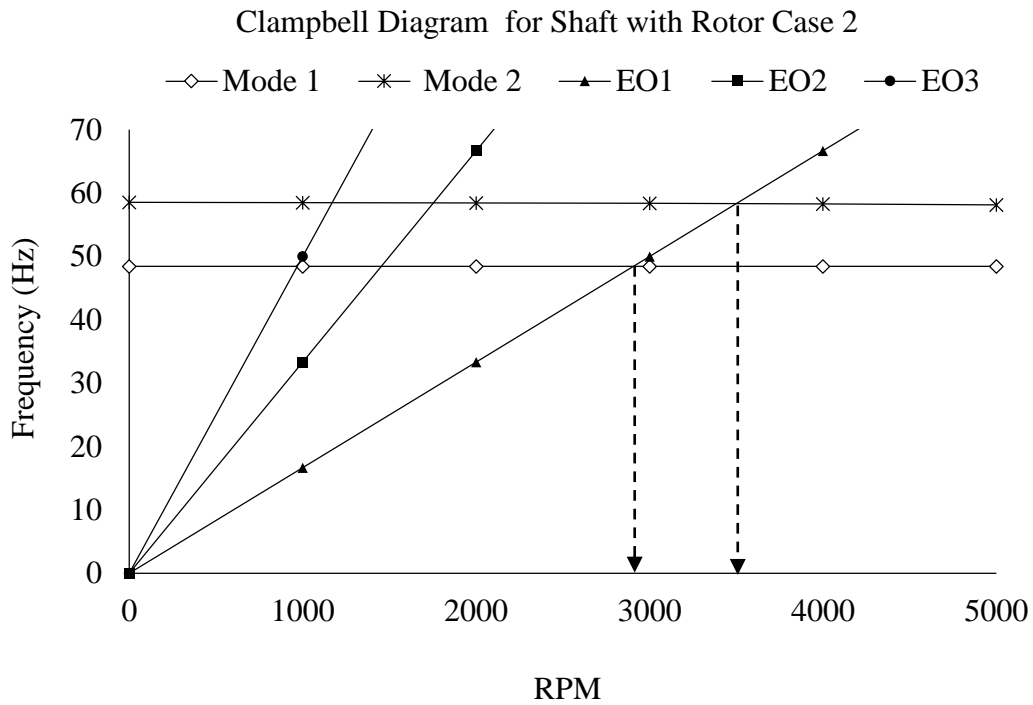


Figure 5.6 Clampbell Diagram for Shaft with Rotor Case 2

Table 5.7 Results Showing Modes, Critical Speeds and Engine Orders For Case 3

	Mode 1(Hz)	Mode 2	Mode 3	Mode 4	Mode 5	1st EO	2nd EO	3rd EO
Critical Speed	3010.2 rpm	3624 rpm						
Rpm	Mode 1(Hz)	Mode 2	Mode 3	Mode 4	Mode 5	1st EO	2nd EO	3rd EO
0	50.17	60.51	137.41	213.21	247.65	0.00	0.00	0.00
1000	50.17	60.50	137.37	213.21	247.75	16.67	33.33	50.00
2000	50.17	60.47	137.25	213.22	248.06	33.33	66.67	100.00
3000	50.17	60.44	137.06	213.22	248.57	50.00	100.00	150.00
4000	50.17	60.38	136.80	213.22	249.28	66.67	133.33	200.00
5000	50.17	60.31	136.46	213.22	250.19	83.33	166.67	250.00

For this Case 3, modes frequency accordance with RPM are shown in the Table 5.7. From the Clampbell diagram shown in Figure 5.7 for the 1st Engine Orders (EO), critical speeds are found to be 3010.2RPM and 3624RPM. Similarly, for the higher engine orders critical speeds can be obtained from diagram. The critical speed for the first mode 3010.2 RPM with frequency of 50.17Hz is quite close to the operating

RPM and the frequency. So, to operate the balancing system with this shaft, different RPM speed should be selected or different configuration shaft can be used.

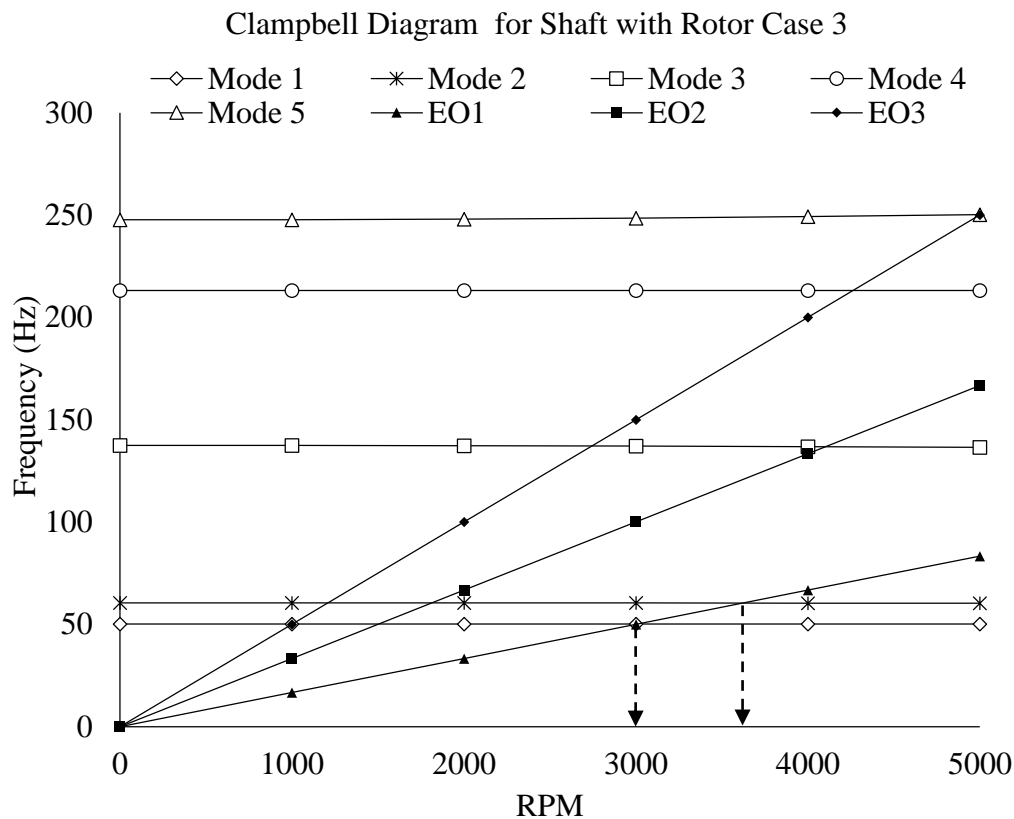


Figure 5.7 Clampbell Diagram for Shaft with Rotor Case 3

5.2.2.6 Selection of Shaft-Rotor System

Three different configurations of the shaft with varying positions of the rotor are being studied. The modal analysis for the deformation at different frequencies and free vibration is carried out with the help of Clampbell diagrams. The amplitude of deformation of Case 2 containing rotor at the center of the shaft was found to be comparatively lower than for the other cases. Similarly, in free vibration analysis, the critical speed of the Case 3 is obtained close to the operational speed of chosen rpm and frequency. This might leads to the resonance and high vibration resulting in the premature failure of the shaft. Taking result of deformation and the free vibration at 0-5000RPM, Case 2 having the rotor position at the center of the shaft is found to be comparatively better design.

5.2.2.7 Mesh Independent Test

The no. of mesh elements is changed for the analysis of the shaft rotor system. For the different element number, the corresponding result of the analysis was calculated. As shown in Figure 5.8 and Figure 5.9, for the increasing number of mesh elements from 180000 to 220000 the deformation value 3.59mm and critical speed for the first mode 2905 rpm and 3500 for the second mode remain almost constant. So, 200000 mesh elements number were chosen for shaft rotor analysis from this mesh independent test result.

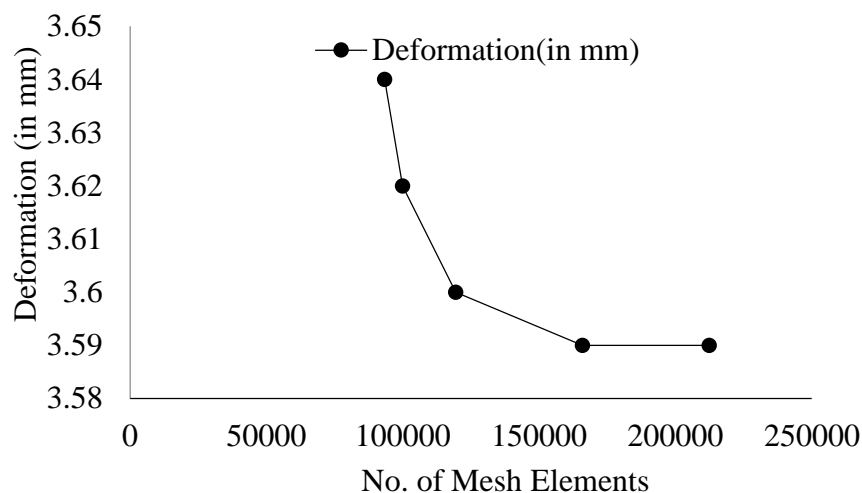


Figure 5.8 Mesh Independent Graph for Deformation

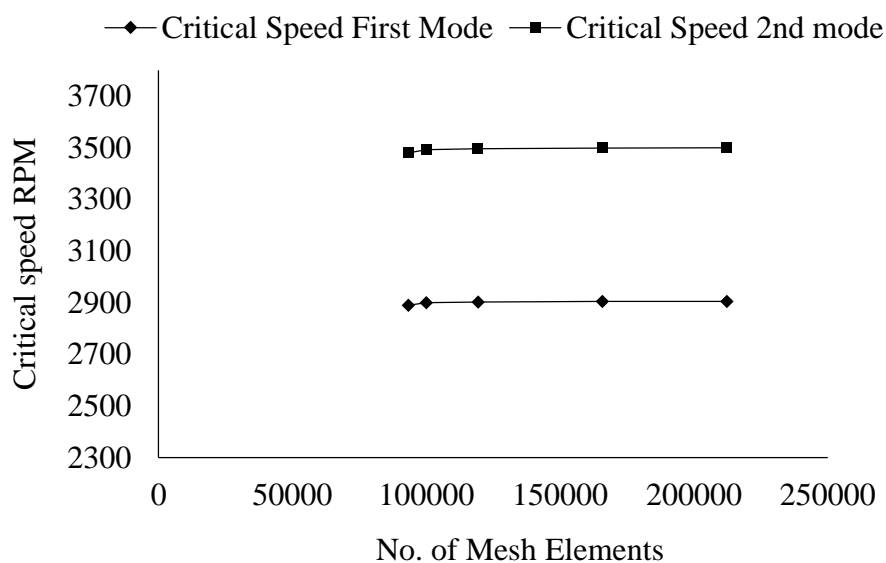


Figure 5.9 Mesh Independent Test Graph For Critical Speed

5.2.3 Suspension System

On the support A of Figure 5.1, the reaction force R_A 539N obtained from Equation no (5.2) is transferred to two supporting bearings. The shaft is tangentially in contact with the bearings with no separation connection. Any imbalance force in the rotor system is transferred to the shaft which in turn is being acted on the bearings. R_{1X} is the horizontal rotor imbalance force which results in the displacement x of the bearing as shown in the Figure 5.10. R_1 is the reaction force from the bearings, the vertical component this is R_{1Y} . Center to center distance for the bearing is 110mm and 70 mm is the diameter of the shaft.

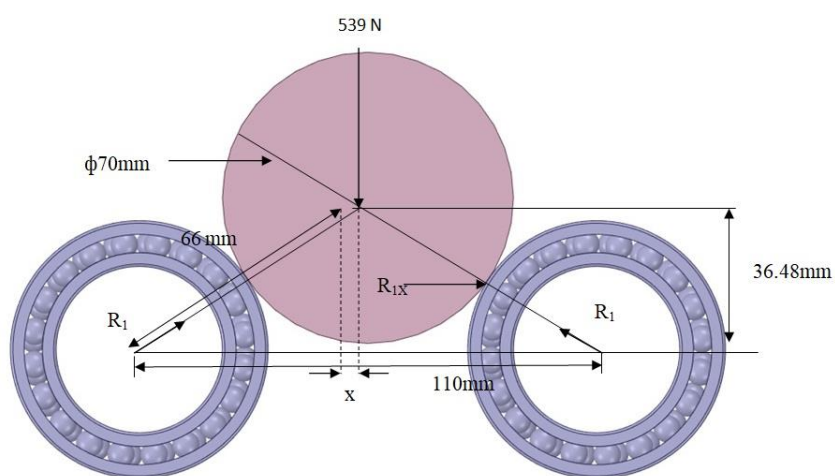


Figure 5.10 Free Body Diagram of Reaction Forces for Shaft and bearing

From the free body diagram and the unbalance weight of 60N, the displacement x is found to be 2.2mm. The calculation is shown in APPENDIX A. Therefore the unbalance weights are vertical R_{1Y} is 269.5N and the horizontal R_{1X} is 60N which can be seen Figure 5.11.

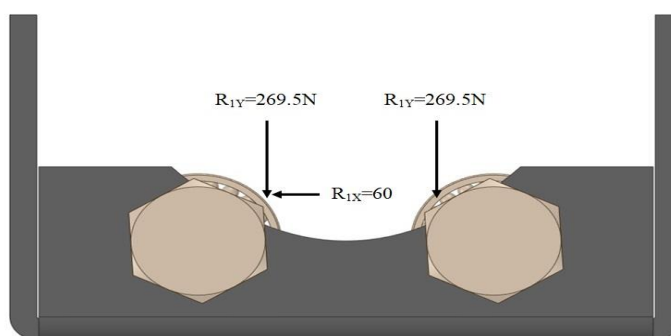
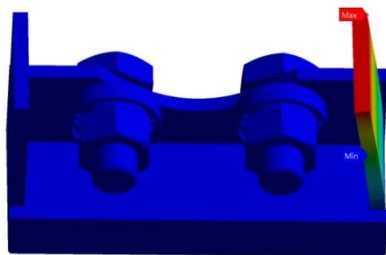


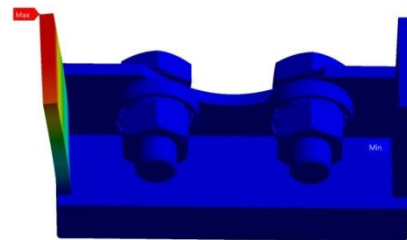
Figure 5.11 Forces acting on Suspension System

The finite element analysis of the suspension system is carried out taking the unbalance forces acting on it. The forces acted upon the bearings which are then being transferred to the other structural components of the suspension system. The suspension system structure is made up of grey cast iron having the ultimate strength 240MPa (Density 7200 Kg/m³) and the bearings are made up of structural steel of yield strength of 1511MPa (Density 7850 Kg/m³).

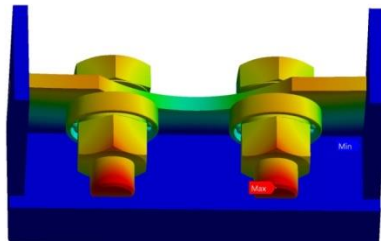
Modal Analysis 301 Hz(D1)



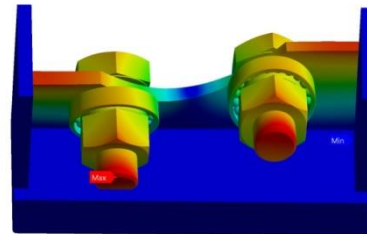
Modal Analysis 324Hz(D2)



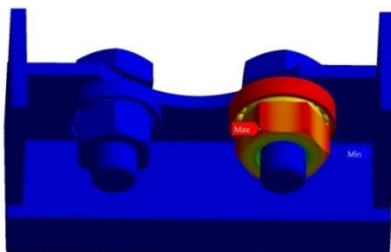
Modal Analysis 605Hz(D3)



Modal Analysis 709Hz(D4)



Modal Analysis 840Hz(D5)



Maximum Deformation(mm)	
301 Hz(D1)	7.051
324Hz(D2)	7.35
605Hz(D3)	3.43
709Hz(D4)	3.45
840Hz(D5)	6.66

Figure 5.12 Deformation of Suspension System for First five modes

The modal analysis of the suspension system is carried out in Ansys. For the load applied in Figure 5.11 and the fixed geometry is applied to the bottom of the system. The corresponding deformations for first five modes were analyzed and the results as shown in Figure 5.12 were obtained. The maximum structural deformation of 7.35mm is obtained for the 2nd mode of 324Hz. This maximum deformation is for the side component rather than the main component, i.e. bearings taking the load.

As the side components are well supported by the spring system, this deformation can be reduced. Similarly, the maximum deformation for the supporting bearing sections is 34.3Hz and 34.4Hz for 3rd and 4th mode respectively.

From the structural analysis of suspension system Figure 5.13 the maximum deformation was found to be 4.13mm and the maximum stress of 12.5MPa. The maximum deformation is obtained in the bolted section of bearing of suspension. As the load is applied in the bearing section, it has been transferred to bolted section, so it came to deform more. Similarly, the maximum stress is seen in the bearing section due to application of load. The analyzed stress value is very less than the Yield strength of material of suspension system, i.e, Grey Cast Iron and structural steel. So, the structure can sustain the system load and work efficiently without reaching to the failure state.

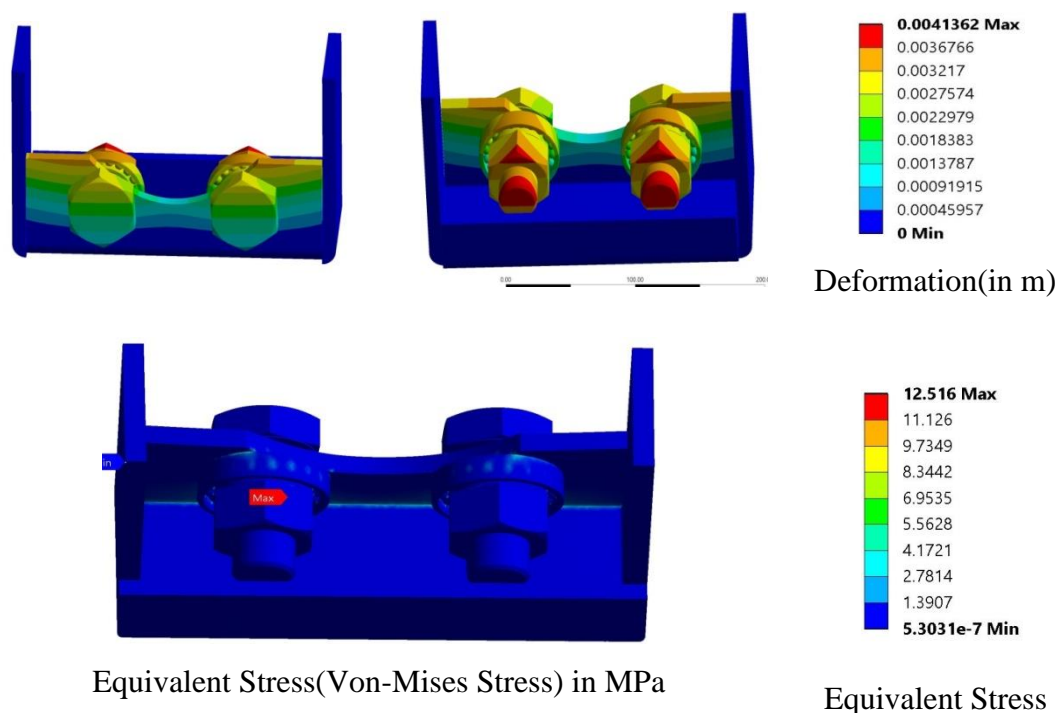
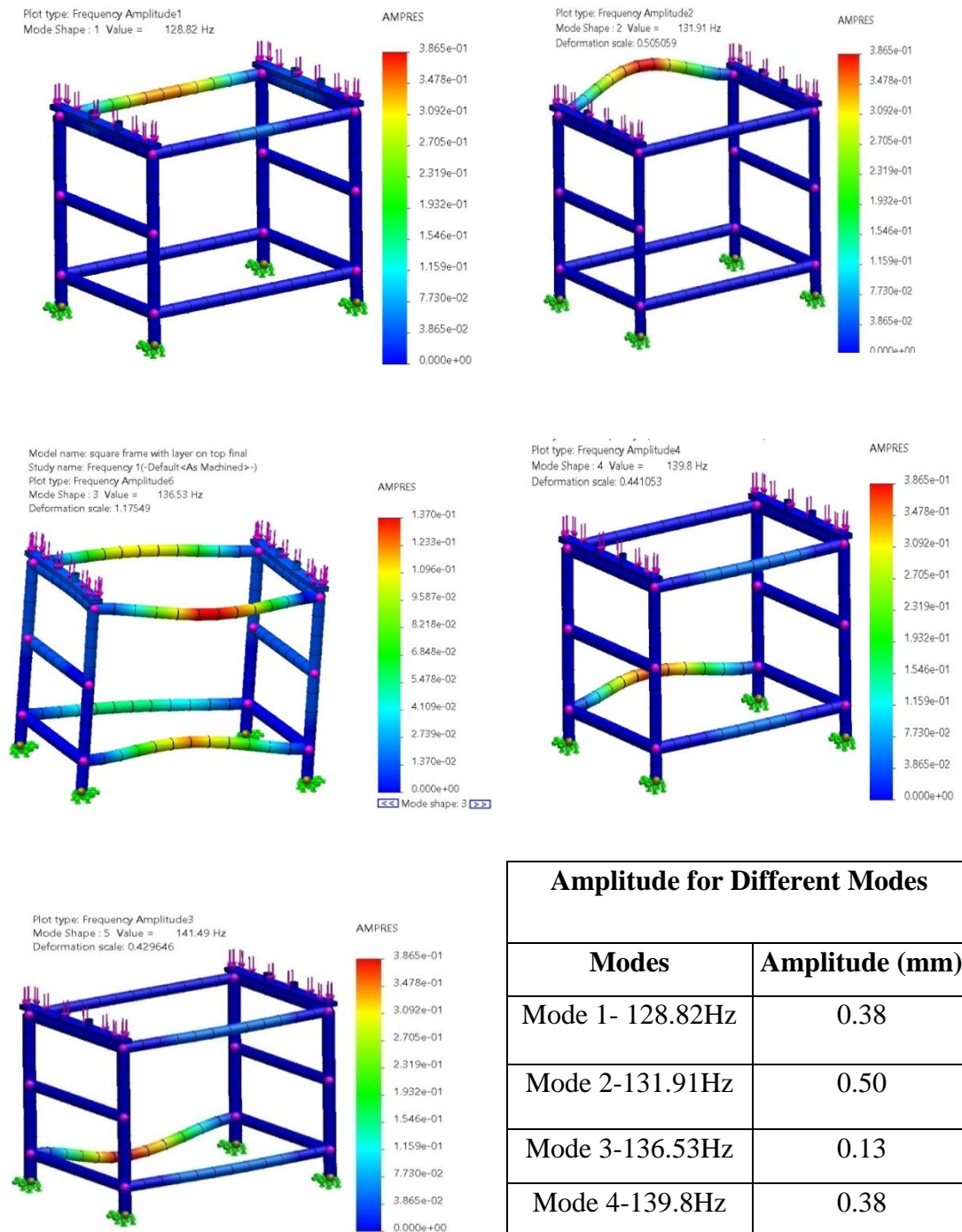


Figure 5.13 Structural Analysis of Suspension System

5.2.4 Machine Frame



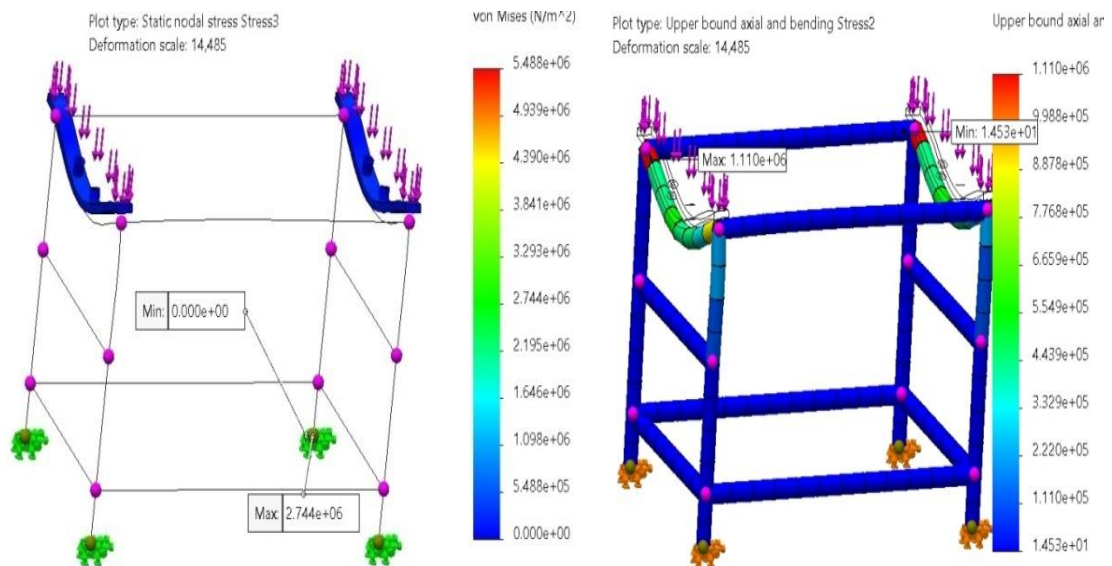
Amplitude for Different Modes	
Modes	Amplitude (mm)
Mode 1- 128.82Hz	0.38
Mode 2-131.91Hz	0.50
Mode 3-136.53Hz	0.13
Mode 4-139.8Hz	0.38
Mode 5-141.49Hz	0.386

Figure 5.14 Modal Analysis of Machine Bench

As shown in Figure 5.14 the modal analysis of machine bench is carried out for first five modes and the corresponding amplitude of vibration is calculated. For the

calculation, the legs of the supports were assigned fixed geometry. The load due to shaft and its components are being divided into two equal forces of 630N and applied at two beams of the machine bench as in Figure 5.14. During the analysis the maximum amplitude of 0.5m was obtained for the frequency of 131.91Hz, the minimum displacement is found for the mode 3 where the magnitude of amplitude is 0.13m for 136.53Hz frequency.

The structural analysis of the machine bench is also carried out with the same load applied for the modal analysis. From the analysis the maximum stress, axial and bending stress, static displacement, strain and factor of safety were found to be 2.744×10^6 Pa, 1.11×10^6 Pa, 11mm, 3.77×10^6 and 1.00×10^{16} respectively as shown in Figure 5.15. The maximum stress is seen in the machine bench standing point or the attachment point of the ground and comparatively minimum in the loading portion. However, the loading portion has more bending and axial stress, displacement, and the applied load is being transferred finally to the ground attachment part of frame leading to maximum stress and highest factor of safety. As the stress value is less than the ultimate stress value of the material, the frame can sustain the load without going to the failure.



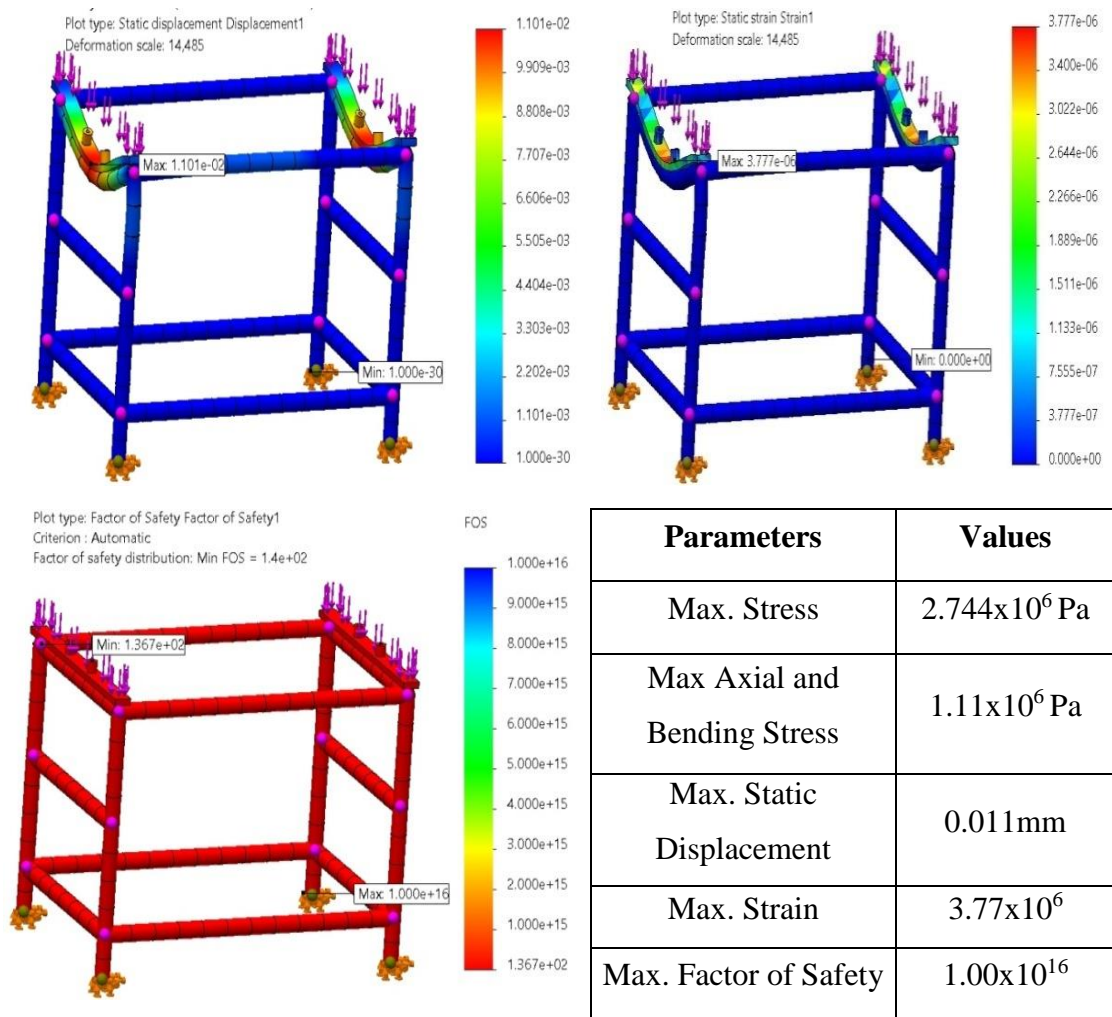


Figure 5.15 Structural Analysis of Machine Bench

5.3 Unbalance System

The disc shaped rotor is chosen for the study having the diameter of 30cm and width of 12cm. The disc has the cylindrical cut at the center with the diameter of 7cm which can be inserted into the shaft. The disc will undergo unbalance if the additional weight is added to it or some part of the rotor is being damaged or removed. Two cases has been studied for the unbalance weight one having cylindrical lumped mass of diameter 5cm and length 4cm at a distance 11cm from the center and other having the cylindrical cut of same dimensions at the same place.

5.3.1 Unbalance System with Lumped mass

The addition of the extra mass will lead to unbalance of the system as shown in Figure 5.16. The centrifugal force generated in the system varies and the eccentricity of the

rotor will also change. The original mass of the rotor disc is 61.76kg, and with the addition of lumped mass of dimension 5cm diameter and 4 cm length, the mass is increased to 62.36kg. The additional residual mass will generate the extra centrifugal force which in-turn impact the balancing of the system.

5.3.2 Unbalance System with Mass Removed

Some portion of the mass is removed from the rotor disc. The mass of the rotor after the removal of portion of dimension 5cm diameter and 4 cm length, the final mass is 61kg as in Figure 5.16. The reduction of the mass will produce unbalance in the system due to reduction in the centrifugal force as per Equation (5.4).

Centrifugal force,

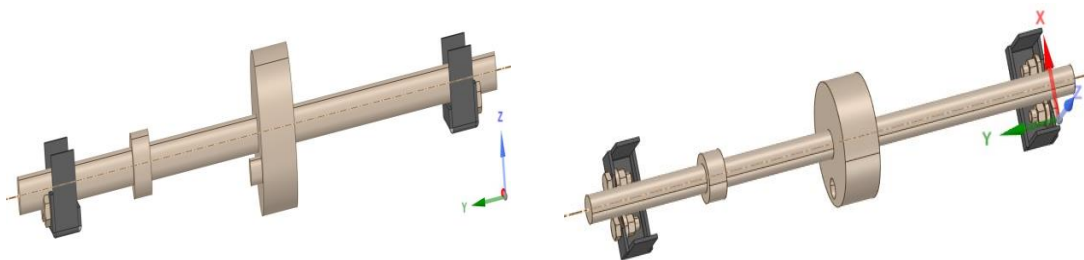
$$F = \frac{mv^2}{r} \quad (5.4)$$

Where,

m is the mass added or removed

v is the rotational velocity

r is the distance from the center



a. Rotor with Lumped Mass

b. Rotor with Mass Removed

Figure 5.16 Unbalance System with Lumped mass and Removed mass

5.3.3 Comparative Study of Unbalance System

The two cases of unbalance system is being studied one with the lumped mass and one with the mass removed. Any changes in the mass of the body vary the centrifugal force, so there will be corresponding change in the modal and the structural properties of the system which will be analyze in the following sub-topics.

5.3.3.1 Campbell Diagram

The Campbell diagram is being plotted for the both cases of unbalances to determine the critical speed, resonance frequency, modes and engine order frequency. The details of Campbell diagram is given in the Table B.1 and Table B.2 of APPENDIX B. The Campbell diagrams for the unbalance mass is shown in Figure 5.17 and Figure 5.18. For Case 2 rotor, critical speed of 2905 and 3500 rpm for the first mode 48.43Hz and 58.53Hz in second mode respectively is already obtained.

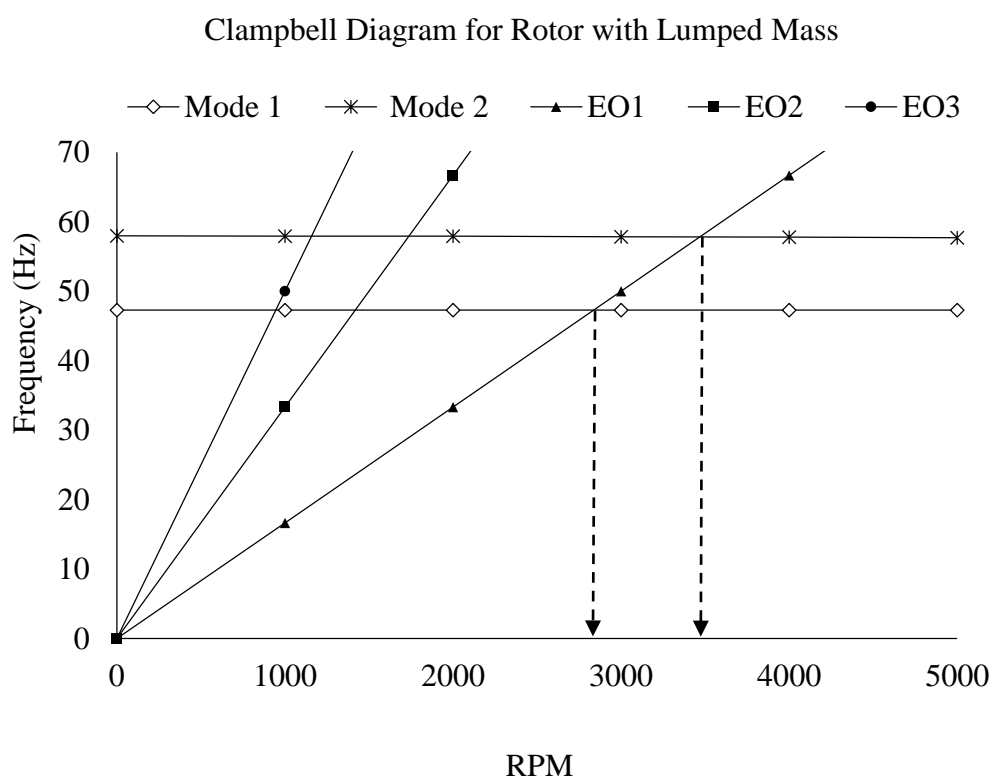


Figure 5.17 Campbell Diagram for Rotor with Lumped Mass

As in the Table B.1 and Figure 5.17, the critical speed is 2837.3 rpm for the first mode at frequency 47.289Hz and 3468.5rpm for the second mode at frequency of 57.94Hz. With the addition of the mass, the critical speed for the first and second mode reduced and the corresponding frequency is smaller than the Case 2 rotor.

In the case of rotor with the mass removed, as in Figure 5.18 and Table B.2 critical speeds values are 2953.3 rpm and 3871 rpm for the first and the second mode, the corresponding frequencies are 49.22Hz and 64.707Hz. These values are bit higher than the values obtained for the Case 2 rotor. So, from the study of unbalanced rotor,

it can be concluded that, if the mass is added to the balanced rotor, it will reduce the critical speed and the mode frequency and the scenario is opposite for the case of mass removed.

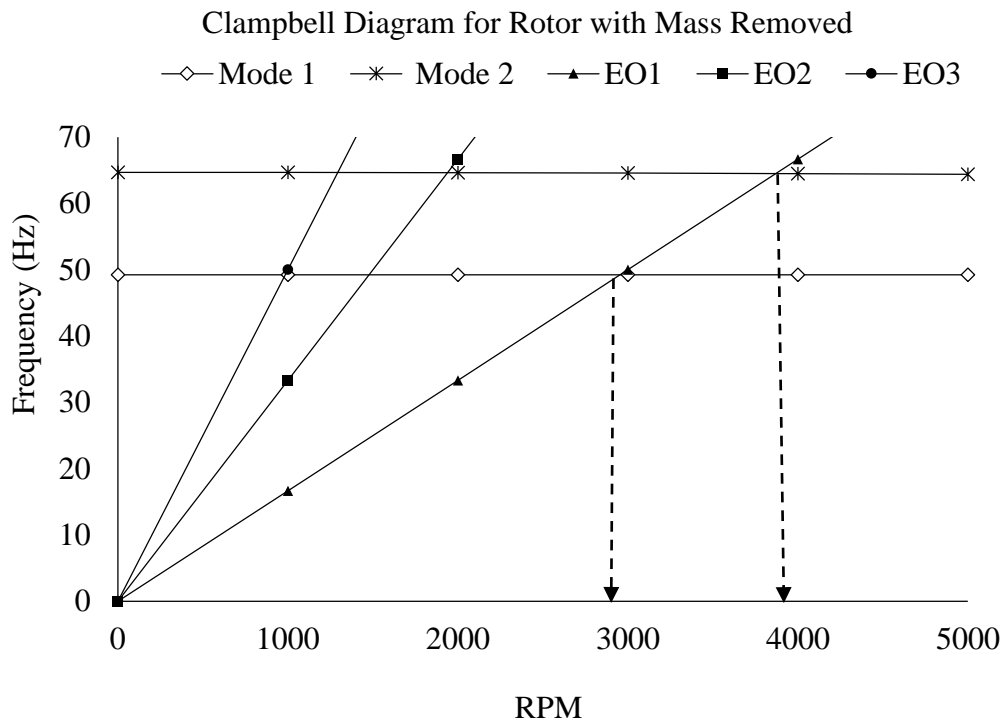


Figure 5.18 Clampbell Diagram for Rotor with Mass Removed

5.3.3.2 Deformation

The comparative study of deformations due to rotation of shaft for the Case 2 and unbalance weight is carried out, which is shown in Figure 5.19, the data related to them is given in Table C.1 of APPENDIX C. Similarly diagrams showing the comparative deformation under the modal frequency are given in of APPENDIX D. From the Figure 5.19, in the first mode, deformation and frequency are quite close to each other, the rotor with mass removed has higher frequency but lower deformation of 3.586mm. As the higher mode proceeds, these parameters are transparent and can be distinguishing from the graph. From fourth and fifth mode, frequency and deformations are in increasing order from rotor with lumped mass, rotor with mass removed to Case 2. The maximum frequency of 271.8Hz is obtained for rotor with mass removed and and maximum deformation value of 5.957mm is obtained for Case 2 rotor at mode 5.

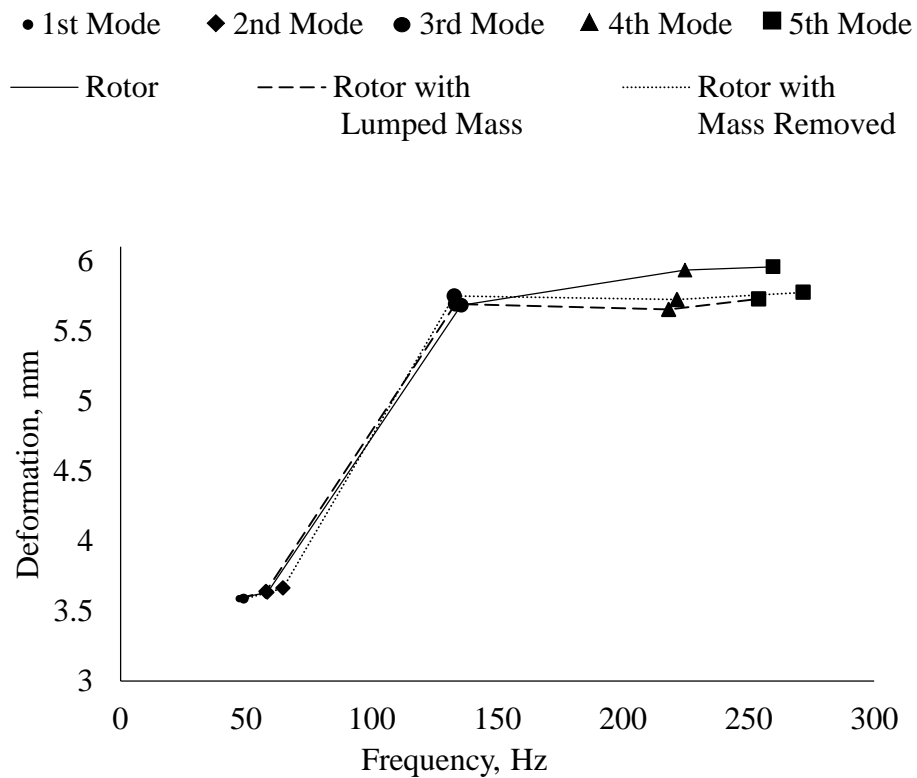


Figure 5.19 Comparative Deformation Diagram

5.3.3.2 Equivalent Stress (Von-Mises Stress)

The comparative study of Equivalent stress due to rotation of shaft for the case 2 and unbalance weight is carried out, which is shown in Figure 5.20, the data related to them is given in Table C.2 of APPENDIX C. Similarly diagrams showing the comparative stress under the modal frequency are given in Table E.1 of APPENDIX E. As in the Figure 5.20, the equivalent stress is higher for the lumped mass and lower for the mass removed. The trend is similar for higher modes 3, 4 and 5. This maximum stress is applied to the bearing support and the minimum stress is at overhanging part of the rotor shaft which can be seen in Table E.1. The maximum equivalent stress is obtained for the rotor with lumped mass with value of 40958Mpa at frequency of 254.09Hz. The maximum stress value is lower than the yield strength value of rotor, shaft and bearings, so this structure can easily overcome the possible material and mechanical failure.

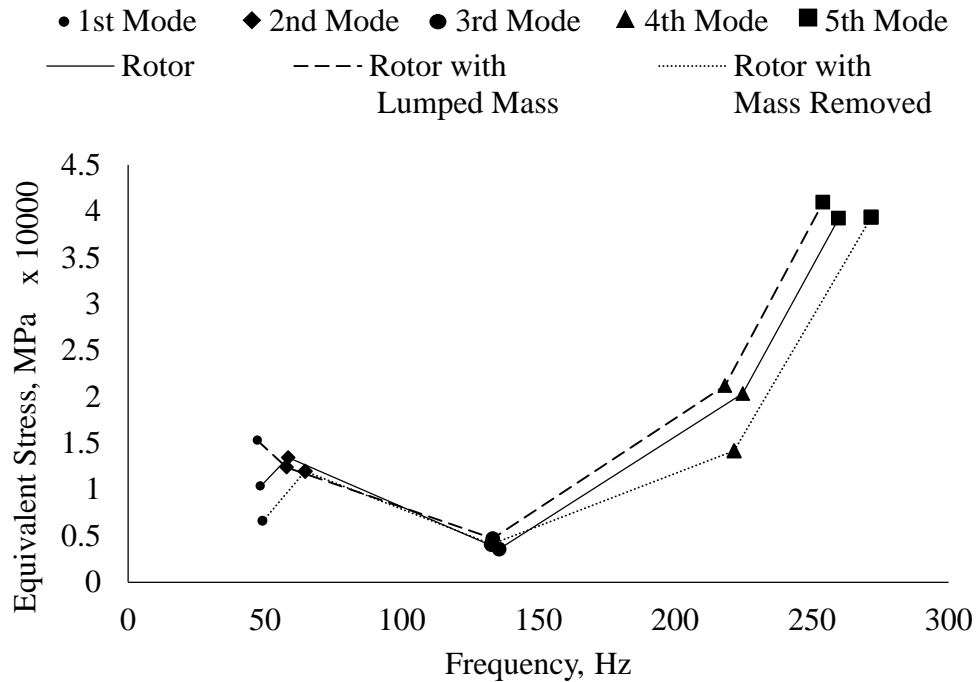


Figure 5.20 Comparative Equivalent Stress (Von Mises) Diagram

5.4 Unbalance Characteristics

The any residual mass or the removal of the mass from the rotor induces the unbalance in the system. The residual mass m_i at certain eccentricity r_i from the center of the rotor develop the centrifugal force $F = m_i r_i \omega^2$. This centrifugal force impose additional stress to the shaft on which rotor is rotated. The permissible unbalance mass for different rotor weight and the speed is calculated as shown in Table 5.8 and APPENDIX F.

The study is carried out for the rotor of weight 600N, 1000N, 1500N, 2000N and 2500N for rpm 1000, 2000, 3000, 4000 and 5000 and corresponding permissible unbalance weight($m_i r_i$) is calculated from the shear stress allowable for the shaft material. The shaft material is made up Alloy Steel and the standard factor of safety of value 6 is used for calculation.

It is found that with the increase in the rpm of the rotor, the permissible unbalance weight also reduces. This conditions is applicable all rotors of aforementioned weight. But with the increase in the rotor weight the permissible unbalance also reduces in the

same manner as shown in Table 5.8, however, the change in value is very small which is shown in Figure 5.21.

Table 5.8 Permissible Unbalance Mass

Dia. in m	$W_t + m_i r_i \omega^2$	W_t (N)	$mr\omega^2$	RPM				
				1000	2000	3000	4000	5000
				$m_1 r_1$	$m_2 r_2$	$m_3 r_3$	$m_4 r_4$	$m_5 r_5$
0.07	484596.95	600	4839	44.135	11.033	4.9039	2.7584	1.7654
			96.95	22947	80737	14385	51842	09179
0.07	484596.95	1000	4835	44.098	11.024	4.8998	2.7561	1.7639
			96.95	75384	68846	61538	72115	50154
0.07	484596.95	1500	4830	44.053	11.013	4.8947	2.7533	1.7621
			96.95	15931	28983	95479	22457	26372
0.07	484596.95	2000	4825	44.007	11.001	4.8897	2.7504	1.7603
			96.95	56478	89119	2942	72799	02591
0.07	484596.95	2500	4820	43.961	10.990	4.8846	2.7476	1.7584
			96.95	97024	49256	6336	2314	7881

For the rotational speed of 3000rpm, the maximum permissible unbalance ($m_i r_i$) in Kg.m is 4.9039kg.m for 600N rotor. The unbalance weight above for this value cannot be sustain by this system as it crosses the allowable shear stress value and develop the crack and damage in the shaft. The detail calculation of the permissible unbalance is given in APPENDIX F.

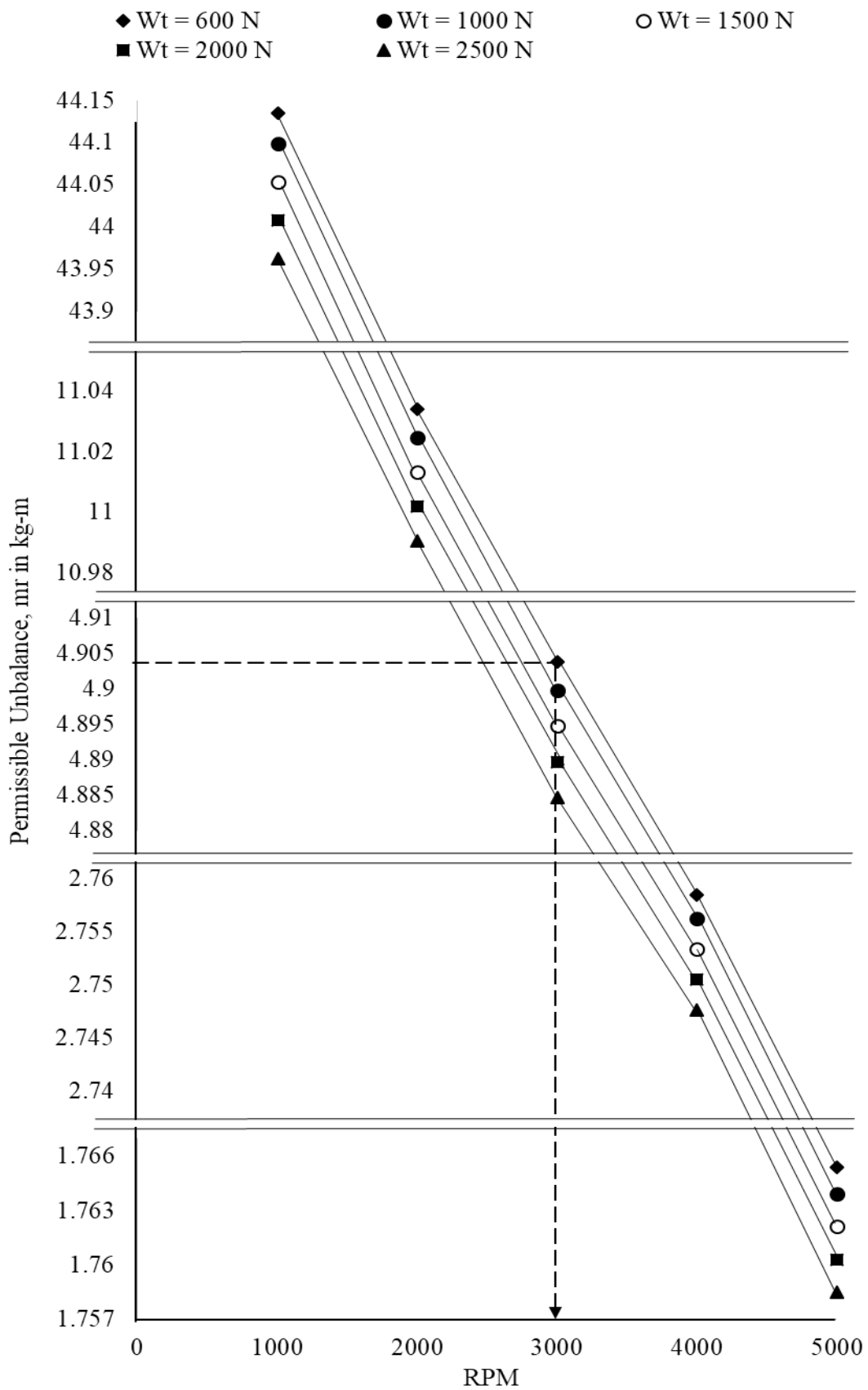


Figure 5.21 Permissible unbalance Weight

CHAPTER SIX: CONCLUSIONS AND RECOMMENDATIONS

6.1 Conclusions

The study has been carried out on design and analysis of rotor balancing system for the industrial purposes. The CAD design of the model is done in Solidworks software, structural and modal analysis of the system is carried out in both Solidworks and Ansys software. The design parameters and operational characteristics of the system have been selected based on the literature reviews and the modern industrial requirements. The rotor balancing system has been studied for vibration characteristics, structural integrity and the unbalance parameters considering different design approaches.

First of all, shaft rotor combination has been studied with the different rotor positions for the case 1, case 2 and case 3. The case 1 and 3 of shaft –rotor system, have deformation value of 136mm and 118mm respectively. However, case 2, with the rotor at the center, have deformation 3.59 mm at 48.27Hz frequency, and the critical speed is 2905 and 3500 RPM. This will avoid possible resonance for the operating speed of 3000RPM, so case 2 is comparatively found to be better design. Similarly, Suspension system and the machine frame were analyzed, deformation value of 4.11mm, 0.011mm and equivalent stress of 12.516 MPa, 2.744 MPa were obtained respectively. The equivalent stress for both components are very small compared to the ultimate stress of grey cast iron material (240MPa). Therefore, the structure can easily sustain load acted on it without any structural failure.

The Unbalance shaft-rotor system is studied considering two cases, one with lumped mass and other with the mass removed. For unbalance system: with addition of cylindrical mass of diameter 5cm and length 4cm at distance 11 cm from center, critical speeds (2837 rpm and 3468 rpm) values were reduced and equivalent stress found to increase. For the case of mass removal, the behaviors were found to be just opposite to the case of mass addition.

Similarly, the permissible unbalance mass found to reduce with the increase in the rpm of the rotor. The rotors with the higher weight have lesser permissible unbalance weight limit with respect to rpm. For our rotor balancing system, at 3000rpm, the permissible residual weight was found to be 4.903Kg.m for the rotor of weight 600N.

6.2 Recommendations

In this research study, the rotor balancing system is designed and analyzed for the vibration, structural and balancing characteristics. This study is just the theoretical approach of the balancing system, the practical or experimental approach will give more details ideas about the system. The rotor balancing for various design parameters like shaft characteristics, material properties, rotor weight, motor rpm, etc can be considered to understand different behaviors of the system. The balancing procedures for unbalance system can be studied using Influence Co-efficient method, Modal Balancing Methods and other balancing approaches, so that the improvement in the balancing system design can be made.

References

- Ashby, M. F. (2011). Material Property Charts. In *Materials Selection in Mechanical Design* (Fourth Edi). Michael F. Ashby. <https://doi.org/10.1016/b978-1-85617-663-7.00004-7>
- Bishop, R. E. D. (1958). Mechanical vibration. In *Nature* (Vol. 182, Issue 4649, p. 1581). <https://doi.org/10.1038/1821581a0>
- Bishop, R. E. D., & Gladwell, G. M. L. (1959). The Vibration and Balancing of an Unbalanced Flexible Rotor. *Journal of Mechanical Engineering Science*, 1(1), 66–77. https://doi.org/10.1243/jmes_jour_1959_001_010_02
- Brecher, C., Spachholz, G., & Paepenmüller, F. (2007). Developments for high performance machine tool spindles. *CIRP Annals - Manufacturing Technology*, 56(1), 395–399. <https://doi.org/10.1016/j.cirp.2007.05.092>
- Bucher, I., & Ewins, D. J. (2001). Modal analysis and testing of rotating structures. *Philosophical Transactions of the Royal Society A: Mathematical, Physical and Engineering Sciences*, 359(1778), 61–96. <https://doi.org/10.1098/rsta.2000.0714>
- Burgos Alconz, S. C., & Zurita V., G. (2019). Designing and Development of a Dynamic Vibration Balancing Machine for Industrial Applications. *Investigacion & Desarrollo*, 19(1), 73–93. <https://doi.org/10.23881/idupbo.019.1-5i>
- Cao, Y., & Altintas, Y. (2004). A general method for the modeling of spindle-bearing systems. *Journal of Mechanical Design, Transactions of the ASME*, 126(6), 1089–1104. <https://doi.org/10.1115/1.1802311>
- Capello, M. A., & Kotlarek, P. (2016). Application of Full Spectrum to Rotating Machinery Diagnostics. *Leading Edge*, 35(6), 549–550. <https://doi.org/10.1190/tle35060549.1>
- Chen, X., & Liu, Y. (2014). Finite element modeling and simulation with ANSYS workbench. In *Finite Element Modeling and Simulation with ANSYS Workbench*. <https://doi.org/10.1201/b17284>
- Das, A. S., Dutt, J. K., & Ray, K. (2010). Active vibration control of unbalanced flexible rotor-shaft systems parametrically excited due to base motion. *Applied Mathematical Modelling*, 34(9), 2353–2369. <https://doi.org/10.1016/j.apm.2009.11.002>
- Deepthikumar, M. B., Sekhar, A. S., & Srikanthan, M. R. (2013). Modal balancing of flexible rotors with bow and distributed unbalance. *Journal of Sound and Vibration*, 332(24), 6216–6233. <https://doi.org/10.1016/j.jsv.2013.04.043>
- Goodman, T. P. (1964). A Least-Squares Method for Computing Balance Corrections. *Journal of Engineering for Industry*, 86(3), 273–277. <https://doi.org/10.1115/1.3670532>

- Grobel, L. . (1953). *Balancing Turbine-Generator Rotors*.
- Guskov, M., Sinou, J. J., & Thouverez, F. (2008). Multi-dimensional harmonic balance applied to rotor dynamics. *Mechanics Research Communications*, 35(8), 537–545. <https://doi.org/10.1016/j.mechrescom.2008.05.002>
- Habasit. (2015). *Positive Drive Belts Engineering Guide Habasit – Solutions in motion*. 6033.
- Han, D. J. (2007). Generalized modal balancing for non-isotropic rotor systems. *Mechanical Systems and Signal Processing*, 21(5), 2137–2160. <https://doi.org/10.1016/j.ymsp.2006.09.004>
- He, J., & Fu, Z.-F. (2001). Basic vibration theory. *Modal Analysis*, 49–78. <https://doi.org/10.1016/b978-075065079-3/50003-6>
- Hongwei, F., Mingqing, J., & Heng, L. (2011). *Program Design of an online Dynamic Balancing System for Grinding-wheel and spindle*.
- International Standard Organization. (2003). Mechanical vibration — Balance quality requirements for rotors in a constant (rigid) state — Part 1: Specification and verification of balance tolerances. *Iso1940-1*, 2, 28. <https://www.iso.org/standard/27092.html>
- ISO 5406. (2014). International Standard International Standard. *61010-1* © Iec:2001, 2014(I), 13.
- Juergen M. Tessarzik. (1975). *Flexible Rotor Balancing By The Influnence Coefficient Method-Multiple Critical Speeds with Rigid Or Flexible Supports*.
- Kang, Y., Sheen, G. J., & Wang, S. M. (1997). Development and modification of a unified balancing method for unsymmetrical rotor-bearing systems. *Journal of Sound and Vibration*, 199(3), 349–369. <https://doi.org/10.1006/jsvi.1996.0652>
- Kellenberger W. (1971). Should a flexible rotor be balanced in N or (N plus 2) planes. *ASME Pap 71-Vibr-71*, 71.
- Knowles, G., Kirk, A., Bingham, C., & Bickerton, R. (2018). Generalised analysis of compensating balancing sleeves with experimental results from a scaled industrial turbine coupling shaft. *Proceedings of the Institution of Mechanical Engineers, Part C: Journal of Mechanical Engineering Science*, 232(19), 3453–3468. <https://doi.org/10.1177/0954406217737106>
- Li, L., Cao, S., Li, J., Nie, R., & Hou, L. (2021). Review of rotor balancing methods. *Machines*, 9(5), 1–16. <https://doi.org/10.3390/machines9050089>
- Meacham, W. L., Talbert, P. B., Nelsonf, H. D., & Cooperriderj, N. K. (1988). Including Residual Bow. *Aerospace*, 4(3), 245–251.
- Nazri, N. A., & Sani, M. S. M. (2017). Finite element normal mode analysis of

- resistance welding jointed of dissimilar plate hat structure. *IOP Conference Series: Materials Science and Engineering*, 257(1). <https://doi.org/10.1088/1757-899X/257/1/012059>
- Neto, R. R., Bogh, D. L., & Flammia, M. (2006). Some experiences on rigid and flexible rotors in induction motors driving critical equipment in petroleum and chemical plants. *Record of Conference Papers - Annual Petroleum and Chemical Industry Conference*, 44(3), 923–931. <https://doi.org/10.1109/PCICON.2006.359699>
- Nicholas, J. C., Gunter, E. J., & Allaire, P. E. (1975). Effect of Residual Shaft Bow on Unbalance Response and Balancing of a Single Mass Flexible Rotor - 1, 2. *American Society of Mechanical Engineers (Paper)*, 75-GT-48, 171–181.
- Palazzolo, A. B., & Gunter, E. J. (1982). Modal balancing of a multi-mass flexible rotor without trial weights. *Proceedings of the ASME Turbo Expo*, 5, 1–11. <https://doi.org/10.1115/82GT267>
- Parkinson, A. G. (1991). Balancing of rotating machinery. *Proceedings of the Institution of Mechanical Engineers, Part C: Journal of Mechanical Engineering Science*, 205(1), 53–66. https://doi.org/10.1243/PIME_PROC_1991_205_091_02
- Parkinson, A. G., Darlow, M. S., & Smalley, A. J. (1984). Balancing flexible rotating shafts with an initial bend. *AIAA Journal*, 22(5), 683–689. <https://doi.org/10.2514/3.8655>
- Portal, C. (1995). *Fundamentals of 3D Design and Simulation*. www.solidworks.com/edureseller.
- Qu, L., Liu, X., Peyronne, G., & Chen, Y. (1989). The holospectrum: A new method for rotor surveillance and diagnosis. *Mechanical Systems and Signal Processing*, 3(3), 255–267. [https://doi.org/10.1016/0888-3270\(89\)90052-6](https://doi.org/10.1016/0888-3270(89)90052-6)
- R.K Bansal. (2014). *Shaft-Design-01.Pdf*.
- Ritto, T. G., Lopez, R. H., Sampaio, R., & Souza De Cursi, J. E. (2011). Robust optimization of a flexible rotor-bearing system using the Campbell diagram. *Engineering Optimization*, 43(1), 77–96. <https://doi.org/10.1080/03052151003759125>
- Salinger, H. E. (1964). Problems in Turbomachinery. In *October*.
- Tessarzik, J. M., Badgley, R. H., & Anderson, W. J. (1972). Flexible rotor balancing by the exact point-speed influence coefficient method. *Journal of Manufacturing Science and Engineering, Transactions of the ASME*, 94(1), 148–158. <https://doi.org/10.1115/1.3428104>
- Thomson, W. T. (2018). Theory of vibration with applications, fourth edition. *Theory of Vibration with Applications, Fourth Edition*, 1–546. <https://doi.org/10.1201/9780203718841>

- Tiwari, R., & Chakravarthy, V. (2006). Simultaneous identification of residual unbalances and bearing dynamic parameters from impulse responses of rotor-bearing systems. *Mechanical Systems and Signal Processing*, 20(7), 1590–1614. <https://doi.org/10.1016/j.ymssp.2006.01.005>
- Tresser, S., Dolev, A., & Bucher, I. (2018). Dynamic balancing of super-critical rotating structures using slow-speed data via parametric excitation. *Journal of Sound and Vibration*, 415, 59–77. <https://doi.org/10.1016/j.jsv.2017.11.029>
- Turpin, A., & Sharan, A. M. (1994). Balancing of rotors supported on bearings having nonlinear stiffness characteristics. *Journal of Engineering for Gas Turbines and Power*, 116(3), 718–726. <https://doi.org/10.1115/1.2906878>
- Urbikain, G., Olvera, D., de Lacalle, L. N. L., & Elías-Zúñiga, A. (2015). Stability and vibrational behaviour in turning processes with low rotational speeds. *International Journal of Advanced Manufacturing Technology*, 80(5–8), 871–885. <https://doi.org/10.1007/s00170-015-7041-2>
- Urbikain, Gorka, Alvarez, A., de Lacalle, L. N. L., Arsuaga, M., Alonso, M. A., & Veiga, F. (2017). A reliable turning process by the early use of a deep simulation model at several manufacturing stages. *Machines*, 5(2), 1–18. <https://doi.org/10.3390/machines5020015>
- Wock, M., & Spachtholz, G. (2003). 3- and Contact Point Spindle Bearings. *Test*, 52(1), 3–8.
- Xu, M., & Marangoni, R. D. (1994). Vibration analysis of a motor-flexible coupling-rotor system subject to misalignment and unbalance, Part I: Theoretical model and analysis. In *Journal of Sound and Vibration* (Vol. 176, Issue 5, pp. 663–679). <https://doi.org/10.1006/jsvi.1994.1405>
- Yang, J., He, S. Z., & Wang, L. Q. (2004). Dynamic balancing of a centrifuge: Application to a dual-rotor system with very little speed difference. *JVC/Journal of Vibration and Control*, 10(7), 1029–1040. <https://doi.org/10.1177/1077546304035603>
- Zhang, Y., Li, M., Yao, H., Gou, Y., & Wang, X. (2021). A modal-based balancing method for a high-speed rotor without trial weights. *Mechanical Sciences*, 12(1), 85–96. <https://doi.org/10.5194/ms-12-85-2021>
- Zhou, S., & Shi, J. (2001). Active balancing and vibration control of rotating machinery: A survey. *Shock and Vibration Digest*, 33(5), 361–371. <https://doi.org/10.1177/058310240103300501>

APPENDIX A

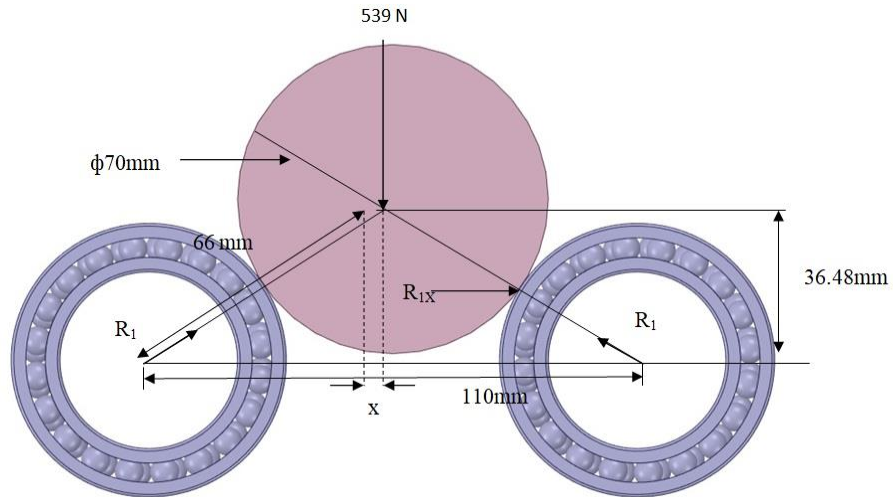
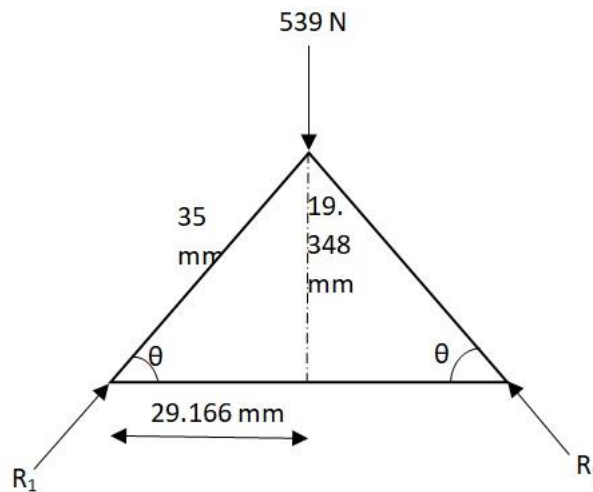


Figure A.1 Free Body diagram of Reaction forces for Shaft and Bearings

This is further simplified into:



$$\theta = \tan^{-1} \left(\frac{36.48}{\left(\frac{110}{2}\right)} \right) = 33.56^\circ$$

$$\sum F_y = 0$$

$$\text{Or, } R_1 \sin \theta + R_1 \sin \theta - 539 = 0$$

$$\text{Or, } 2R_1 \sin 33.56^\circ = 539$$

Therefore,

$$R_1 = 487.509 \text{ N}$$

$$R_{1y} = R_1 \sin \theta = 269.5 \text{ N}$$

$$R_{1x} = R_1 \cos \theta = 269.5 \text{ N}$$

Let us assume that the horizontal displacement of x mm generated by unbalanced force of magnitude 60 N. The horizontal displacement, x mm, is calculated as follows.

$$539 \times x = 60 \times 19.348$$

$$x = 2.2 \text{ mm}$$

APPENDIX B

Table B.1 Results for Rotor with Lumped Mass

	Mode 1	Mode 2	Mode 3	Mode 4	Mode 5	EO1	EO2	EO3
Critical Speed	2837.3 rpm	3468.5 rpm	NONE	NONE	NONE	NONE		
RPM	Mode 1	Mode 2	Mode 3	Mode 4	Mode 5	EO1	EO2	EO3
0	47.289	57.94	133.29	218.28	254.09	0	0	0
1000	47.289	57.929	133.26	218.28	254.2	16.6667	33.3333	50
2000	47.289	57.897	133.16	218.28	254.52	33.3333	66.6667	100
3000	47.289	57.843	133.01	218.28	255.04	50	100	150
4000	47.289	57.768	132.8	218.28	255.77	66.6667	133.333	200
5000	47.289	57.673	132.54	218.28	256.71	83.3333	166.667	250

Table B.2 Results for Rotor with Mass Removed

	Mode 1	Mode 2	Mode 3	Mode 4	Mode 5	EO1	EO2	EO3
Critical Speed	2953.3 rpm	3871. rpm	NONE	NONE	NONE			
RPM	Mode 1	Mode 2	Mode 3	Mode 4	Mode 5	EO1	EO2	EO3
0	49.222	64.707	132.81	221.61	271.8	0	0	0
1000	49.222	64.694	132.79	221.61	271.89	16.6667	33.3333	50
2000	49.222	64.656	132.72	221.61	272.19	33.3333	66.6667	100
3000	49.222	64.594	132.62	221.61	272.67	50	100	150
4000	49.222	64.506	132.47	221.61	273.35	66.6667	133.333	200
5000	49.222	64.394	132.28	221.61	274.21	83.3333	166.667	250

APPENDIX C

Table C.1 Comparative Deformation Data

Modes	Rotor		Rotor with Lumped Mass		Rotor with Mass Removed	
	Frequency (Hz)	Deformation (mm)	Frequency (Hz)	Deformation (mm)	Freq (Hz)	Deform (mm)
1	48.427	3.596	47.289	3.59	49.222	3.586
2	58.531	3.633	57.94	3.64	64.707	3.664
3	135.6	5.683	133.29	5.692	132.81	5.75
4	224.77	5.933	218.28	5.653	221.61	5.723
5	259.85	5.957	254.09	5.728	271.8	5.775

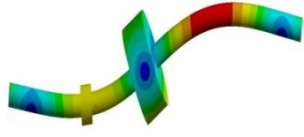
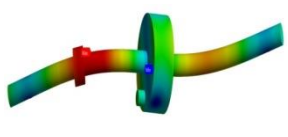
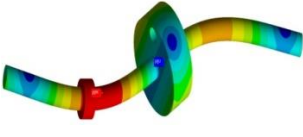
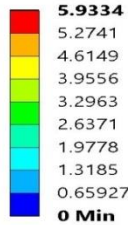
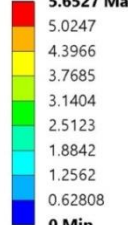
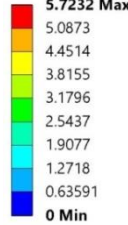
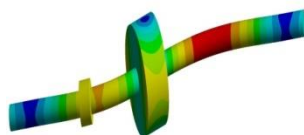
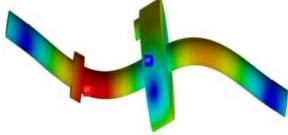
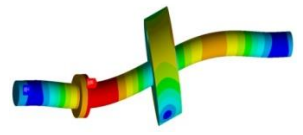
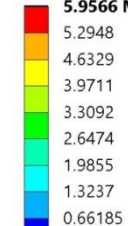
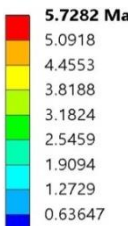
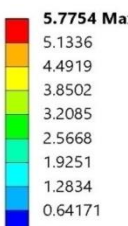
Table C.2 Comparative Equivalent Stress (Von Mises Stress)

Modes	Rotor		Rotor with Lumped Mass		Rotor with Mass Removed	
	Freq. (Hz)	Equiv. Stress (MPa)	Frequency (Hz)	Equivalent Stress (MPa)	Freq (Hz)	Stress (MPa)
1	48.427	10347	47.289	15283	49.222	6580.9
2	58.531	13433	57.94	12389	64.707	11959
3	135.6	3563.5	133.29	4727.1	132.81	4102.3
4	224.77	20330	218.28	21203	221.61	14153
5	259.85	39238	254.09	40958	271.8	39348

APPENDIX D

Table D.1 Comparative Deformation Diagrams

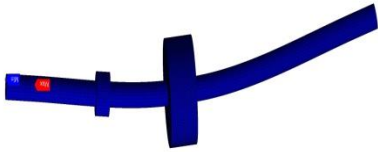
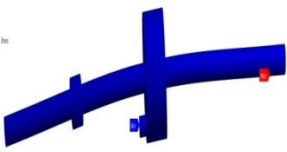

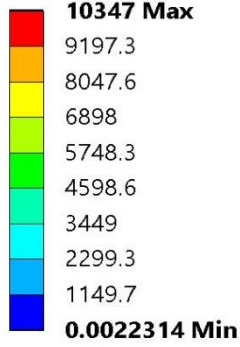
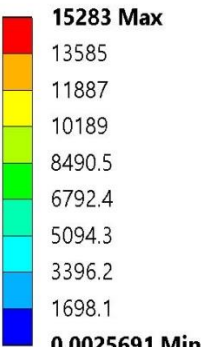
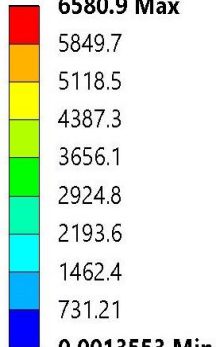
Mode	Rotor	Rotor With Lumped Mass	Rotor With Mass Removed
1st			
D(in mm)	<p>3.5958 Max 3.1963 2.7967 2.3972 1.9977 1.5981 1.1986 0.79906 0.39953 0 Min</p>	<p>3.5904 Max 3.1915 2.7925 2.3936 1.9947 1.5957 1.1968 0.79787 0.39893 0 Min</p>	<p>3.5863 Max 3.1878 2.7893 2.3909 1.9924 1.5939 1.1954 0.79695 0.39848 0 Min</p>
Freq.	48.427 Hz	47.289Hz	49.222Hz
2 nd			
D(in mm)	<p>3.6325 Max 3.2289 2.8253 2.4217 2.018 1.6144 1.2108 0.80722 0.40361 0 Min</p>	<p>3.6402 Max 3.2357 2.8313 2.4268 2.0223 1.6179 1.2134 0.80893 0.40447 0 Min</p>	<p>3.6639 Max 3.2568 2.8497 2.4426 2.0355 1.6284 1.2213 0.81421 0.4071 0 Min</p>
Freq.	58.531Hz	57.94Hz	64.707Hz
3 rd			
D(in mm)	<p>5.6825 Max 5.0511 4.4197 3.7883 3.1569 2.5256 1.8942 1.2628 0.63139 0 Min</p>	<p>5.6923 Max 5.0598 4.4274 3.7949 3.1624 2.5299 1.8974 1.265 0.63248 0 Min</p>	<p>5.7498 Max 5.111 4.4721 3.8332 3.1944 2.5555 1.9166 1.2777 0.63887 0 Min</p>
Freq.	135.6Hz	133.29Hz	132.81Hz

4 th			
D(in mm)	 <p>5.9334 Max 5.2741 4.6149 3.9556 3.2963 2.6371 1.9778 1.3185 0.65927 0 Min</p>	 <p>5.6527 Max 5.0247 4.3966 3.7685 3.1404 2.5123 1.8842 1.2562 0.62808 0 Min</p>	 <p>5.7232 Max 5.0873 4.4514 3.8155 3.1796 2.5437 1.9077 1.2718 0.63591 0 Min</p>
Freq.	224.77Hz	218.28Hz	221.61Hz
5 th			
D(in mm)	 <p>5.9566 Max 5.2948 4.6329 3.9711 3.3092 2.6474 1.9855 1.3237 0.66185 0 Min</p>	 <p>5.7282 Max 5.0918 4.4553 3.8188 3.1824 2.5459 1.9094 1.2729 0.63647 0 Min</p>	 <p>5.7754 Max 5.1336 4.4919 3.8502 3.2085 2.5668 1.9251 1.2834 0.64171 0 Min</p>
Freq.	259.85Hz	254.09Hz	271.8Hz

Note: The notation D means the deformation in mm, Freq means the Frequency in Hz

APPENDIX E

Table E.1 Comparative Equivalent Stress Diagram

Rotor	Rotor With Lumped Mass	Rotor With Mass Removed
		
		
Max Equivalent Stress	Max Equivalent Stress	Max Equivalent Stress
10347Mpa	15283Mpa	6580.9 Mpa
At Bearing Contact on Side A	At Bearing Contact on Side B	At Bearing Contact on Side B

Note: The red arrow in the figure indicates the region of maximum stress whereas the blue arrow head indicates the region of minimum stress.

APPENDIX F

Tensile Yield Strength of Steel, $\sigma_y = 1511$ MPa

According to the maximum shear stress theory, $\tau_{max} = \frac{\sigma_y}{2} = 755.5$ MPa

Factor of Safety, FoS = 6

$$\tau_{allowable} = \frac{\tau_{max}}{FoS} = 125.92 \text{ MPa}$$

Sample Calculation:

Total Shear Force acting on the shaft, $V = W_t + m_i r_i \omega^2$

Where,

W_t is the total weight of the rotor, m_i is the unbalanced mass, r_i is eccentricity due to the unbalanced mass and ω is the angular velocity.

Case 1:

$$W_t = 600N$$

$$\omega = 2\pi f = 2\pi \times \frac{1000}{60} \quad (\text{For RPM} = 1000)$$

$$= 104.72 \text{ rad/sec}$$

$$\text{Therefore, } V = 600 + m_1 r_1 \times 104.72^2$$

Total Shear Stress acting on the shaft,

$$\tau = \frac{V}{\text{Area of Shaft}} = \frac{W_t + m_i r_i \omega^2}{\frac{\pi d^2}{4}} = \frac{((600 + m_1 r_1 \times 104.72^2) \times 4)}{\pi \times 0.07^2} \quad (\text{F.1})$$

Considering critical condition for failure,

$$\tau = \tau_{allowable}$$

$$\text{or, } \tau = 125.92 \text{ MPa} = 125.92 \times 10^6 \text{ N/m}^2 \quad (\text{F.2})$$

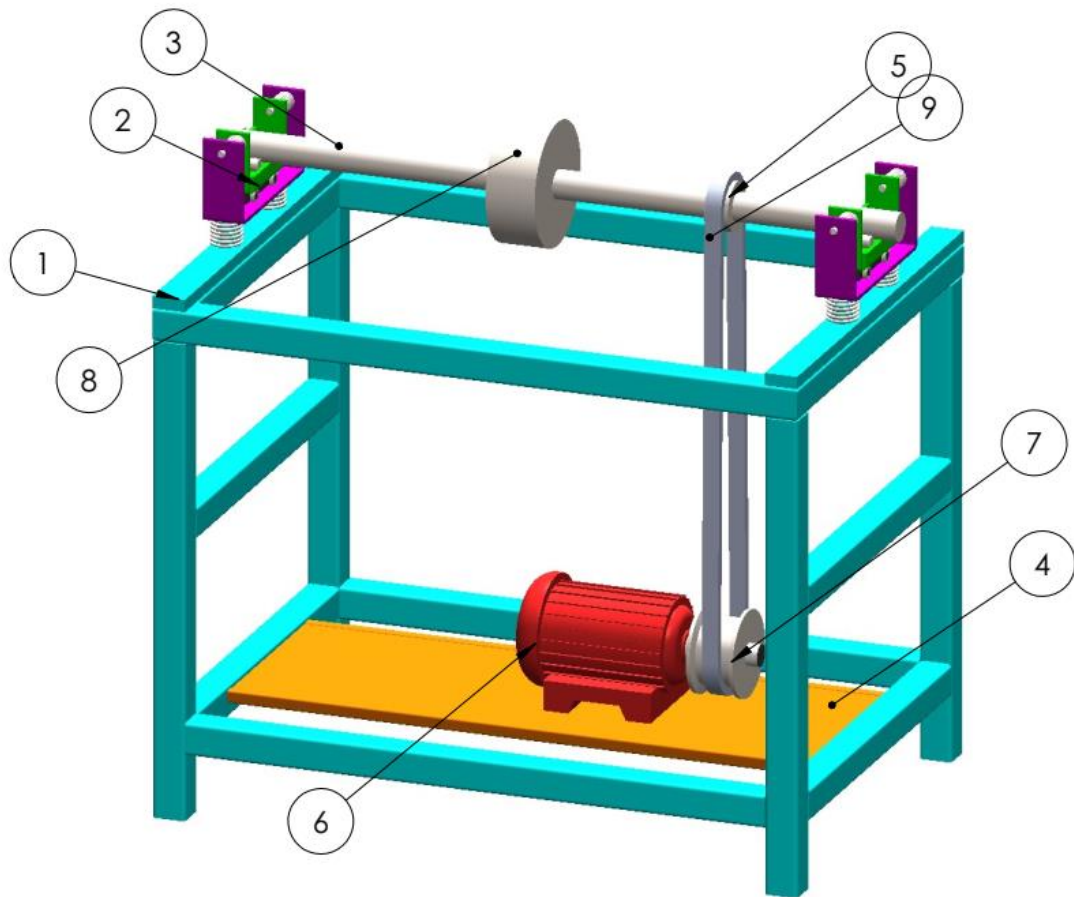
From Equation (F.1) and (F.2),

$$125.92 \times 10^6 = \frac{((600 + m_1 r_1 \times 104.72^2) \times 4)}{\pi \times 0.07^2}$$

Therefore, $m_1 r_1 = 44.135$ kg.m.

APPENDIX G

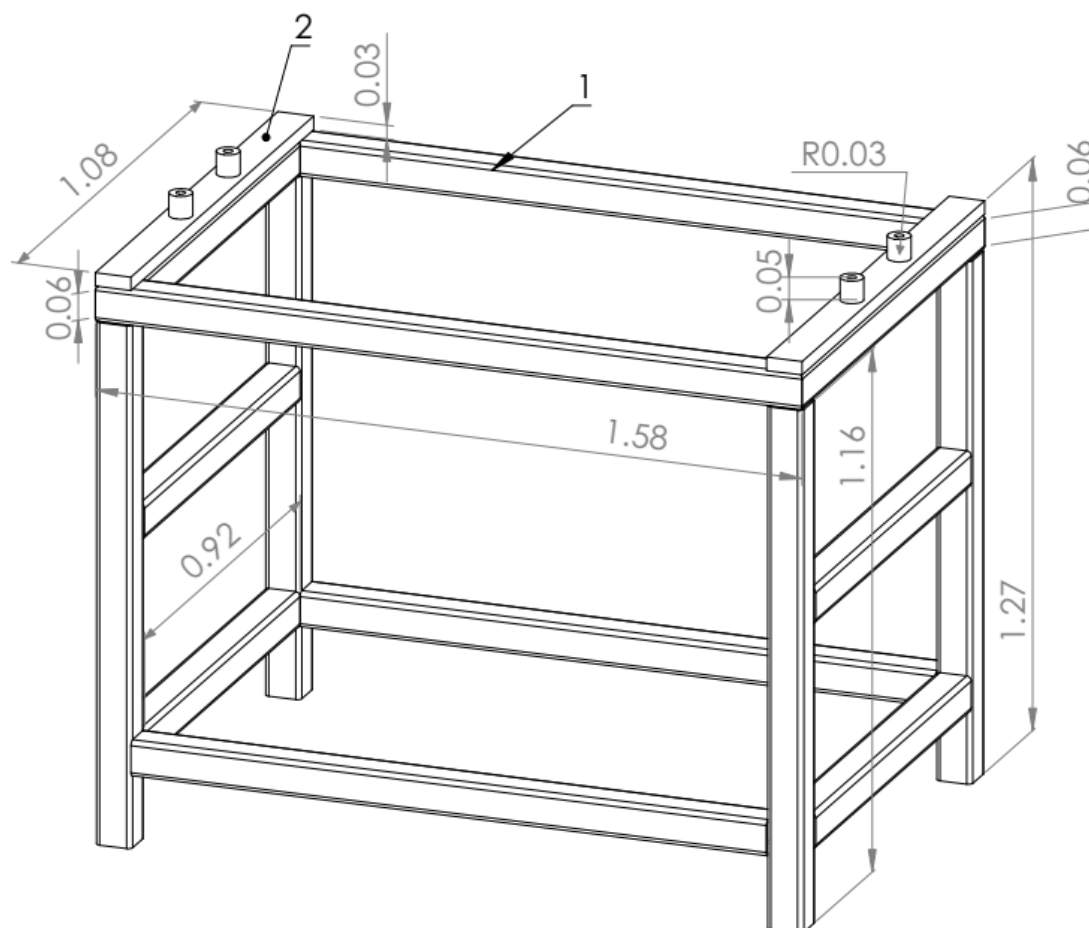
Rotor Balancing System Design



ITEM NO.	NOMENCLATURE	QTY.
1	Machine Bench	1
2	Suspension System	2
3	Shaft	1
4	Motorbase	1
5	Pulley-Shaft	1
6	Motor	1
7	Pulley-Motor	1
8	Rotor	1
9	Belt	1

APPENDIX H

Machine Bench

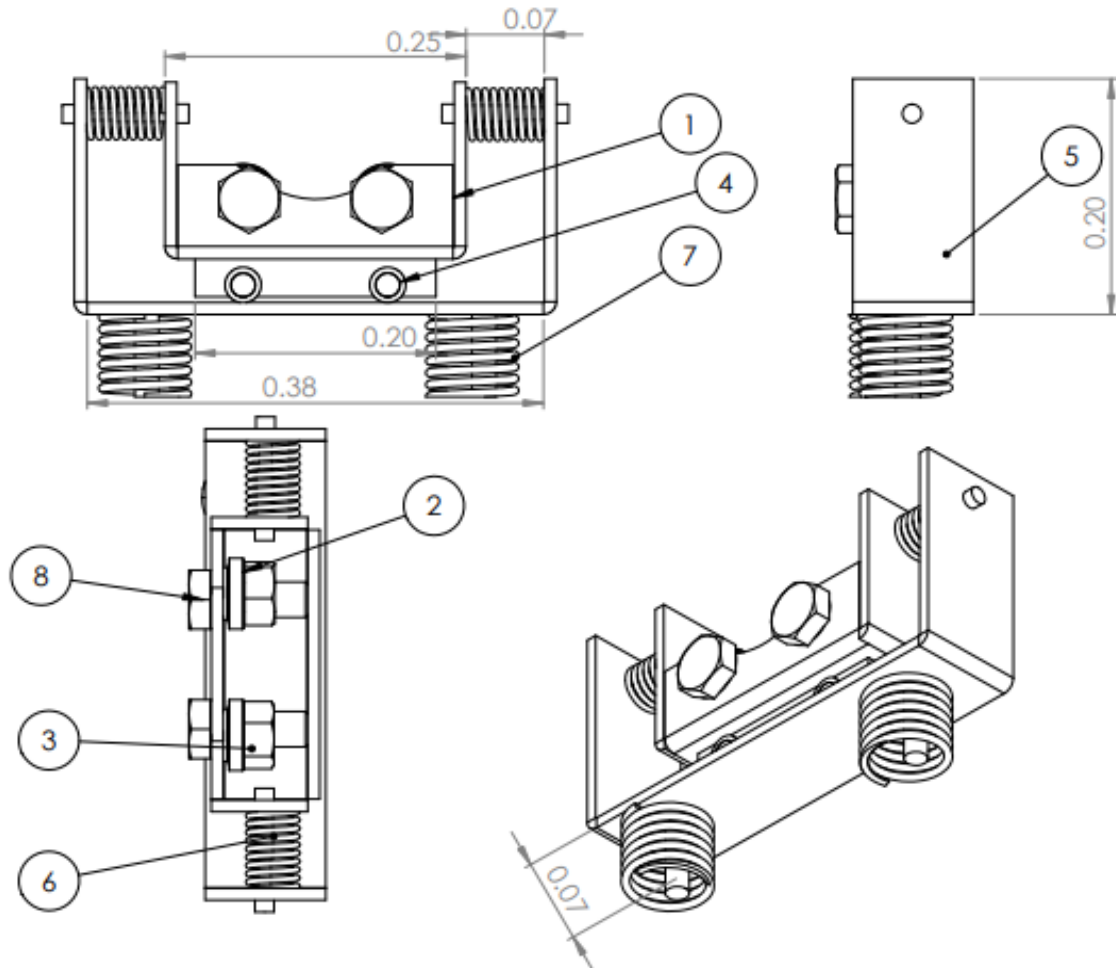


ITEM NO.	NOMENCLATURE	DESCRIPTION	QTY.
1	Square Tube	80mmx80mmx5mm	14
2	Suspension System Base	1080mmX80mmx30mm	2

Note: All dimensions are in meters (m).

APPENDIX I

Suspension System – Item No. 2 as per APPENDIX G

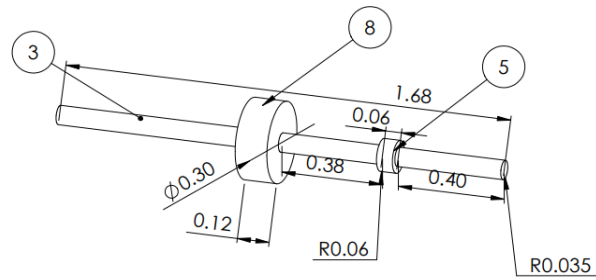


ITEM NO.	NOMENCLATURE	QTY.
1	Small Bracket	1
2	ISO 355-4 - 4CB30 - 16,SI,NC,16 Bearing	2
3	Hexagon Nut ISO - 7414 - M30 - W - N	2
4	Roller	4
5	Large Bracket	1
6	Spring small	2
7	Spring big	2
8	ISO 7412 - M30 x 80 --- 49-WN Bolt	2

Note: All dimensions are in meters (m).

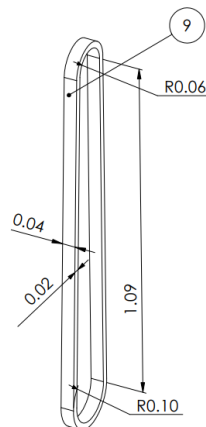
APPENDIX J

Shaft Rotor System



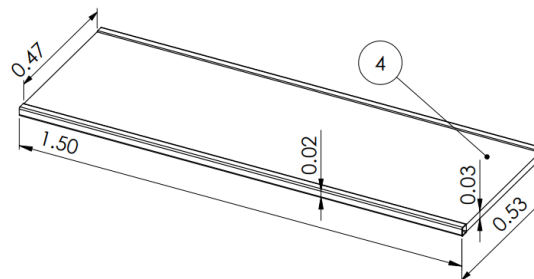
ITEM NO.	NOMENCLATURE	QTY.
3	Shaft	1
5	Pulley-Shaft	1
8	Rotor	1

Belt



ITEM NO.	NOMENCLATURE	QTY.
9	Belt	1

Motorbase



ITEM NO.	PART NUMBER	QTY.
4	Motorbase	1

Note: All dimensions are in meters (m).